IOWA STATE UNIVERSITY
Digital Repository

1973

Bonding modes of species chemisorbed on tungsten single crystal faces

Leon William Anders

Iowa State University

Follow this and additional works at: https://lib.dr.iastate.edu/rtd

Part of the Physical Chemistry Commons

Recommended Citation

www.manaraa.com

INFORMATION TO USERS

This material was produced from a microfilm copy of the original document. While the most advanced technological means to photograph and reproduce this document have been used, the quality is heavily dependent upon the quality of the original submitted.

The following explanation of techniques is provided to help you understand markings or patterns which may appear on this reproduction.

1. The sign or "target" for pages apparently lacking from the document photographed is "Missing Page(s)". If it was possible to obtain the missing page(s) or section, they are spliced into the film along with adjacent pages. This may have necessitated cutting thru an image and duplicating adjacent pages to insure you complete continuity.

2. When an image on the film is obliterated with a large round black mark, it is an indication that the photographer suspected that the copy may have moved during exposure and thus cause a blurred image. You will find a good image of the page in the adjacent frame.

3. When a map, drawing or chart, etc., was part of the material being photographed the photographer followed a definite method in "sectioning" the material. It is customary to begin photoing at the upper left hand corner of a large sheet and to continue photoing from left to right in equal sections with a small overlap. If necessary, sectioning is continued again — beginning below the first row and continuing on until complete.

4. The majority of users indicate that the textual content is of greatest value, however, a somewhat higher quality reproduction could be made from "photographs" if essential to the understanding of the dissertation. Silver prints of "photographs" may be ordered at additional charge by writing the Order Department, giving the catalog number, title, author and specific pages you wish reproduced.

5. PLEASE NOTE: Some pages may have indistinct print. Filmed as received.

74-9098

ANDERS, Leon William, 1940-
  BONDING MODES OF SPECIES CHEMISORBED ON
  TUNGSTEN SINGLE CRYSTAL FACES.

  Iowa State University, Ph.D., 1973
  Chemistry, physical

Bonding modes of species chemisorbed

on tungsten single crystal faces

by

Leon William Anders

A Dissertation Submitted to the

Graduate Faculty in Partial Fulfillment of

The Requirements for the Degree of

DOCTOR OF PHILOSOPHY

Department: Chemistry
Major: Physical Chemistry

Approved:

Signature was redacted for privacy.

In Charge of Major Work

Signature was redacted for privacy.

For the Major Department

Signature was redacted for privacy.

For the Graduate College

Iowa State University
Ames, Iowa

1973

TABLE OF CONTENTS

LIST OF TABLES

LIST OF FIGURES

CHAPTER I. INTRODUCTION

In recent years it has become experimentally possible to study the chemisorption of gases on single crystal planes of metal surfaces. This permits observation of chemisorption on metal surfaces of known structure, in contrast to earlier polycrystalline techniques. In the absence of direct spectroscopic observation, many indirect methods have been utilized in an attempt to assign molecular structures to various adsorbed states. Low energy electron diffraction (LEED) studies have uncovered the symmetry relationship between the substrate and the adsorbate. Flash desorption spectroscopy (FDS) has been used to determine the number of bonding states and kinetics and the energy of desorption from these states. From these techniques it has been clearly demonstrated in the last few years that gases chemisorbed on surfaces exhibit marked variations in structure and kinetics with crystal structure, but the investigators have not been able to assign positively bonding structures to the chemisorbed species.

This work was stimulated by the investigation by Tamm and Schmidt (1, 2) of hydrogen chemisorption on various tungsten single crystal surfaces. In the case of hydrogen on a W(100) surface, other investigators (3, 4, 5) have also reported results. From these findings, various conflicting models have been proposed. Tamm and Schmidt (1) proposed a mixture of atomic and molecular species; Estrup and

Anderson (3) as well as Madey and Yates (4) proposed that hydrogen atoms were bonded at a single site. Later Yonehara and Schmidt (5) proposed that hydrogen atoms were bonded at different sites.

The early part of this work was concerned with developing a qualitative description of chemisorbed hydrogen on W(100), W(110), and W(111). This was extended, following a suggestion by Dr. L. S. Bartell, by an Extended Hückel Molecular Orbital (EHMO) investigation to elucidate the bonding and structure of chemisorbed species on an array of atoms representing a truncated surface. The W(100) crystal face was chosen as the adsorbing surface, with hydrogen nitrogen, and oxygen as adsorbates. The hydrogen (1-5), nitrogen (6-9), and oxygen (10-12) on W(100) systems all have received experimental investigation, and it is generally concluded that the adsorbates are dissociated in their most strongly adsorbed state not only on a polycrystalline surface, but also a single crystal surface of tungsten. Although they are dissociatively adsorbed, molecular hydrogen and nitrogen desorb in FDS experiments. Molecular oxygen will not desorb in FDS experiments, but the dissociatively adsorbed oxygen desorbs as oxides of tungsten and even as atomic oxygen (13).

In developing an overall understanding of the bonding between a chemisorbed species and a surface, the literature was searched for experimental evidence which would yield insight into the problem.

Besides the above diatomic gases which have been used in chemisorption studies to probe the properties of a surface, NO and CO also have been used extensively. On polycrystalline tungsten, Yates and Madey (14) reported that NO chemisorbs nondissociatively at room temperature, but dissociation occurred at elevated temperatures (~ 500 - $600°$K). From the NO dissociation molecular nitrogen is desorbed and the majority of the oxygen is desorbed as oxides of tungsten. Weinberg and Merrill (15) report similar results on the W(100) surface and also found that when all of the nitrogen is desorbed, a typical (2 x 1) oxygen pattern remains (10).

In contrast to these common diatomic molecules, CO has been assumed to be associatively adsorbed on tungsten surfaces. Clavenna and Schmidt (16) recently reported CO was probably associatively adsorbed on a W(100) surface with the possible exception of the adsorbed state which desorbed at $\sim 1425°$K. More recent results (17-19) have been reported supporting a dissociatively adsorbed model for CO on polycrystalline tungsten. In Table I, a comparison is made between the desorption of associatively adsorbed states (molecular) and dissociatively adsorbed states (atomic) for the diatomic molecules of interest. The behavior of hydrogen, oxygen, nitrogen, and nitrous oxides has been well documented with regard to the separation of the two possible adsorbed states. As indicated by Goymour and King (17),

Table I. A comparison of thermal desorption data of diatomic molecules from a W(100) surface.

| Molecule | D_e (Kcal/mole) | Molecular State | | Atomic State | |
		Desorption Temperature (°K)	Activation Energy for Desorption (Kcal/mole)	Desorption Temperature (°K)	Activation Energy for Desorption (Kcal/mole)
H_2 (1)	104	100°	—	450°	26
				600°	32
O_2 (11-13)	118	—	—	Desorbs as metal oxides	
NO (14, 15)	150	520°	—	1100°	47 (N_2)
N_2 (8)	225	180°	10	1250°	74
CO (16)	256	400°	21	(?)	(?)
				1025°	57
				1150°	62
				1425°	74

it has been maintained in the literature that even the states of CO

desorbing at a temperature from ~1000 - 1425°K have resulted from

associatively adsorbed CO. In Table I the desorption activation

energies and temperatures for these high temperature states of CO

are similar to those for nitrogen states known to be dissociatively

adsorbed.

It therefore seemed desirable to re-examine the question of CO

dissociation on tungsten, and a study of mixed adsorption of $C^{16}O$ and

$^{18}O_2$ on (100), (110) and (111) tungsten single crystal faces was under-

taken for this purpose. Very recently and while the present study was

in progress, Goymour and King (17-19) have presented evidence, based

on polycrystalline FDS experiments, for dissociative adsorption of CO

on tungsten and have presented a model for such adsorption.

CHAPTER II. MOLECULAR ORBITAL INVESTIGATION OF ATOMIC SPECIES CHEMISORBED ON A W(100) SURFACE

Introduction

Today there is no available experimental technique or any combination of techniques which can be used to assign unequivalently a bonding structure between an adsorbate species and the atoms of a surface. The advent of metal single crystal surfaces in chemisorption research has brought about increased speculation as to the preferred bonding structures for chemisorbed species. Unfortunately, no general overall understanding has emerged which can serve to predict sites and preferred structure for new systems based on previous knowledge. Certainly, there is no reason to suspect that chemisorbed atoms like hydrogen, nitrogen, oxygen, etc. would exhibit strange and unusual bonding properties when interacting with the atoms of a metal surface. The bonding properties of most atoms are generally known and their roles in a particular chemical compound are usually predictable. If a surface chemist were able to develop guidelines from which bonding between an adatom and surface atoms could be predicted, he would be able to understand and describe more concretely surface processes of current concern.

In this study, a molecular orbital approach was used in hopes that some guidelines could be established for predictions of

chemisorption bonding. A simple molecular orbital technique developed by Hoffmann (20), which was sensitive to bonding geometries, was utilized in this study. Hoffmann extended the Hückel Molecular Orbital technique which depended only on the interactions of adjacent atoms to include all interactions. Therefore, it is referred to as the Extended Hückel Molecular Orbital (EHMO) technique. A listing of the computer program used for the molecular orbital calculations can be found in Appendix D.

Results and Discussion

This study was restricted to the tungsten (100) surface with adatoms of hydrogen, nitrogen, and oxygen. The application of the EHMO technique to the surface "molecules" formed by

$$W_n(100) + X \rightarrow W_n(100)X$$
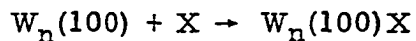
is described in Appendix A. The tungsten surface was represented by a finite array of tungsten atoms (W_n) to which the adatom could bond forming the surface "molecule" $W_n X$.

The results and a full description of the molecular orbital calculations for hydrogen, nitrogen, and oxygen atoms chemisorbed to the various sites on a W(100) surface are found in Appendices A, B, and C respectively.

The tungsten (100) surface has three symmetric bonding sites as illustrated in Fig. 1a. An adatom at site A will be coordinated to
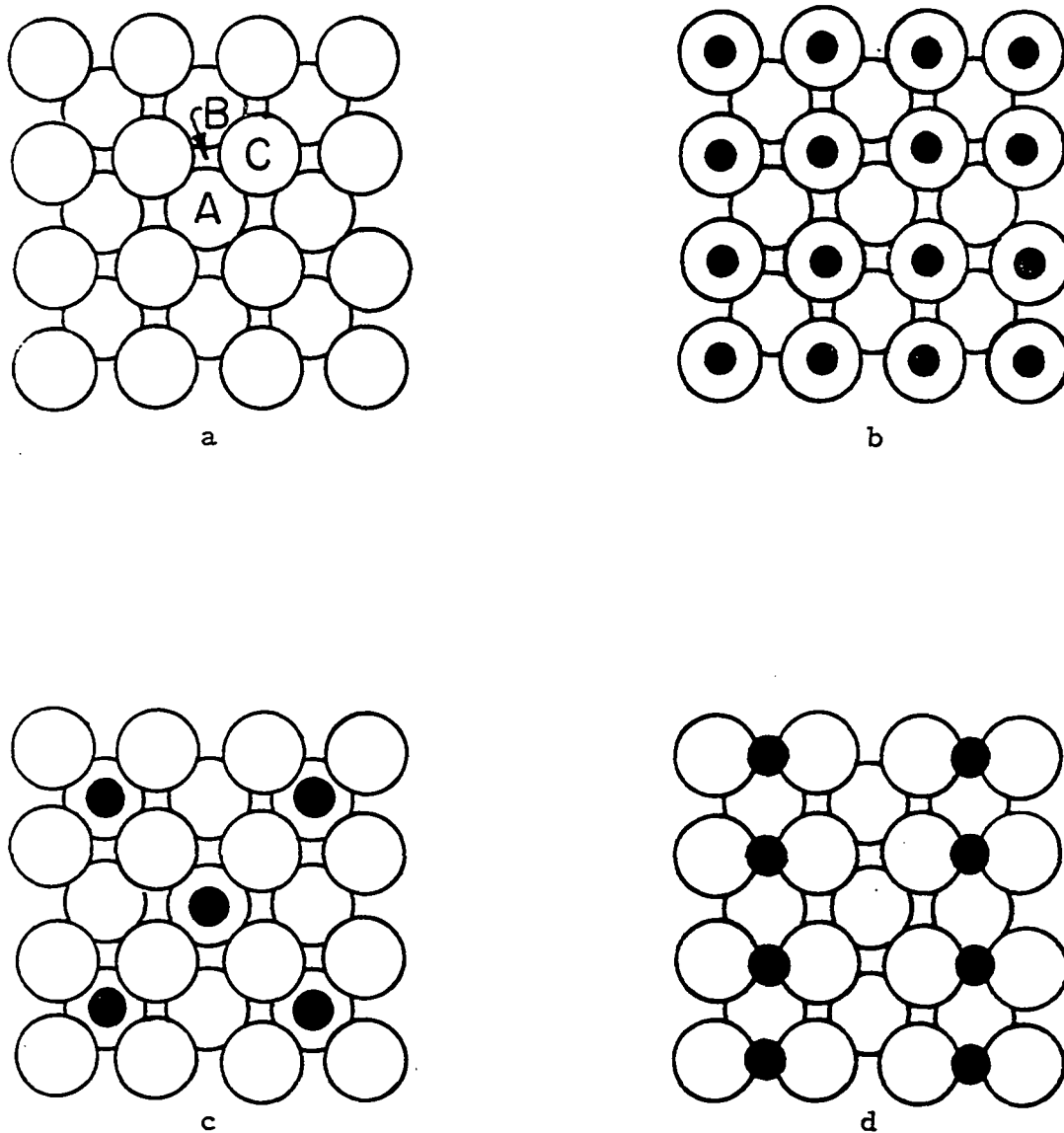
Fig. 1. Bonding structure of chemisorbed atoms on the W̄(100) surface
(a - W(100) surface A - 5 CN site, B - 2 CN site, C - 1 CN
site, b - hydrogen bonded at 1 CN sites in a (1 x 1) structure,
c - nitrogen bonded at 5 CN sites in a C(2 x 2) structure and
d - oxygen bonded at 2 CN sites in a (2 x 1) structure).

five surface atoms (5 CN), at site B to two surface atoms (2 CN), and at site C to a single surface atom (1 CN). It was found that hydrogen (Appendix A) preferred the 1 CN site, the nitrogen (Appendix B) preferred the 5 CN site, and oxygen (Appendix C) preferred the 2 CN site. It appears that each adatom selected a site on the tungsten (100) surface determined by the bonding properties of the adsorbate atom.

The most direct tests of the above bonding models are the LEED patterns of stable structures of these adatoms. The adsorption of hydrogen on a W(100) surface leads to a (1 x 1) pattern (3, 5) or one hydrogen atom for every surface atom. Such a structure, as shown in Fig. 1b, is consistent with hydrogen bonded at every 1 CN site. After annealing a nitrogen adsorbed layer a C(2 x 2) structure (7, 8) is produced on a W(100) surface. From the knowledge (Appendix B) that nitrogen selected the 5 CN site because of the ability of the p_x and p_y orbitals to bond to the four atoms surrounding the 5 CN site, it is not unreasonable that nitrogen atoms would select a C(2 x 2) surface struc-ture (Fig. 1c). In this structure, a nitrogen atom is surrounded by four empty adjacent 5 CN sites. The p_x and p_y orbitals of nitrogen can form strong bonds with the four atoms around this site. LEED has observed a stable (2 x 1) oxygen (10) surface structure on the W(100) surface. A (2 x 1) surface structure results if the oxygen atoms occupy the 2 CN sites on a W(100) surface as illustrated in Fig. 1d. Each

oxygen atom is bonded to two surface atoms, and each surface atom to one oxygen atom.

Summary and Conclusions

The bonding properties of chemisorbed species on metal surfaces appear to be very similar to those expected from their usual bonding characteristics. Where there is no activation for dissociation (usually the case for diatomic molecules) the atoms of an adsorbing molecule will select sites where they can best satisfy their valency requirements and maximize the bonding interactions with the surface atoms. These guidelines should be able to help understand additional chemisorbed systems. One example will be used to indicate the transferability of derived results. In Fig. 2, a W(110) surface is illustrated. There are three probable sites for a chemisorbed species to be located. If an oxygen atom were bonded to this surface, either site A or site B would satisfy its divalent property. At site B, the tungsten atoms are touching and probably would not form a stable bond with an oxygen atom. Site A appears attractive to an atom with a higher valency, because of its high coordination number. Although the four atoms are not equally spaced at this site, two atoms are separated by 3.16Å and the other two by 4.46Å. To the oxygen atom, this site is very similar to the 2 CN site on the W(100) surface. If the oxygen atoms were to produce a surface structure as illustrated in Fig. 2,
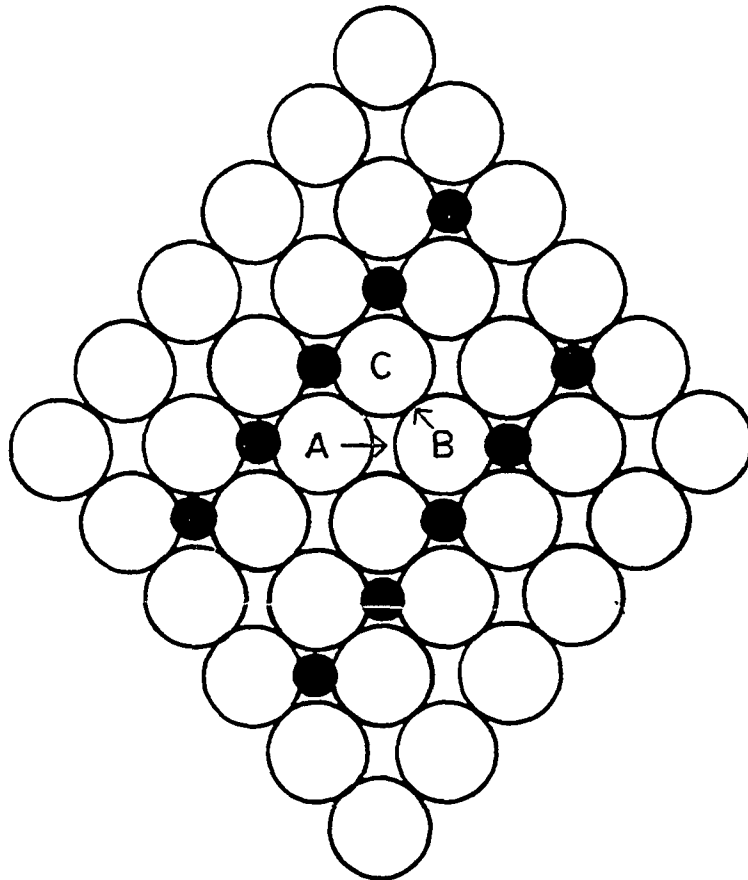
Fig. 2. Proposed surface structure of oxygen atoms at 2CN sites on a W(110) surface.

the bonding between the oxygen atoms and the surface atoms would be identical to that on the W(100) surface. Each oxygen is bonded to two tungsten atoms and these tungsten atoms are not bonded to any other oxygen atom. This surface structure is a p(2 x 1) and a resulting LEED pattern should be observed. Tracy and Blakely (21) have reported such a structure for oxygen adsorption on a W(110) surface.

The usefulness of this basic understanding will be illustrated in the next chapter when selecting preferred sites for C and O adatoms and associatively adsorbed CO and O_2 on the single crystal surfaces of tungsten (100, 110, and 111) crystal faces.

CHAPTER III. CO AND $^{18}O_2$ CO-ADSORPTION ON SINGLE CRYSTAL SURFACES OF TUNGSTEN

Introduction

The interaction of CO with tungsten has been extensively studied and reviews of the literature have recently been published (22-24). On tungsten as on most metal surfaces, it has generally been accepted that CO is nondissociatively chemisorbed. All common diatomic gases including CO exhibit multiple peaks in the desorption spectra from Flash Desorption Spectrometry (FDS), but for CO, unlike the other diatomic gases, it has been assumed that even the high temperature desorption peaks result from undissociated adsorbed CO.

Very recently Goymour and King (17-19) have shown that a model based on dissociative chemisorption of CO can more satisfactorily explain their experimental results. They have presented the following facts in a brief history (17) of related experimental evidence which has been reported in favor of and against the hypothesis of dissociative adsorption:

(1) The argument of Ehrlich, Hickmott, and Hudda (25) that their failure to find traces of C or O residues on their surfaces following CO chemisorption implies associative chemisorption is not compelling. The major desorption product from a mixture of C and O adatoms appears always to be CO, and in this case it is scarcely

surprising if little C and O residues remain after heating a CO adlayer.

Thus Becker et al. (26) and Singleton (27) found that carbon impurities

are removed as CO from a tungsten surface when that surface is heated

to 2000°K in an oxygen ambient.

(2) The energy balance for dissociative adsorption is (24)

$$q_{co} = q_o + q_c - D_{co}$$

where q_x is the adsorption heat of species x and D_{co} is the

dissociation energy of gaseous CO (256 Kcal/mole). From Brennan

and Graham (28) $q_o = 163$ Kcal/mole, and from Redhead (29) $q_c \cong 170$

Kcal/mole; therefore q_{co} is 77 Kcal/mole. If the activation energy

for adsorption is zero, then q_{co} can be compared with the activation

energy for desorption of CO from the various surfaces of tungsten

which are listed in Table II. These comparisons indicate that

it is thermodynamically feasible for CO to be dissociated on tungsten

surfaces.

(3) Madey et al. (30) observed isotopic mixing in the β states

of CO from mixed adsorption of $^{12}C^{18}O$ and $^{13}C^{16}O$. Their

explanation was based upon a four-centered complex formed by the

interaction of two adsorbed CO molecules, although dissociative

adsorption is also a very plausible explanation. Madey and Yates (31)

later reported that isotopic exchange occurred on W at temperatures

between 1300 and 2200°K where the steady state CO coverage is very

Table II.   A comparison of activation energy of desorption for CO on various tungsten surfaces.

Tungsten Surface	State	E_{d0} (Kcal/mole)
Polycrystalline	β_1	53
W (4)	β_2	100
W(100) (12)	β_3 (<0.1)	93
	β_3 (>0.1)	74
	β_2	62
	β_1	57
W(110) (13)	β_1	40 - 55
	β_2	67

small and it is difficult to see why desorption should take place preferentially through a four-centered complex. It was also shown by Madey et al. (30) that isotopic exchange does not occur in the α states but only in the β states of CO.

(4) Propst and Piper (32), using the relatively low resolution energy-loss technique, observed a strong vibrational band attributed to the β-CO state on W(100) which they claimed could only be explained by the presence of atomically adsorbed C and O.

These facts along with the kinetic and surface stoichiometry data reported by Goymour and King (17) and also the mixed adsorption of CO and $^{18}O_2$ very recently reported by Goymour and King (19) strongly suggest that β-CO is dissociatively adsorbed on tungsten. The object of the present work was to use $^{18}O_2$ which will dissociatively adsorb on W surfaces as a chemical probe in mixed adsorption experiments on single crystal surfaces of tungsten (100, 110, 111) to test the hypothesis of dissociatively adsorbed CO. Isotopic mixing of oxygen in the desorbed CO molecules could serve as primary evidence for the hypothesis. It should also be possible to vary the ratio of $C:^{16}O:^{18}O$ adsorbed on the surface and if the CO is dissociatively adsorbed the ratio of $C^{16}O$ and $C^{18}O$ desorbed from the W surfaces should also vary. If more than one β (dissociated CO) state exist on a particular surface, then the ability of the adsorbed

$^{18}O_2$ to displace any or all of these states, or the ability of the co-adsorbed $^{18}O_2$ to alter the energy of CO desorption (e.g. lowering the temperature of the maximum desorption of an adsorbed state) are also of interest.

Experimental Procedure

The ultra-high vacuum Pyrex apparatus is schematically illustrated in Fig. 3. During bake-outs to ~350°C, the system was pumped by a mercury diffusion pump trapped with liquid nitrogen. At the end of the bake-out, with the oven still hot, the pumping was shifted to an Ultek 20 L/sec differential ion pump. After cooling of the apparatus, background pressures of ~ 10^{-10} Torr were routinely obtained. Pressures were measured with an Electron Technology Inc. ion gauge equipped with a thoriated iridium filament controlled with a Granville-Phillips ionization gauge controller. The reaction cell was also equipped with a quadrupole mass spectrometer (QMS) (Electronic Associates Inc.) enabling partial pressures of the various gaseous species to be monitored. The tungsten single crystals were cut from a 7 mm diameter rod of 99.998% purity. The rod was properly aligned by back reflectance x-ray patterns according to the procedure outlined by Wood (33). Sample wafers ~20 mil thick were spark cut from the rod to expose selected single crystal surfaces. These wafers were mechanically polished to a mirror finish. Back reflectance x-ray
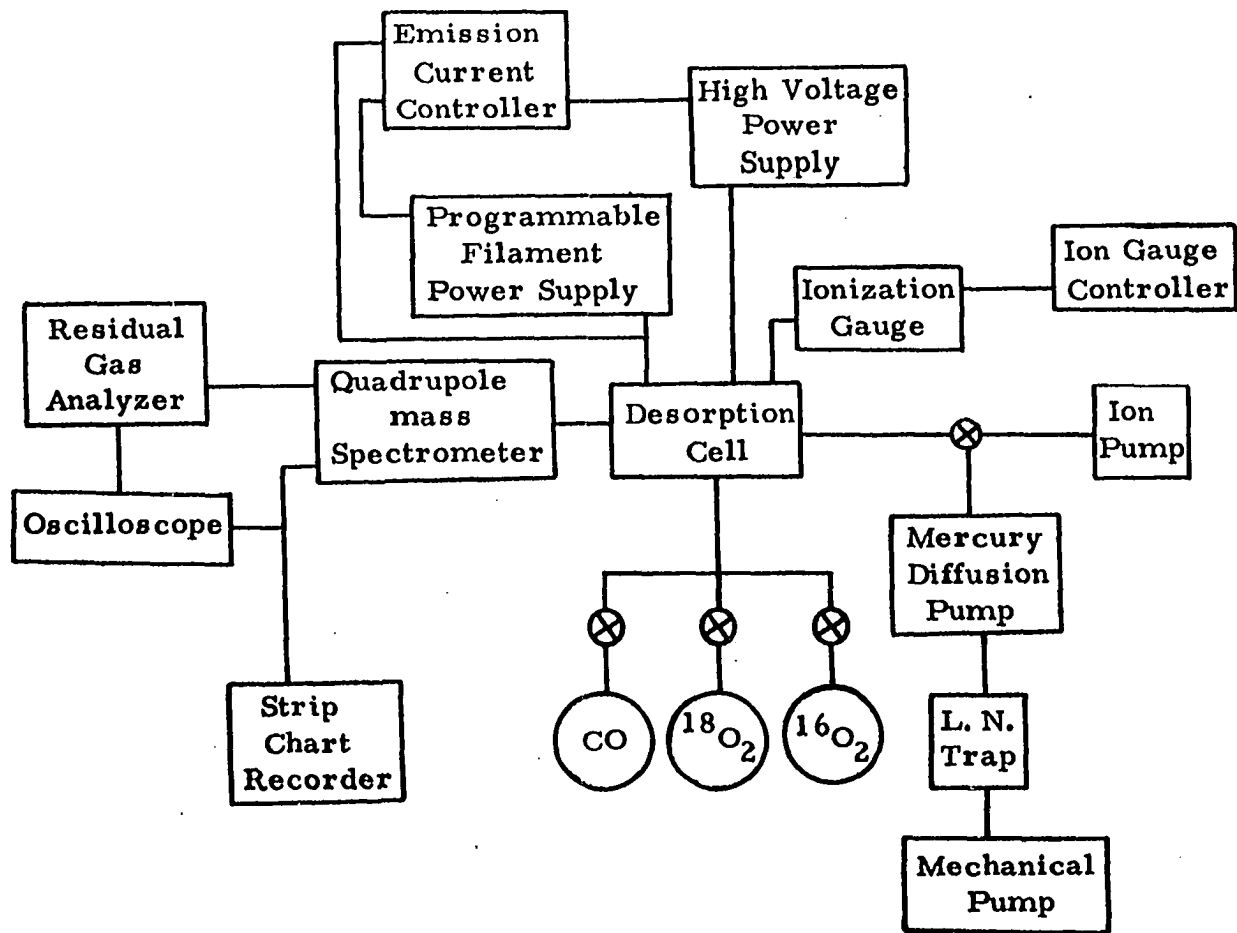
Fig. 3. A schematic diagram of the experimental apparatus for flash desorption
spectrometry.

patterns indicated that the three crystal surfaces (100), (110), and (111) were oriented to within 1.5° of the nominal orientations. For each of the crystals the edge area was about 10% of the total area. Each single crystal surface sample was mounted to a 15 mil tungsten main support rod which was attached to a pyrex dewar via a 45 mil tungsten rod. A thermocouple (W vs. Re) was also attached to each sample. Generally, the crystals were heated in vacuo to 2200°K by electron bombardment until a background pressure of less than 10^{-8} Torr could be obtained (about 24 hours); this was interspersed with flashes to at least 2600°K for several minutes each. During the cleaning period, the crystals were also flashed to 2000°K for several minutes in an O_2 atmosphere of $\sim 10^{-6}$ Torr. At the end of this procedure the crystal could be flashed to above 2000°K without a measurable pressure increase.

The heating of the crystal by electron bombardment was accomplished by maintaining the crystal +400 volts above filament potential and by preselecting an emission current with which to bombard the sample. With a controller which monitored the emission current and signalled a programmable filament power supply, a filament temperature could be maintained to give the proper emission current. The calibrated thermocouple was used to obtain time-temperature curves for various emission currents for each sample. Emission currents could then be selected which gave linear heating rates over

the temperature ranges of interest. The flash desorption curves were all recorded as ion current (y axis) vs. time (x axis); the latter could be converted to a temperature scale from the above heating curves.

In the following experiments, the desorption species of principal concern were $C^{16}O$ and $C^{18}O$ molecules. Therefore, the QMS was set to sweep mass (m/e⁻) 28-30 at a rate of six sweeps per second. The ion current of each mass on each sweep was recorded by a high speed chart recorder enabling each species to be monitored simultaneously for each flash desorption spectrum.

The dosing gases were controlled by variable leak valves. The $^{18}O_2$ was obtained from YEDA R&D Co. LTD, a Division of Miles Laboratories, and was 99.29% $^{18}O_2$. The $C^{16}O$ was C.P. Grade, 99.5% CO, obtained from Matheson Co. The CO was vacuum distilled prior to use as the dosing gas. The dosing pressure of each gas was monitored with the QMS which was calibrated with the ionization gauge.

Results and Discussion

Mixed adsorption of CO and $^{18}O_2$ on a W(100) surface

A series of CO desorption spectra obtained from a W(100)

surface after varying exposures to CO at room temperature are shown

in Fig. 4. These are very similar to those found in the literature (16,

34) for the interaction for CO with this single crystal surface. Yates

and King (34) reported three bonding states: α which desorbed at

$\sim$400°K and two higher temperature states β_1 and β_2. The desorption

temperatures for these states were not reported. Clavenna and

Schmidt (16) also reported an α state desorbing at $\sim$ 400°K; with an

ultra-high vacuum system which apparently had a higher pumping speed,

they were able to resolve the next state which compares to the β_1 state

of Fig. 4 into states which they labeled β_1 desorbing at $\sim$1040°K and

β_2 desorbing at $\sim$1130°K. These two states combined desorbed at a

temperature centered at $\sim$1100°K and compares with the β_1 state in

Fig. 4 which desorbs at $\sim$1060°K and with the β_1 states reported by

Yates and King (34). The higher temperature state β_2 in Fig. 4 desorbs

at $\sim$ 1450°K which compares with a state desorbing at $\sim$1480°K and

labeled β_3 by Clavenna and Schmidt. The spectra reported by

Clavenna and Schmidt better resolve the $\beta_1 - \beta_2$ group and the higher

temperature β_3 state than the spectra of Fig. 4. The β_2 state in Fig.

4 is only clearly observed in curves A and B and unfortunately because
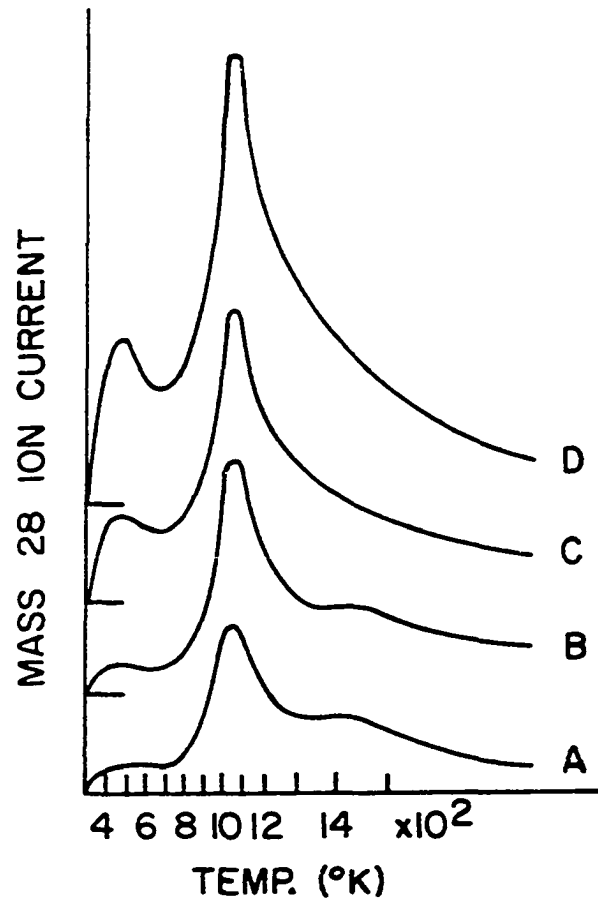
Fig. 4. Flash desorption spectra of CO adsorbed on a W(100) surface
(A - 2.4L, B - 4.5L, C - 9.0L, and D - 18.2L (1 Langmuir
(L) = 10^{-6} Torr-sec.)).

of poor resolution at larger CO coverages (curves C and D of Fig. 4),

the tail of the flash desorption spectra of the β_1 state covers up the β_2

state. The resolution of a flash desorption spectra can be improved

primarily by controlling two experimental parameters: the pumping

speed of the system and the heating rate. The design of the system and

size of the pump determine the pumping speed, therefore, this can not

be changed after construction of the system and in the experiments of

this study, the heating rate was optimized for the best resolution

possible. The only other observable difference between the spectra in

Fig. 4 and those previously reported (16, 34) is the amount of CO

desorbed in the α state. Yates (35) suggested that possibly the crystal

was not cool enough during the dosing period to accommodate a larger

amount of CO adsorbed in the α state. Yates and King (34) using ESD

were able to resolve the α state into two substates α_1 (340° K) and α_2

(380° K). Yates (35) indicated that the α_1 state was very labile and

could be desorbed by pumping on the system, whereas the α_2 state was

more stable. Although cool water flowed through the dewar reservoir,

Yates (35) thought that the temperature of the crystal might have been

high enough during dosing to preclude formation of the α_1 state, so

that only the α_2 state appeared in Fig. 4.

Using LEED and FDS, Anderson and Estrup (36) reported that

two β states resulted from room temperature adsorption of CO on the

W(100) surface. The initial adsorption produced a (1 x 1) LEED pattern, and upon heating the surface to desorb the β_1 state at $\sim 1150°$K, the remaining CO, the β_2 state, produced a C(2 x 2) LEED pattern. This β_2 state desorbs at $\sim 1380°$K. These β states compare remarkably well with those found in this study and elsewhere (16, 34). They were able to readsorb CO upon the β_2 (C(2 x 2) structure) state to produce a structure indistinguishable from that resulting from adsorption on a clean surface.

The results of first dosing the W(100) surface with CO followed by a dose of $^{18}O_2$ are shown in Figs. 5 - 8. In these figures, the flash desorption curves of both $C^{16}O$ and $C^{18}O$ are shown (recorded simultaneously as previously explained). In Fig. 5, the surface was dosed with a 2.4L dose of $C^{16}O$ followed by increasing dosages of $^{18}O_2$ as indicated for curves B-F. It is observed that most of the $C^{18}O$ is desorbed in the β_1 state. It is difficult to observe any peak of $C^{18}O$ desorbing from the β_2 state, in fact at larger $^{18}O_2$ doses (curves E and F) even the $C^{16}O$ which desorbed from the β_2 state has been displaced. The amount of $C^{16}O$ desorbing in the α state increases slightly as the coverage of $^{18}O_2$ increases and seems to reach a limiting value as observed from curves E and F. The isotopic mixing of oxygen in the CO molecules desorbed from the β_1 state suggests CO has been dissociatively adsorbed. A suggestion that associatively
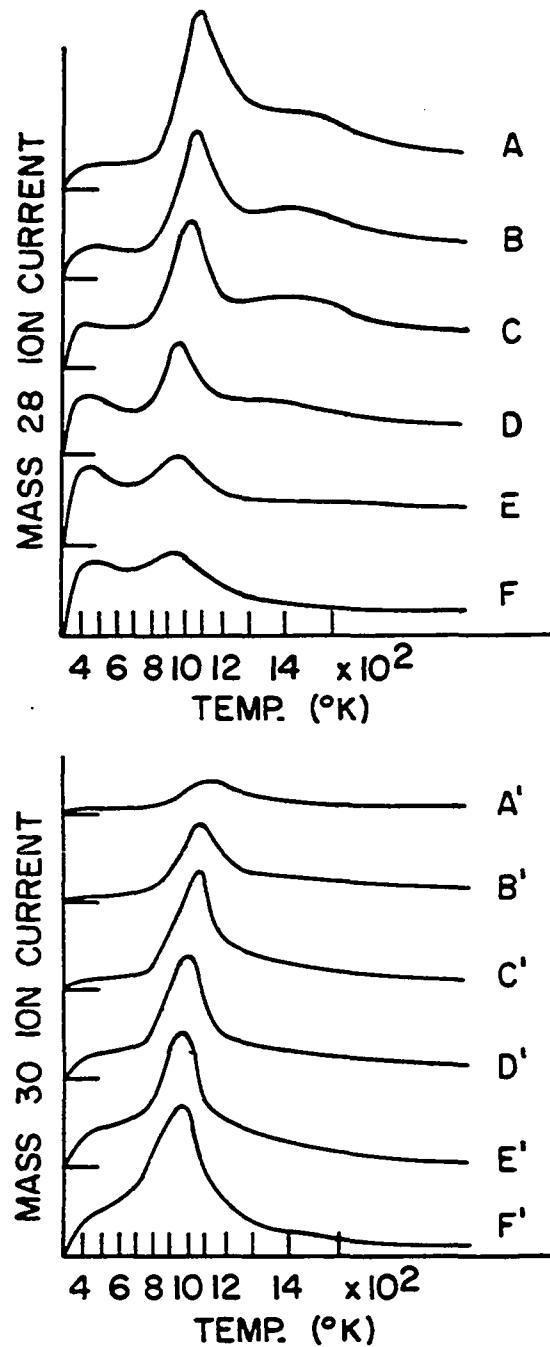
Fig. 5. Flash desorption spectra of CO from a W(100) surface predosed with 2.4L of $C^{16}O$ followed with increasing dosages of $^{18}O_2$ (A - 0.0L, B - 1.2L, C - 2.6L, D - 5.3L, E - 10.7L and F - 21.3L).
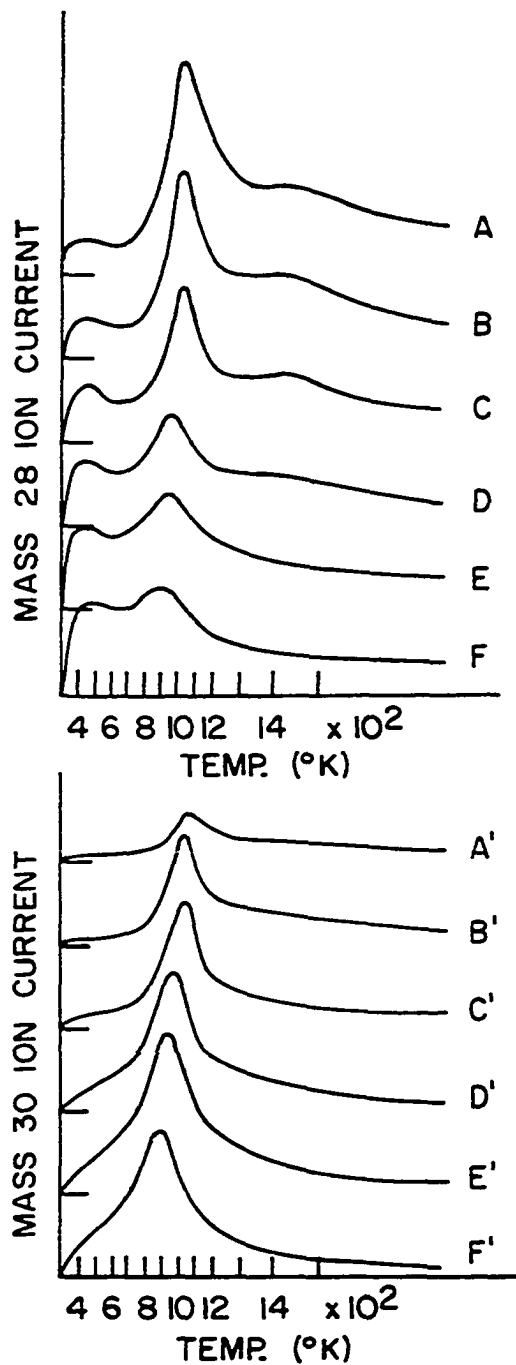
Fig. 6. Flash desorption spectra of CO from a W(100) surface predosed with 4.5 L of $C^{16}O$ followed with increasing dosages of $^{18}O_2$ (A - 0.0L, B - 1.2L, C - 2.6L, D - 5.3L, E - 10.7L and F - 21.3L).
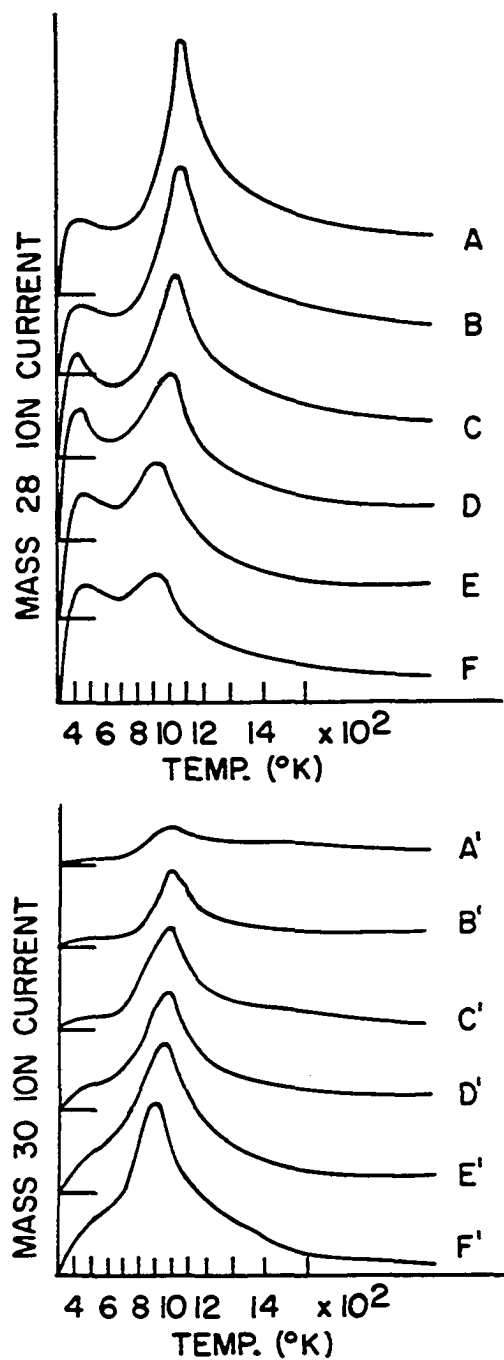
Fig. 7. Flash desorption spectra of CO from a W(100) surface predosed
with 9.0L of $C^{16}O$ followed with increasing dosages of $^{18}O_2$
(A - 0.0L, B - 1.2L, C - 2.6L, D - 5.3L, E - 10.7L and
F - 21.3L).
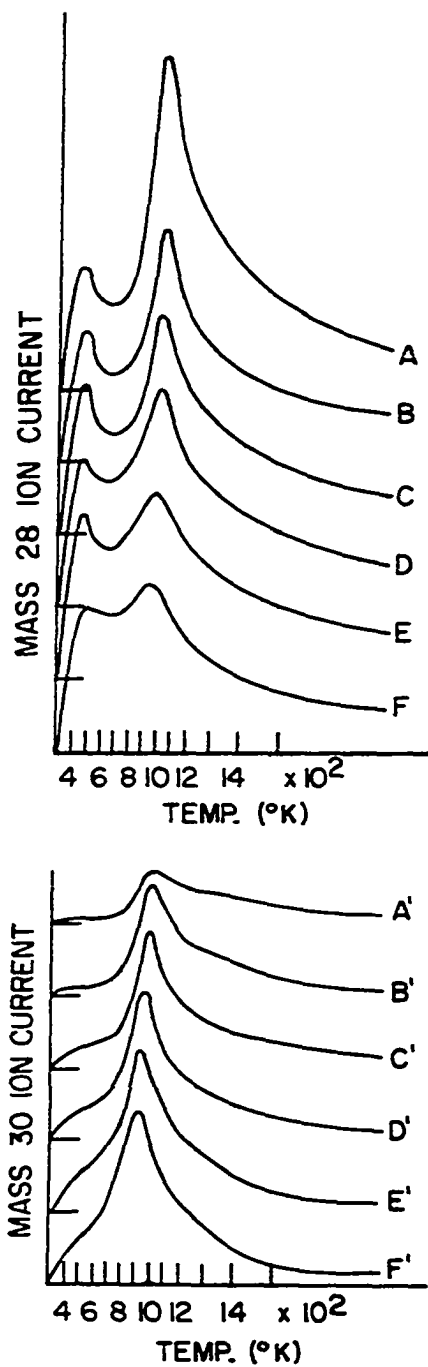
Fig. 8. Flash desorption spectra of CO from a W(100) surface predosed
with 18.2L of CO followed with increasing dosage of $^{18}O_2$
(A - 0.0L, B - 1.2L, C - 2.6L, D - 5.3L, E - 10.7L and
F - 21.3L).

adsorbed CO in an α state could be converted to dissociated CO in the β states as a result of heating during the flash desorption technique is not supported by the above facts. If CO were only associatively adsorbed at room temperature, then dosing with $^{18}O_2$ a surface with preadsorbed CO should block the sites needed for the conversion of α-CO to β-CO. This conflicts with results shown in Figs. 5-8; therefore, the CO must be adsorbing in the β states at room temperature. With larger $^{18}O_2$ doses (curves D-F), it also must be noted that some $C^{18}O$ is desorbed from the α state. Therefore, at very high coverages of $^{18}O_2$, the associatively adsorbed α-CO must be able to interact with the adsorbed $^{18}O_2$. In Fig. 6, where the surface was predosed with 4.5 L dose of $C^{16}O$ followed with increasing $^{18}O_2$ doses, the observations are the same as those stated above. Figures 6 and 7 with predose 9.0 L of $C^{16}O$, and Fig. 8 with predose of 18.2 L of $C^{16}O$ all show that as the $^{18}O_2$ coverage increases, there is a decrease in the temperature of the desorption peak maximum for the β_1 state.

The flash desorption spectra of a set of experiments where a W(100) surface was predosed with varying amounts of $^{18}O_2$ always followed by the same dose of $C^{16}O$ are shown in Fig. 9. It is observed that the $^{18}O_2$ initially blocks sites for CO to adsorb in the β state, but creates sites for more CO to adsorb associatively in α states; as the
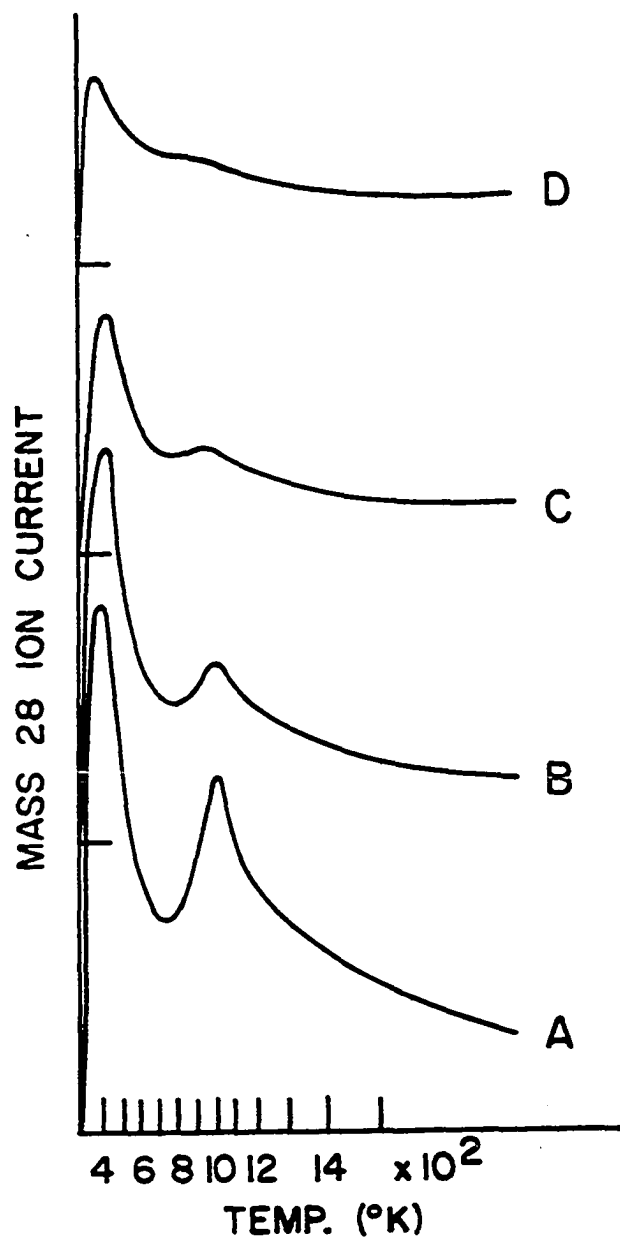
Fig. 9. Flash desorption spectra of CO from a W(100) surface predosed
with increasing dosages of $^{18}O_2$ (A - 2.6L, B - 5.3L, C - 10.7L
and D - 21.3L) followed by a constant dose of $C^{16}O$ (9.0L).

amount of preadsorbed $^{18}O_2$ increases, it eventually also blocks the

CO from adsorbing in the α state. If the W(100) surface were

saturated with $^{18}O_2$, it would prevent the surface from adsorbing any

CO. From Fig. 9 it must also be observed that isotopic mixing of the

oxygen in the desorbed CO molecules still occurs primarily in those

desorbed in the β state.

It is possible to estimate the amount of CO desorbed from the

surface by determining the area under each of the flash desorption

curves. The total amounts of CO ($C^{16}O$ and $C^{18}O$) desorbed from all

states in each of the four experiments (Figs. 5 - 8) are plotted in Fig.

10. It is evident that in a given experiment with a constant $C^{16}O$

predose, the amount of CO desorbed is independent of the $^{18}O_2$ coverage.

This shows that $^{18}O_2$ is unable to displace any of the preadsorbed $C^{16}O$.

Figure 11 plots the ratio of $C^{18}O:CO_{total}$ as a function of $^{18}O_2$ dose on

the surface for each of the experiments in which $C^{16}O$ was preadsorbed.

Each $C^{16}O$ predosed surface appears to reach a limiting ratio

($C^{18}O:CO_{total}$) as the amount of $^{18}O_2$ dosed increases to a saturated

level. The limiting ratios for each predosed surface are plotted in

Fig. 12 as functions of the $C^{16}O$ predose. The limiting $C^{18}O:CO_{total}$

ratio at low $C^{16}O$ dose appears to be ~ 0.75 and at high $C^{16}O$ dose

appears to be ~ 0.24.
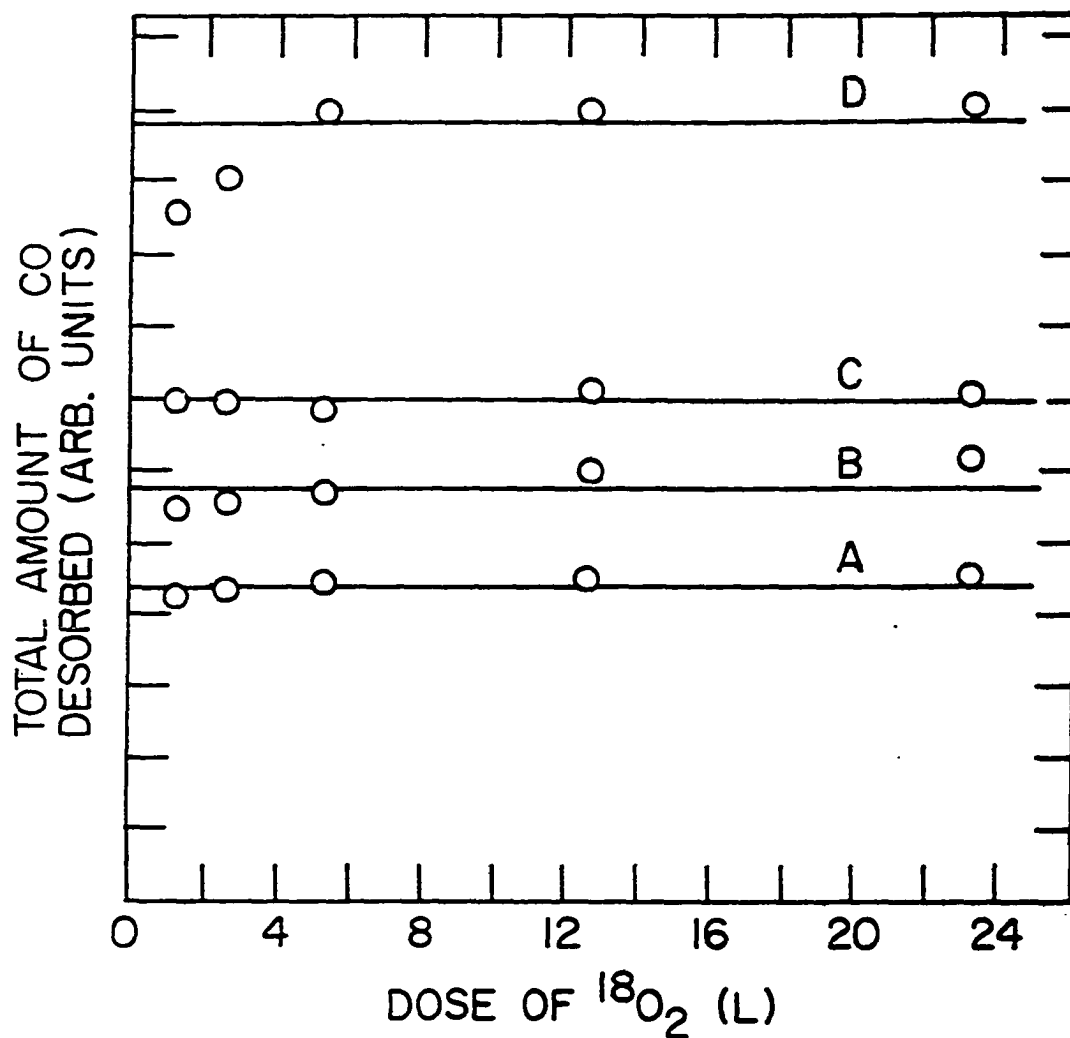
Fig. 10. Total amount of CO ($C^{16}O + C^{18}O$) desorbed from a W(100) surface where the surface was predosed with $C^{16}O$ (A - 2.4L, B - 4.5L, C - 9.0L and D - 18.2L) with increasing dosages of $^{18}O_2$ (1.2L, 2.6L, 5.3L, 10.7L and 21.3L) in each set of $C^{16}O$ doses.
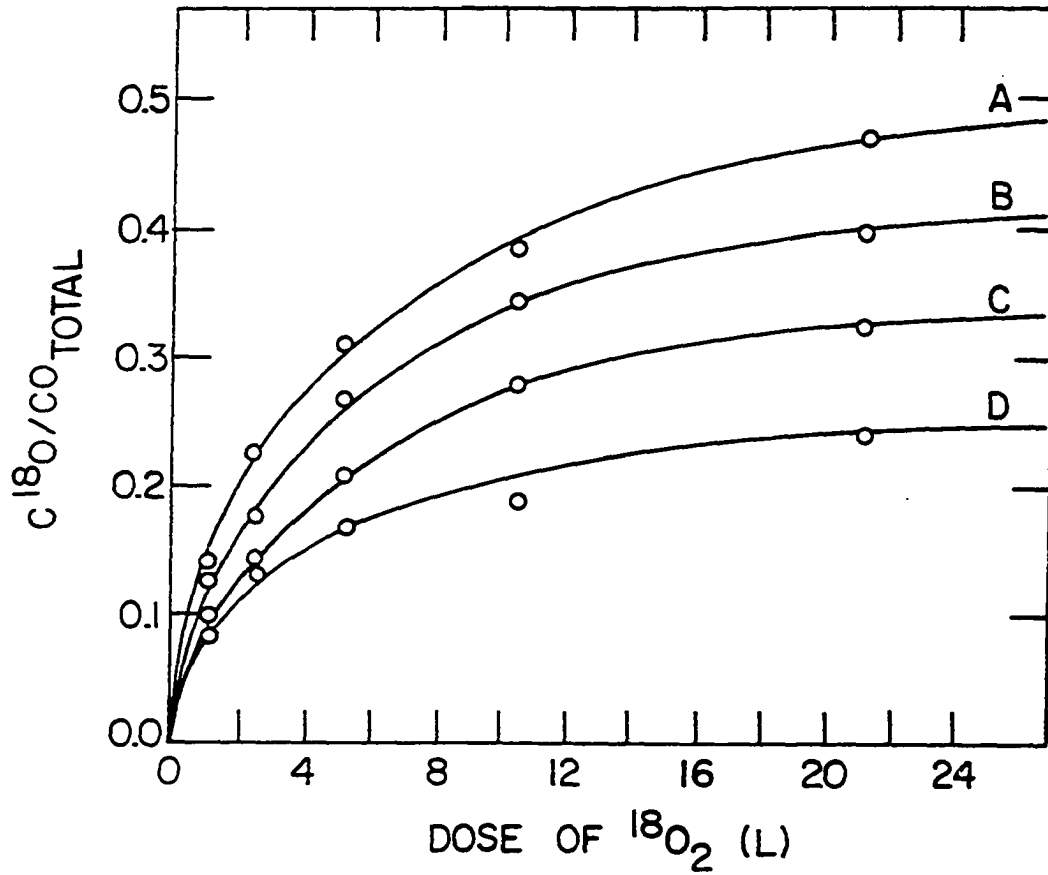
Fig. 11. The ratio of $C^{18}O/CO_{total}$ desorbed from a W(100) surface predosed with $C^{16}O$ (A - 2.4 L, B - 4.5 L, C - 9.0 L and D - 18.2 L) with increasing dosages of $^{18}O_2$ (1.2 L, 2.6 L, 5.3 L, 10.7 L and 21.3 L) in each set of $C^{16}O$ doses.
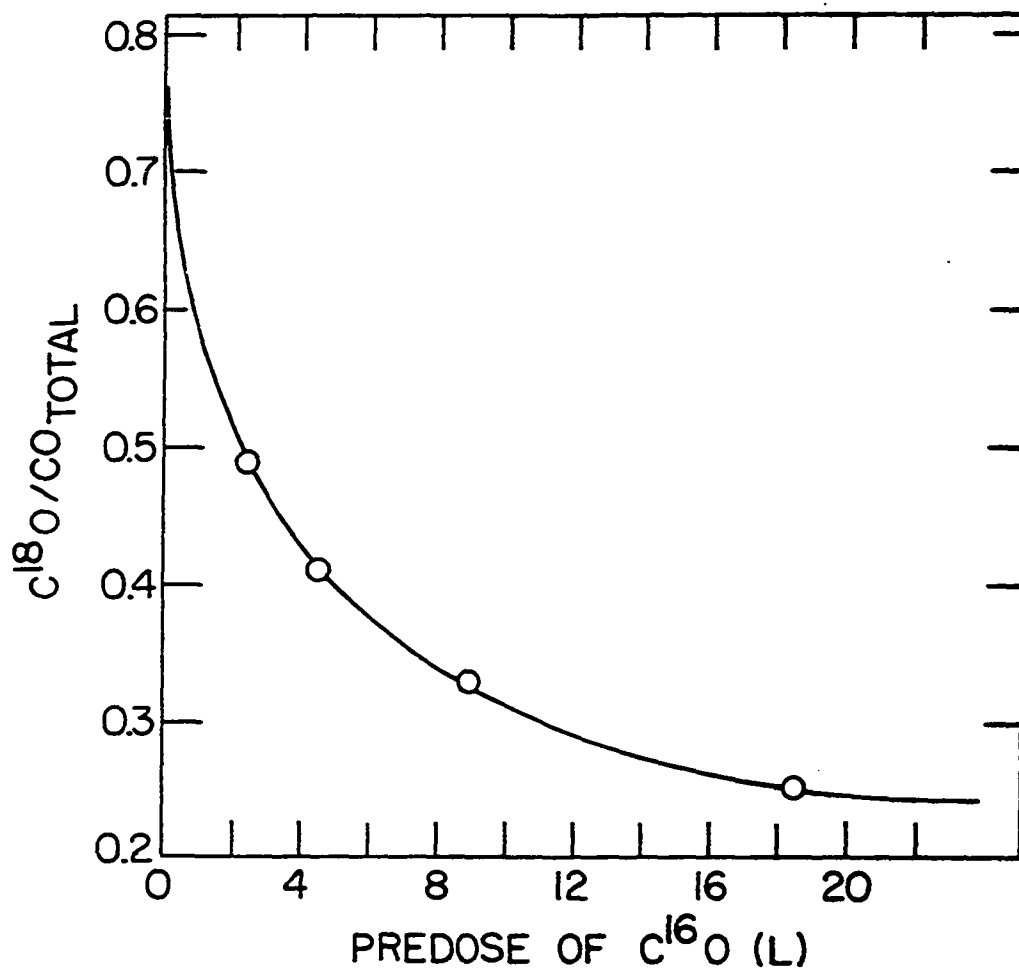
Fig. 12. The limiting ratio of $C^{18}O/CO_{total}$ desorbed from a W(100) surface predosed with $C^{16}O$ (2.4L, 4.5L, 9.0L, and 18.2L) followed by a saturated dose of $^{18}O_2$.

Before proposing a model which is consistent with the above results of mixed adsorption of $C^{16}O$ and $^{18}O_2$ on a W(100) surface, it would be appropriate to first summarize the experimental observations.

(1) The FDS spectra of CO desorbed from a W(100) surface exhibited three bonding states: α, β_1, and β_2. Because the amount of α desorbed was smaller than other reported results, it is assumed that only the more stable α_2 state was present on the W(100) surface.

(2) Preadsorbed CO was not displaced from the surface by dosing with $^{18}O_2$ (Fig. 10).

(3) The adsorption of $^{18}O_2$ on a CO covered surface eliminated the β_2 state of adsorbed CO. There was a small increase in CO desorbed in the α_2 state which appeared to reach a rather low limiting value. The fact the amount of CO desorbing in the α state does not continue to increase provides evidence that there is no conversion from an α state to β state. With increasing $^{18}O_2$ coverage, the temperature of maximum desorption for the β_1 state shifted to lower temperatures.

(4) From mixed adsorption of CO and $^{18}O_2$, isotopic exchange of oxygen occurred in the desorbed CO molecules primarily in the β_1 state and also to a very small extent in the α state at very high $^{18}O_2$ coverages.

(5) At very low preadsorbed coverages of CO followed by a

saturating dose of $^{18}O_2$, the ratio of $C^{18}O:CO_{total}$ desorbed appeared to reach a limiting value of $\sim.75$. At a saturated coverage of CO followed by a saturating dose of $^{18}O_2$, the ratio of $C^{18}O:CO_{total}$ appeared to reach a lower limiting value of $\sim.24$.

(6) With increasing coverages of preadsorbed $^{18}O_2$, it is possible to decrease the amount of CO which can be adsorbed on the surface. The β states are the first to be blocked by the preadsorbed $^{18}O_2$. As the sites for the β states are blocked, there is an increasing amount of CO desorbed in the α state, but at still higher $^{18}O_2$ coverages, the α state is also blocked for CO adsorption.

Goymour and King (17-19) have very recently published results for CO adsorption on polycrystalline tungsten from which they concluded CO was dissociatively adsorbed. They have proposed a model (17) based on the W(100) surface which was consistent with their kinetic and surface stoichiometric results from their polycrystalline work. The essence of the model proposed by Goymour and King is schematically illustrated in Fig. 13. They proposed that at room temperature a CO molecule would dissociate into C and O adatoms in the β state occupying the 5 CN sites marked A in Fig. 13. Nitrogen has been shown (Appendix B) to prefer the 5 CN site, and its 2p orbitals were influential in this preference; the carbon atom for the same reason should prefer this site. This is not, as shown in Appendix C, a
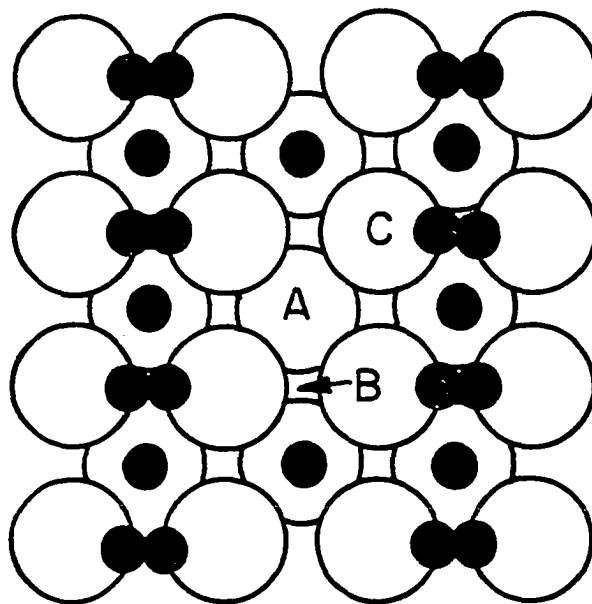
Fig. 13. Possible sites occupied by chemisorbed species resulting from co-adsorption of $C^{16}O$ and $^{18}O_2$ on a W(100) surface (A - 5 CN site, B - 2 CN site, C - 1 CN site, ● - C or O adatoms and ●● associatively adsorbed oxygen).

preferred site for oxygen adsorbing alone, but presumably the carbon

is able to influence the oxygen to select a 5 CN site when co-adsorbed

(the LEED results indicate that C and O must select the same kind of

site in CO adsorption). It has been shown (18) that, if the CO adsorption

occurs by dissociation into these sites and requires the availability of

5 CN sites in adjacent pairs, then random adsorption will lead to a

maximum coverage of CO in the β state in which only 85% of the

available 5 CN sites are occupied. It was proposed (18) that the

remaining 5 CN sites could adsorb an associated CO molecule in an α

state or two associated CO molecules in an α state at the 2 CN sites

(B in Fig. 13) adjacent to an empty 5 CN site. ESD (34, 37) has resolved

two α states; the low temperature α_1 state is labile (35) and yields a

CO^+ ion by ESD and the high temperature α_2 state yields an O^+ ion by

ESD. These two α states might well correspond to the two α sites

suggested by Goymour and King (18). Suppose the α_1 state is bonded

at site B and the α_2 state at site A in Fig. 13. In the former case

the carbon atom is presumably bonded to two tungsten atoms, and lies

above their plane. Its desorption as CO^+ on ESD seems likely. In the

latter case the carbon atom is coordinated to 5 tungsten atoms and is

nestled down into the plane of surface atoms. The bonding of carbon

to tungsten is presumed stronger, and to oxygen weaker, than at site B.

Loss of O^+ from this configuration on ESD seems reasonable. If the C

and O atoms from the dissociated CO molecule in the β state are bonded at the 5 CN sites, it is very probable that the electrons would not be able to desorb any ionic species. Yates and King (34) have reported that they were unable to desorb any ions by the ESD technique when only the β states are present on a W(100) surface.

The observations which have been summarized above can readily be explained based upon the above model for dissociatively adsorbed CO. The initial interaction of a CO molecule with the W(100) surface is probably at either a 1 CN or 2 CN site (C or B of Fig. 13). If two adjacent 5 CN sites (A of Fig. 13) are available then the CO molecule will dissociate into C and O adatoms at these sites. If only one 5 CN site is empty, we will assume that the CO will bond associatively at this site. The bonding state of CO observed in the flash desorption spectra of Fig. 4 from a W(100) surface can be assigned bonding sites based on the above model for CO adsorption. The CO desorbed in the β_1 and β_2 states would be C and O adatoms bonded at the 5 CN sites. The CO desorbed in the α state (α_2) would be associatively adsorbed CO molecules occupying the 15% of 5 CN sites not occupied by C and O adatoms. The fact that CO desorbed as two states β_1 and β_2 from C and O adatoms in the same sites can be explained by lateral interactions as has been done in other systems (H on W(100) and N in W(100)). When the CO desorbs from the surface, as the β_1 state, it will be

assumed to be occurring by the recombination of adjacent C and O adatoms. The remaining C and O adatoms are undergoing rearrangement to form a more stable surface structure, a β_2 state, which desorbs at a higher temperature. This explanation is also consistent with the LEED observations of Anderson and Estrup (36).

The results summarized above where oxygen was co-adsorbed on the surface to serve as a chemical probe add support to the model of dissociatively adsorbed CO; the isotopic mixing of the oxygen in the CO molecules desorbed in the β states is particularly significant.

Goymour and King (19) have shown by ESD that oxygen adsorbed onto a CO saturated surface seemed to be identical in population and ESD cross section to the $\beta_1 - O_2$ state formed by oxygen adsorption on clean W with oxygen preadsorbed in the β_2 state. Although it does not desorb as a molecular oxygen, it has been described as an associated adsorbed O_2 species (38-40) on a clean polycrystalline tungsten surface. The primary ESD product of this species is an O^+ ion. When heating the surface, this species undergoes a change which occurs between 600 and 900° K and the ESD product is no longer an O^+ ion.

From the above discussion, it can be assumed that the oxygen adsorbed on W(100) with preadsorbed CO is molecular oxygen. From ESD results on polycrystalline tungsten, this molecularly adsorbed state begins to dissociate at about 600-900° K. Therefore, as the β_1

state of CO desorbs at ~1060°K, the carbon atoms have a random

selection of the two isotopes of oxygen resulting in a mixture of $C^{16}O$

and $C^{18}O$ desorbed for the β states. The small amount of isotopic

mixing in the α_2 state could result from the possibility that the

associatively adsorbed CO in desorbing from a 5 CN site could interact

with a molecularly adsorbed oxygen; the probability of such interaction

should increase with increasing oxygen saturation and this is what is

observed.

The β_2 state of dissociated CO has been proposed as resulting

from C and O atoms in a C(2x2) structure formed after the β_1 state

has desorbed and the C and O atoms have rearranged to seek a more

stable bonding configuration. The presence of adsorbed oxygen could

prevent this rearrangement and therefore all the CO would be desorbed

at a temperature characteristic of the β_1 state. The presence of the

adsorbed oxygen with which the surface tungsten atoms must also bond

will cause those bonds between the tungsten atoms and those of the C

and O adatoms to be weakened. Therefore, as there is an increase of

oxygen adsorbed on a W(100) surface, preadsorbed CO (C and O adatoms)

bonds should be weakened, and the CO should desorb at lower

temperatures as observed.

Goymour and King (19) found that oxygen would displace part of

the α-CO from their polycrystalline tungsten surface which was

saturated with CO. They found no displacement of the CO desorbed in
the β state. In this study, oxygen did not displace any of the pre-
adsorbed CO on a W(100) surface (Fig. 10). According to the model
just presented, it would be difficult for the adsorbed oxygen which is
assumed to be occupying sites above the surface atoms to displace any
preadsorbed CO (which is assumed to be occupying 5 CN sites whether
associatively (α) or dissociatively (β) adsorbed). On the other hand, -
any CO preadsorbed in the more labile α_1-CO state might be displaced.
Goymour and King (19) reported the α-CO which was not displaced from
their polycrystalline surfaces shifted to a higher desorption temperature.
This supports the hypothesis of two bonding states of α-CO with the
α_2-CO being more stable and not displaced by the adsorbing oxygen.

In Fig. 9 it was observed that with an increasing preadsorbed
oxygen dose the adsorption of CO in the β states was decreased while
adsorption in the α_2 state was mutually increased. According to our
model, the β states are dissociated and a pair of vacant adjacent 5 CN
sites is needed to adsorb β-CO. Oxygen preadsorption will reduce
adjacent pairs of empty sites much more than single sites (which suffice
for associative α_2-CO adsorption) and therefore as observed a decrease
in CO desorbed as β and increased in α-CO. With increased coverages
of oxygen, even these sites were blocked for CO adsorption and at a
saturated coverage of oxygen, the surface should be blocked to any CO

adsorption.

By an assessment of sites available for adsorbed α-CO, β-CO
and $^{18}O_2$ it is possible to offer an explanation for the limiting ratio of
$C^{18}O:CO_{total}$ which is desorbed from the surface. It has been assumed
that the β states of adsorbed C and O atoms occupy 5 CN sites. With a
low initial CO dose, the C atom will have one adjacent 5 CN site occupied
by its initial oxygen partner and three empty adjacent sites. It can also
be assumed that, as the $^{18}O_2$ adsorbs on this tungsten surface with low
coverage of adsorbed CO, it dissociates and will be influenced by the C
adatoms to occupy the surrounding three empty 5 CN sites. Then as the
CO desorbed, the C atom will have a choice of one ^{16}O and three ^{18}O
atoms with which to combine. This should lead, at very low CO cover-
ages, to a ratio of 3:4 (.75) for the $C^{18}O:CO_{total}$ desorbed from the
surface, and this is what Fig. 11 shows. At saturated coverages of CO,
Goymour and King (18) determined that about 15% of the 5 CN sites
capable of adsorbing C and O atoms from dissociated CO were not
occupied. These sites have adjacent 5 CN sites which are occupied,
resulting from random adsorption.

On a tungsten surface which is saturated with preadsorbed CO,
the β-CO is in the form of C and O adatoms at 5 CN sites in a (1 x 1)
surface structure. A saturated dose of $^{18}O_2$ upon this C and O adatom
layer results in co-adsorption and as reported above, oxygen is

molecularly bonded to the surface. The most reasonable structure for such a chemisorbed species is one bridging from site C to site C (Fig. 13). Each oxygen will be bonded to a single tungsten atom, and a single bond will exist between the oxygen atoms. The co-adsorbed oxygen molecules could easily occupy every other set of surface atoms in every row. This (2×1) structure of associatively adsorbed $^{18}O_2$ is formed on the surface (Fig. 13).

Therefore, from a surface with saturated preadsorbed CO followed with a dose of saturating $^{18}O_2$, 15% of the CO desorbed is α-$C^{16}O$ from associatively adsorbed CO. The remaining 85% of the 5 CN sites are occupied by C and O adatoms in a (1×1) structure. This (1×1) unit mesh defines a surface structure of one adatom per unit mesh and assuming LEED can not distinguish between C and O adatoms, then the (1×1) structure contains either one carbon or one oxygen atom. It would require two unit meshes (2×1) to contain a CO molecule. If the C adatom in this structure will recombine only with O adatoms, then the carbon has a choice of ^{16}O and ^{18}O if the associatively adsorbed $^{18}O_2$ has dissociated at the temperatures of β-CO desorption. If the co-adsorbed oxygen dissociates according to

$$\underset{*}{\overset{O}{\diagup}} - \underset{*}{\overset{O}{\diagdown}} \rightleftarrows 2 \underset{*}{\overset{O}{|}}$$
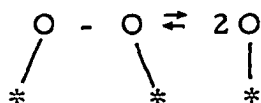
then, as assumed, each (2×1) unit mesh should contain three oxygen

atoms ($^{16}O + 2^{18}O$) and one carbon atom. It is very unlikely that the above dissociation is complete when β-CO desorbs. If one-half the oxygen molecules have dissociated, coupled with the probability that only one-half of these are dissociating next to a C adatom, then the carbon has a choice of oxygen isotopes in the ratio of $^{16}O:^{18}O$ which is 1:.5. Therefore, from the 85% of the sites occupied by C and O adatoms, 57.5 molecules of CO will be desorbed from every 100 sites occupied. Based upon the above assumptions, one-third of these CO molecules would be $C^{18}O$. From the arguments above, the limiting ratio of $C^{18}O:CO_{total}$ desorbed should be $\sim$.24 which compares well with the value of $\sim$.23 determined from Fig. 12.

Mixed adsorption of CO and $^{18}O_2$ on a W(110) surface

The flash desorption spectra of CO from a W(110) surface are shown in Fig. 14. At low coverages only a β state is present which desorbs at $\sim$ 1100°K. As the coverage increases, an α state desorbing at a much lower temperature ($\sim$400°K) appears and the β state increases and appears to split into 2 states, β_1 and β_2, desorbing at $\sim$ 920°K and $\sim$1100°K respectively. In the present study, $^{16}O_2$ occasionally was found in the ambient when heating the crystal to higher temperatures for cleaning. It was also observed that the size of the β_1 state depended upon the amount of $^{16}O_2$ which appeared in the ambient. This dependence is depicted in Fig. 15 which indicates that the splitting

46
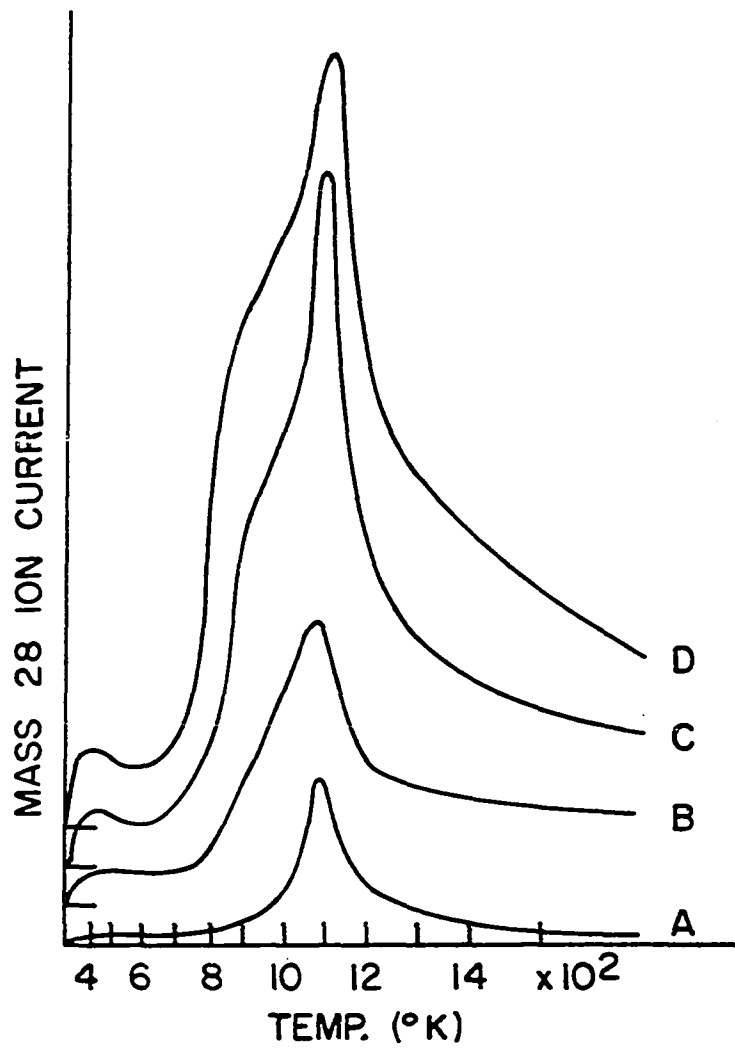
Fig. 14. Flash desorption spectra of CO adsorbed on a W(110) surface
(A - 2.5 L, B - 4.4 L, C - 9.2 L and D - 18.6 L).

47
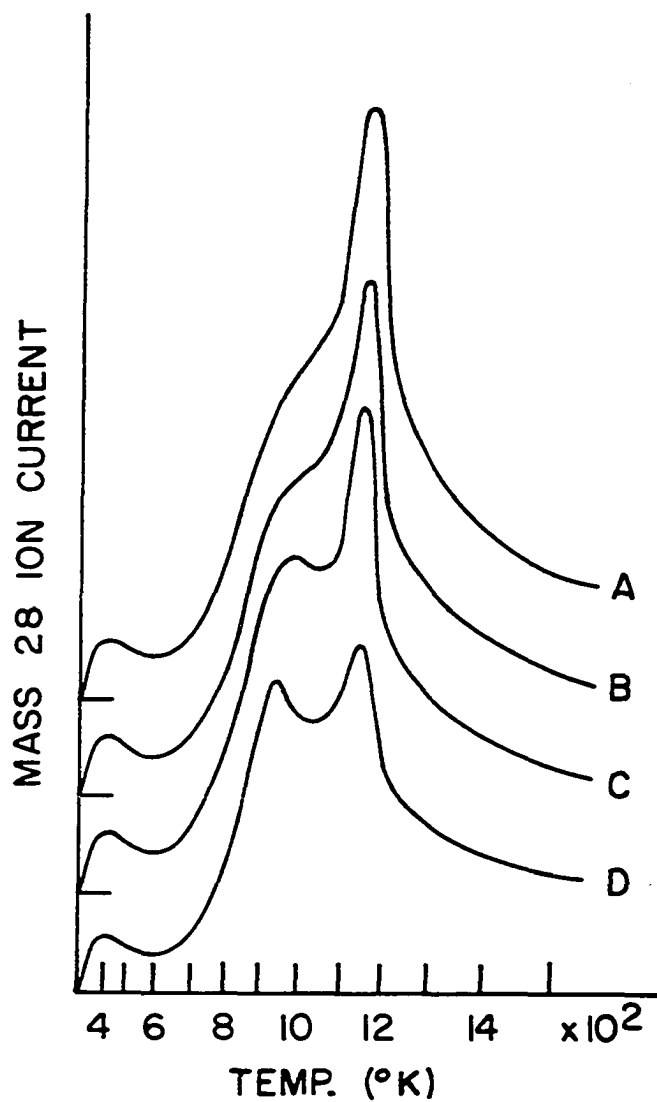
Fig. 15. Flash desorption spectra of CO from a W(110) where CO was dosed (18.6L) simultaneously with $^{18}O_2$ (A - ~.05L, B - .15L, C - .60L and D - 1.80L) from the ambient.

of the β state into β_1 and β_2 results from interactions of co-adsorbed species on the surface.

May and Germer (41) reported two peaks in their flash desorption spectra of CO from a W(110) surface, a β state at $\sim 1100°$K and an α state at $\sim 450°$K. Kohrt and Gomer (42) observed, in their step desorption spectra from CO adsorbed on a W(110) surface at 100°K, a virgin state (v) desorbing at $\sim 390°$K and two β states, β_1 desorbing at $\sim 980°$K and β_2 desorbing at $\sim 1120°$K. From their findings, they concluded that heating the surface to 400-600°K after it was saturated with virgin CO caused some of the CO to desorb, but that some of the virgin CO was converted irreversibly to the β states. They reported that the surface was able to accommodate approximately one-half the number of CO molecules in beta configurations as in virgin configuration. After formation of the beta layer, they report that additional CO could be adsorbed on the surface at 100°K. In their step desorption spectra this CO desorbed at $\sim 150°$K and at $\sim 300°$K. They labeled these states α_1 and α_2 respectively.

In the mixed adsorption experiments of CO followed by $^{18}O_2$ (Figs. 16-19), it was observed that as the amount of $^{18}O_2$ dosed on the surface increased, the β_2 state was gradually displaced until all the CO desorbed as the β_1 state. The temperature of maximum desorption for the β_1 state even shifted to lower temperature as the amount of
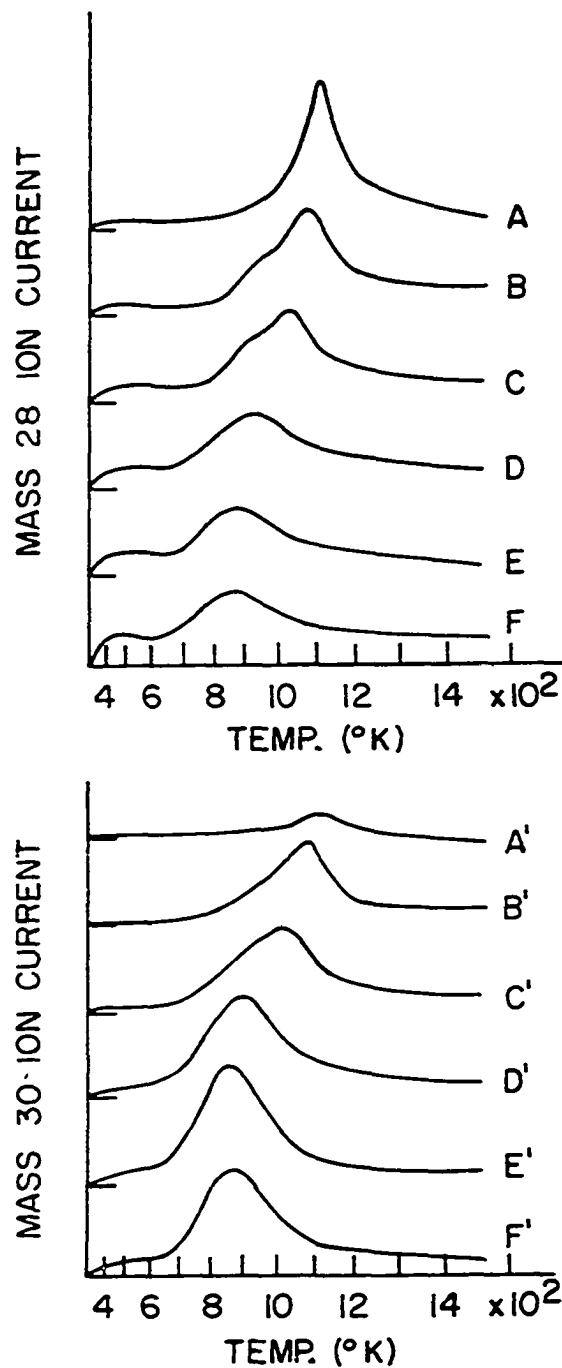
Fig. 16.   Flash desorption spectra of CO from a W(110) surface
predosed with 2.5 L of $C^{16}O$ followed with increasing dosages
of $^{16}O_2$ (A - 0.0 L,   B - 1.2 L,   C - 2.6 L,   D - 5.3 L,   E - 10.7 L
and F - 21.3 L).
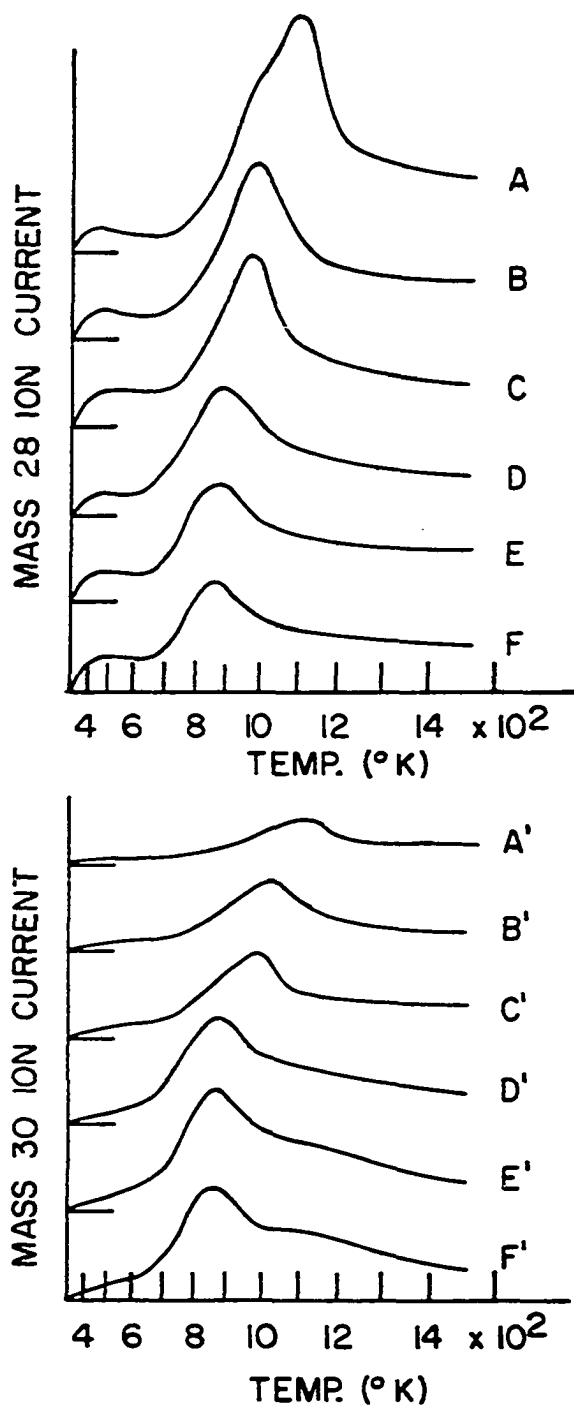
Fig. 17.   Flash desorption spectra of CO from a W(110) surface
predosed with 4.4L of $C^{16}O$ followed with increasing dosages
of $^{18}O_2$ (A - 0.0L, B - 1.2L, C - 2.6L, D - 5.3L, E - 10.7L
and F - 21.3L).
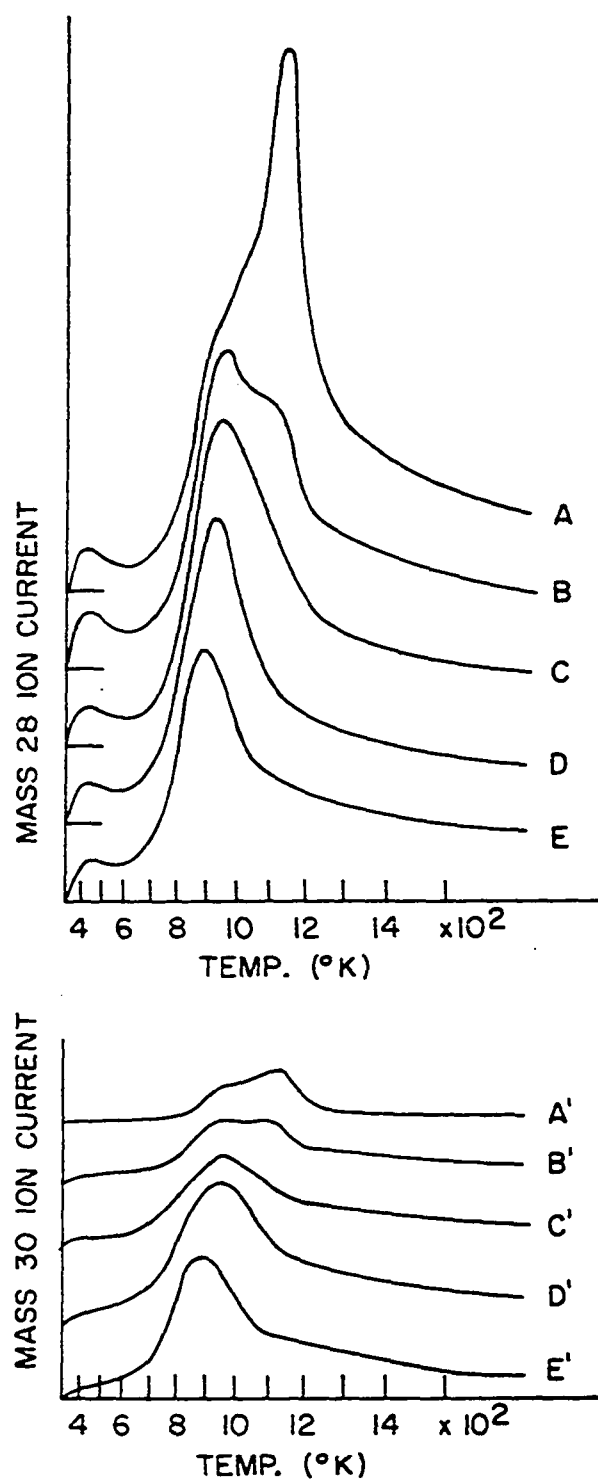
Fig. 18. Flash desorption spectra of CO from a W(110) surface
predosed with 9.2L of $C^{16}O$ followed with increasing dosages
of $^{18}O_2$ (A - 0.0L, B - 1.2L, C - 2.6L, D - 5.3L, E - 10.7L
and F - 21.3L).

52
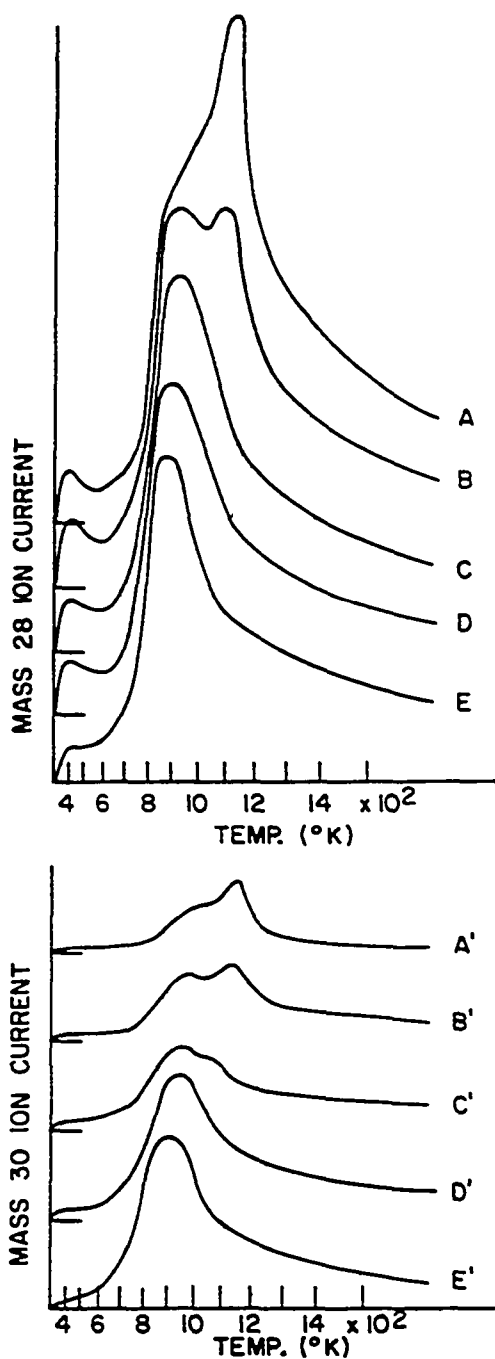
Fig. 19. Flash desorption spectra of CO from a W(110) surface predosed
with 18. 6L of $C^{16}O$ followed with increasing dosages of $^{18}O_2$
(A - 0.0L, B - 1.2L, C - 2.6L, D - 5.3L, E - 10.7L and
F - 21.3 L).

$^{18}O_2$ on the surface increased. As the amount of $^{18}O_2$ on the surface

increased following the predose of CO, there was no large increase in the

amount of CO desorbed in the α state. Such an observation would have

been expected if α-CO was being converted to β-CO by heating the

surface during the flash desorption.

Figures 16-19 also show that isotopic mixing of the oxygen in

the CO molecules desorbed from the β states is extensive, but that it

is negligible in those desorbed from the α state. In a given experiment

the CO molecules ($C^{16}O$ and $C^{18}O$) desorb simultaneously as evidenced

by their substantially identical FDS temperatures of peak maxima.

If the surface is predosed with $^{18}O_2$, the oxygen is able to block

the adsorption of CO. In Fig. 20, a small dose of $^{18}O_2$ (curve A)

displaces the β_2 state first and causes a slight increase in the amount

of CO desorbed in the α state. With larger doses of $^{18}O_2$, the amount

of CO desorbed from the surface decreases and the temperature of

maximum desorption of the β_1 state is again shifted to lower

temperatures until finally it is almost impossible to adsorb any CO on

the oxygen covered surface. Figure 20 also illustrates the desorption of

$C^{18}O$ in these experiments. It is observed that as the $^{18}O_2$ dosed

increases the amount of $C^{18}O$ desorbed first increases (curves A - C of

Fig. 20), then decreases (curves C-D) because the amount of CO on the

surface decreases. There is almost no $C^{18}O$ desorbed from the
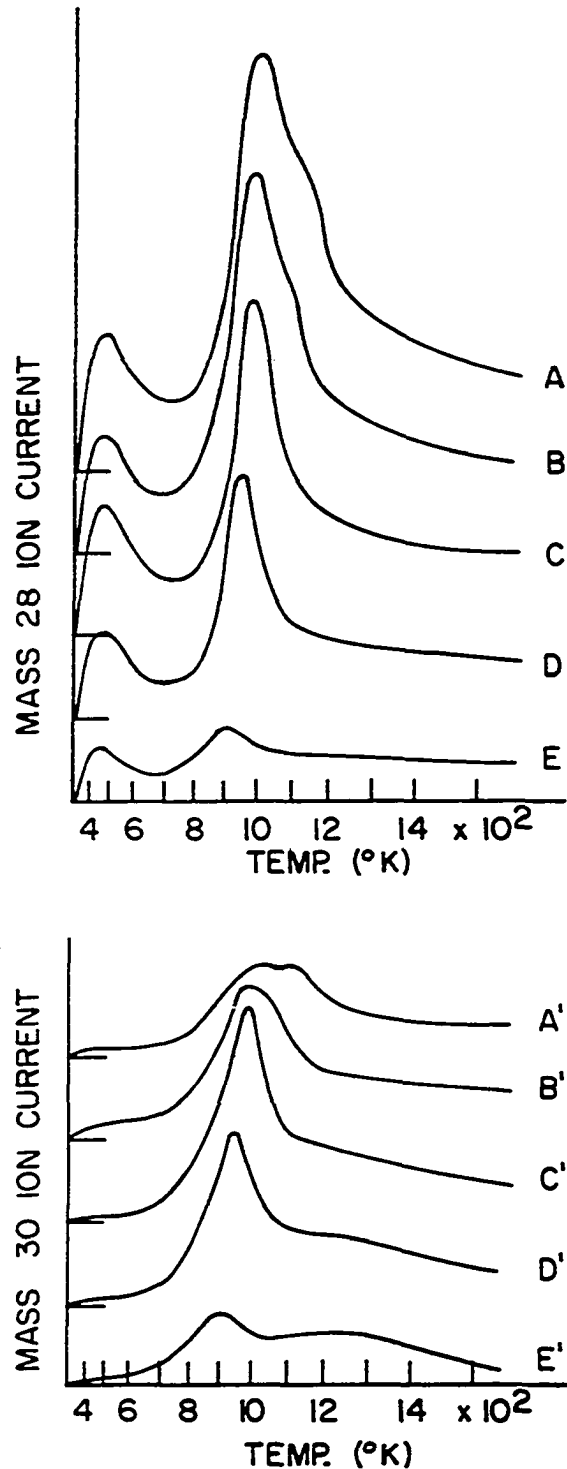
Fig. 20. Flash desorption spectra of CO form a W(110) surface predosed with increasing dosages of $^{18}O_2$ (A - 1.2L, B - 2.6L, C - 5.3L, D - 10.7L, and E - 21.3L) followed by a constant dose of $C^{16}O$ (9.2L).

surface as α-CO.

The total amounts of CO desorbed from the W(110) surface in each of the experiments as determined from the area under flash desorption curves are plotted in Fig. 21. A constant amount of CO is desorbed from the surface after being predosed with a constant amount of CO followed by increasing coverages of $^{18}O_2$; this proves that the oxygen is not able to displace any of the CO adsorbed on the surface at room temperature.

The ratios of $C^{18}O:CO_{total}$ desorbed from the surface in each of the experiments (Figs. 16-19) are plotted in Fig. 22. In each experiment, there appears to be a limiting ratio of $C^{18}O:CO_{total}$ desorbed. The limiting ratios for each of the four sets of experiments are plotted in Fig. 23. At low coverages of preadsorbed CO followed by a saturated dose of $^{18}O_2$, the limiting ratio is $\sim.5$ and for a surface saturated with preadsorbed CO followed by a saturated dose of $^{18}O_2$, the limiting ratio is $\sim.25$.

The above results will be summarized before proposing a consistent model.

(1) CO adsorbed on a W(110) surface at room temperature desorbs as an α-state at $\sim 400°$K and as two β states, β_1 at $\sim 920°$K and β_2 at $\sim 1100°$K. The separation into two states appears to result from interactions of co-adsorbed species on the surface.
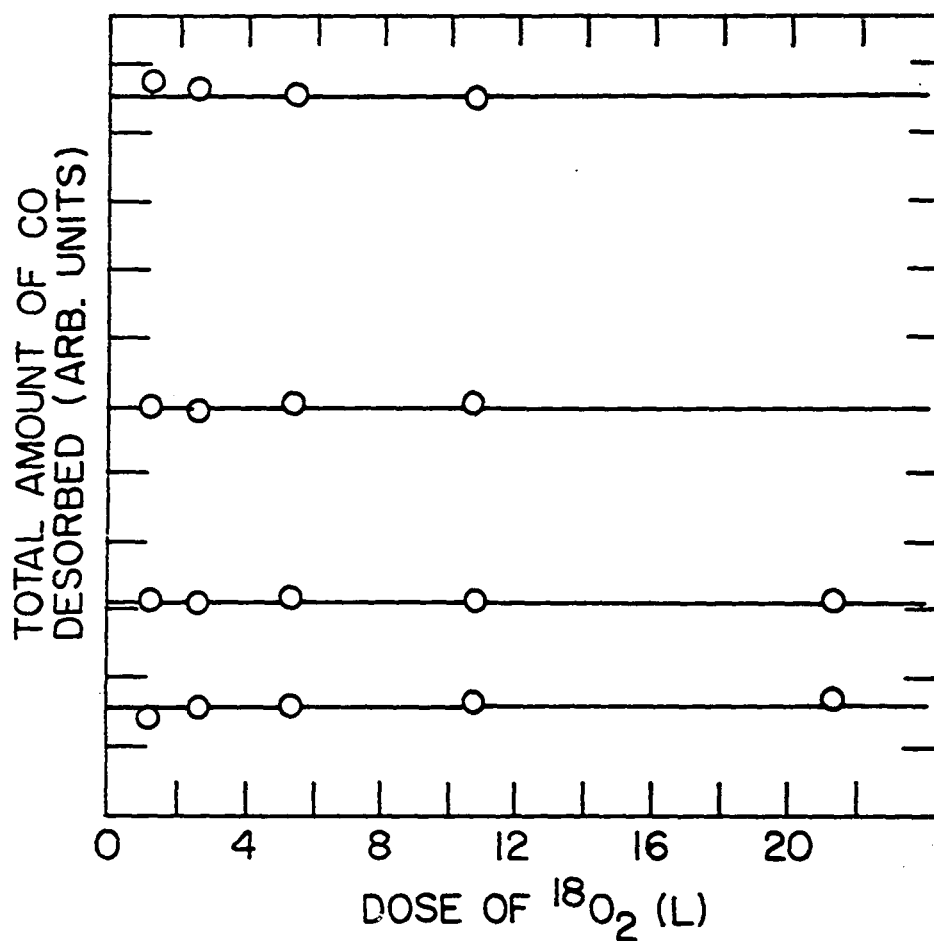
Fig. 21. Total amount of CO ($C^{16}O + C^{18}O$) desorbed from a W(110) surface where the surface was predosed with $C^{16}O$ (A - 2.5 L, B - 4.4L, C - 9.2L and D - 18.6L) with increasing dosages of $^{18}O_2$ (1.2L, 2.6L, 5.3L, 10.7L and 21.3L) in each set of $C^{16}O$ doses.
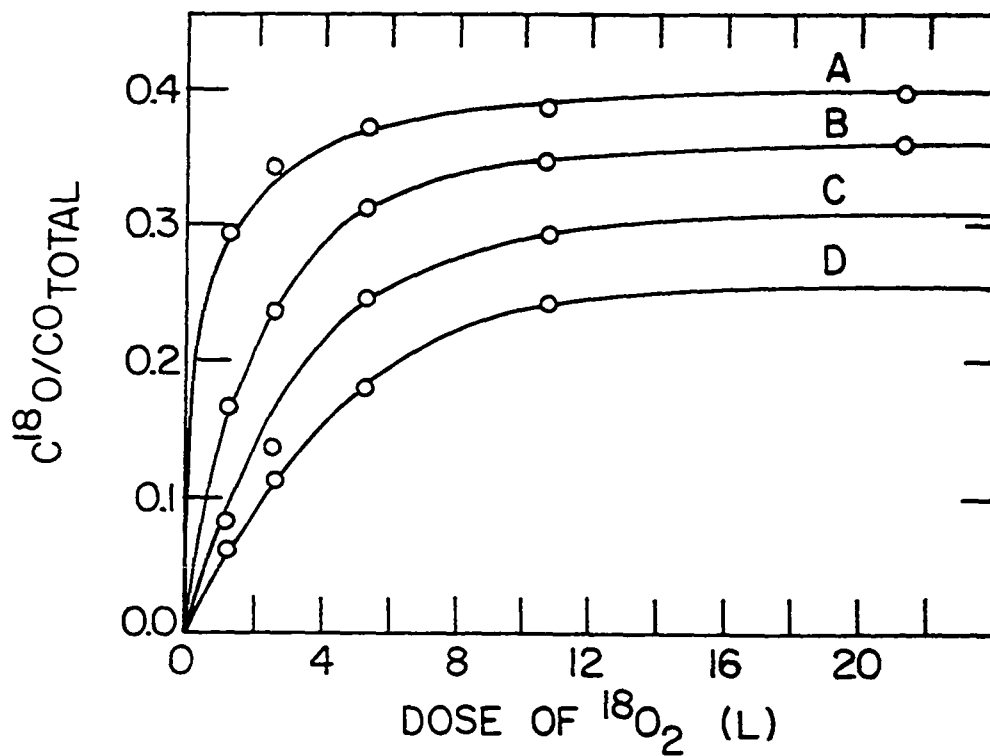
Fig. 22. The ratio of $C^{18}O/CO_{total}$ desorbed from a W(110) surface predosed with $C^{16}O$ (A - 2.5 L, B - 4.4 L, C - 9.2 L and D - 18.6 L) with increased dosages of $^{18}O_2$ (1.1 L, 2.4 L, 5.3 L, 10.6 L and 21.2 L) in each set of $C^{16}O$ doses.
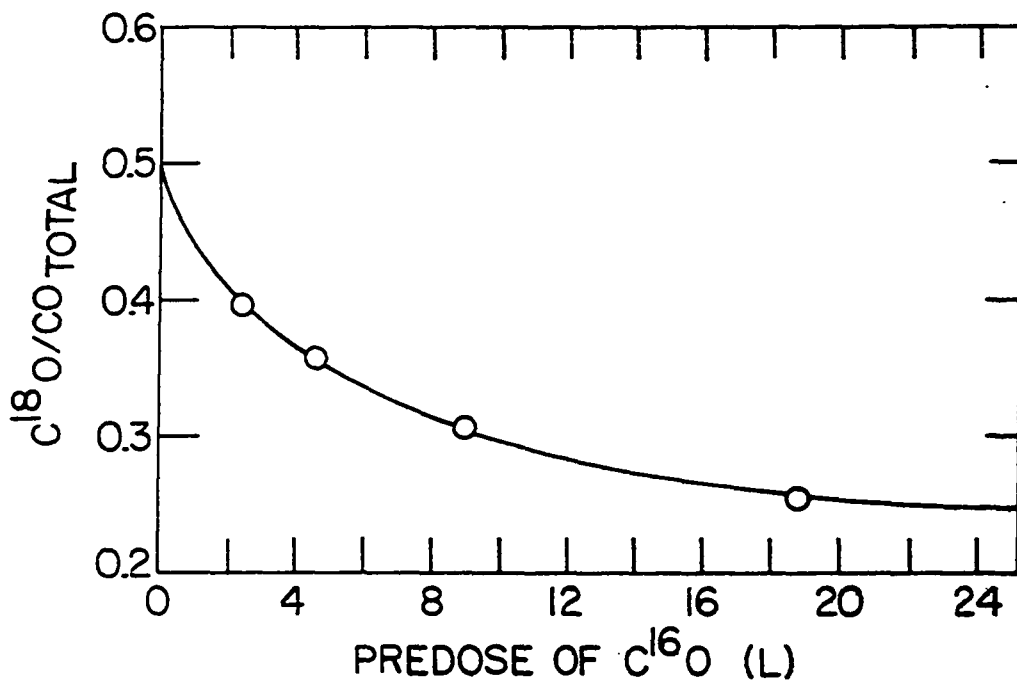
Fig. 23. The limiting ratio of $C^{18}O/CO_{total}$ desorbed from a W(110) surface predosed with $C^{16}O$ (2.5L, 4.4L, 9.2L and 18.6L) followed by a saturated dose of $^{18}O_2$.

(2) Preadsorbed CO was not displaced from the surface by dosing with $^{18}O_2$ nor was there any extensive increase in the amount of CO desorbed in the α state. The lack of such an observation suggests no conversion is occurring between adsorbed states.

(3) Mixed adsorption of CO and $^{18}O_2$ results in isotopic mixing of the oxygen in the CO molecules desorbed from the β states and very little mixing in the CO molecules desorbed in the α state.

(4) From a low coverage of CO followed with a saturated coverage of $^{18}O_2$, the limiting ratio of $C^{18}O:CO_{total}$ desorbed from the surface is $\sim.5$ and from a saturated coverage of CO and $^{18}O_2$, the limiting ratio is $\sim.25$.

(5) A surface saturated with preadsorbed $^{18}O_2$ first preferentially blocks CO adsorption in the β state and slightly increases the amount of CO desorbed as α-CO (Fig. 20). As the amount of preadsorbed $^{18}O_2$ was increased, the amount of CO adsorbed in all states decreased.

The above results suggest a model for adsorption of CO on the W(110) surface similar to that for the W(100) surface. The CO which desorbs in the β states, where there is extensive isotopic mixing of the oxygen when it is co-adsorbed with $^{18}O_2$, will be assumed to be in the form of C and O adatoms. The CO desorbed as the α state is proposed to be associatively adsorbed CO. In the flash desorption of

the adsorbed CO, a point of concern is the conversion of α-CO to the

β-CO by the heating process. If the CO were preadsorbed associatively

on the surface, the co-adsorbed $^{18}O_2$ should be able to block the sites

for the conversion of α-CO to β-CO. Since increasing doses of $^{18}O_2$

on a surface with preadsorbed CO leads to no increase in the amount of

CO desorbing in the α state, it appears that there is no conversion

from an associatively adsorbed CO in an α state to a β state.

The above model should also be consistent with other reported

results for the adsorption of CO on the W(110) surface. Kohrt and

Gomer (42) reported the formation of a virgin state, when dosing a

W(110) surface at a temperature of 100°K or lower with CO. In a step

desorption experiment, virgin CO desorbed at 200-450°K, followed by

the desorption of two beta states, β_1 at ~970°K and β_2 at ~1120°K.

Because of the complex kinetics observed from the desorption of the

virgin state, they suggested there was competition between desorption

and conversion to β state, with the latter predominating at low θ.

If after forming the virgin state by dosing a surface at 100°K or less,

they heated the surface to only 450-600°K where all the virgin state had

desorbed, they were then able to readsorb CO forming a new state.

This state was different from the original low temperature virgin

state and was labeled α. It desorbed as α_1 at ~150°K and α_2 at

~300°K. This also supports the hypothesis that the CO adsorbed in

the virgin state is converted irreversibly to the β states.

In view of the model proposed for dissociative adsorption of CO, it must be reasoned that the W(110) surface at $\sim 100°K$ is not able to dissociatively adsorb CO. Therefore, it adsorbs the CO associatively as virgin CO, but when the surface is heated to 450-600°K where half of the virgin CO desorbs, the remaining CO dissociates to C and O adatoms. Tungsten with this chemisorbed layer is able to adsorb additional CO associatively as the α states observed by Kohrt and Gomer (42). In this study, the CO was dosed on a W(110) surface at room temperature, and as observed the β states formed immediately and were not formed by the conversion of associative adsorbed CO molecules. With larger doses of CO, as the β states were saturated, a small amount of CO adsorbed associatively (no isotopic mixing) as an α-CO. This compares with the α_2-CO state desorbed at $\sim 300°K$ observed by Kohrt and Gomer.

On the W(110) surface there are three symmetric sites available for the chemisorbed species. These sites are indicated in Fig. 24. At site A, a chemisorbed species could possibly be coordinated to four surface atoms. Although two of the surface atoms are farther away, the two nearer surface atoms are separated by the same distance as those forming a 2 CN site on the W(100) surface. Although the two tungsten atoms are touching at site B, a chemisorbed

Fig. 24. Possible sites occupied by chemisorbed species from co-
adsorption of CO and $^{18}O_2$ on a W(110) surface (A - 2 CN
site, B - 2 CN' site, C - 1 CN site, ● - C or O adatoms
and ●● - associatively adsorbed oxygen).

species could be coordinated to these surface atoms. At site C, a chemisorbed atom would be coordinated to a single surface atom.

May and Germer (41) reported a C(9x5) pattern from a W(110) surface with CO adsorbed in the β state. Such patterns are of very little help in assigning possible sites and stoichiometry for the adsorbed species. In a LEED study of oxygen on the W(110) surface, Tracy and Blakely (21) reported that atomically chemisorbed oxygen produced a p(2x1) pattern. This structure corresponds to one-half a monolayer of oxygen atoms. The p(2x1) structure can be produced by the O adatoms occupying every other row of sites A as marked in Fig. 24. With the O adatoms in this surface structure, the bonding shows great similarity to the bonding of O adatoms at 2 CN sites on the W(100) surface where it produced a (2x1) LEED pattern. In the (2x1) structure on W(100), each O adatom was bonded to two surface tungsten atoms, and these tungsten atoms were not bonded to any other O adatoms. If the O adatoms on a W(110) surface occupied the proposed sites indicated in Fig. 24, then each oxygen atom would also be bonded to two of the surface tungsten atoms, and these two tungsten atoms would not be directly involved in the bonding of O adatoms at adjacent sites. At full oxygen coverage, each tungsten atom would be bonded to a single oxygen atom which is consistent with the bonding model also proposed for the W(100) surface. The carbon atom should

seek a site of the highest coordination number possible to satisfy its multi-valency. On the W(110), this would be site A (Fig. 24). Therefore, it is very likely that the C adatoms would occupy the same sites as the O adatoms.

In dissociative adsorption of CO on the W(110) surface, the C and O adatoms should occupy every other row of sites A (Fig. 24). In order to observe $C^{16}O$ and $C^{18}O$ as desorbed CO molecules, it must be possible to adsorb $^{18}O_2$ upon a W(110) surface with preadsorbed $C^{16}O$. And as indicated by the plots in Fig. 21, the adsorbed $C^{16}O$ is not displaced by the adsorption of $^{18}O_2$. Therefore, the $^{18}O_2$ must be co-adsorbed with the preadsorbed CO. As was concluded for the W(100) surface, it will be assumed that the $^{18}O_2$ will be associatively adsorbed. The adsorbed $^{18}O_2$ could be bridged across site A bonding to the two distant tungsten atoms. The adsorbed oxygen could be occupying every other site A between the rows of C and O adatoms. The sum of the amount of CO desorbed in the β_1 and β_2 states is a constant in a set of experiments where the same predose of $C^{16}O$ is followed by increased $^{18}O_2$ coverages. The shift in the desorption of the β-CO all to β_1-CO (lower temperature state) is not likely to result from site changes of C and O adatoms, but rather from weakened bonds between surface atoms of tungsten and the C and O adatoms due to the co-adsorbed $^{18}O_2$. At the temperatures where

the β_1-CO desorbs, the associatively co-adsorbed $^{18}O_2$ will be dissociating and the O adatoms will want to occupy sites A between the rows of C and O adatoms. Therefore, every tungsten atom would be coordinated to two adatoms, a structure certainly not as stable as the previous structure where every tungsten atom was coordinated to only one adatom.

In Fig. 15 the presences of two β states in flash desorption spectra were attributed to co-adsorbed $^{16}O_2$ which was noticed to be varying in the ambient. In fact it is very likely that the β_1 state exists only as a result of some co-adsorbed species (not necessarily always oxygen). The β_1 state could desorb from the surface where the C and O adatoms are co-adsorbed with $^{18}O_2$ according to the above bonding scheme where co-adsorbed species are trying to occupy all of the A sites available (Fig. 24). The β_2 state could be assumed to result from the surface were only C and O adatoms are bonded in the p(2x1) structure. The co-adsorption could also account for the C(9x5) LEED pattern reported by May and Germer (41), because May, Germer and Chang (43) later reported a C(11x5) LEED pattern resulting from experiments of known co-adsorption of oxygen and carbon monoxide on the W(110) surface.

When the surface was predosed with increasing amounts of $^{18}O_2$, followed with constant doses of $C^{16}O$, the amount of $C^{16}O$

adsorbed on the surface decreases. In Fig. 20, it is observed that a surface with preadsorbed oxygen has a larger amount of CO desorbing in the α state than in any experiment (Figs. 15-18) where the surface was predosed with $C^{16}O$. It should also be noted, even in the $^{18}O_2$ predosed surfaces followed with a dose of $C^{16}O$, that there is no $C^{18}O$ desorbed in the α state. The CO desorbed in the β states is desorbed primarily as β_1 with isotopic exchange of the oxygen occurring. The increase in the amount of α-CO desorbed from the surface where the CO was dosed on a surface with preadsorbed $^{18}O_2$ occurred as a result of the O adatoms blocking sites for dissociation by the depletion of adjacent empty A sites, but allowed single A sites to exist for associatively adsorbed CO.

At very small coverages of preadsorbed $C^{16}O$, it should be possible to complete the p(2x1) structure with ^{18}O adatoms. In the limiting case of small coverages, the C and ^{16}O adatoms from the dissociated CO molecule should occupy adjacent sites in the p(2x1) structure, and remaining sites in this structure should be occupied by ^{18}O adatoms. As the carbon atoms desorb, it then has a choice of two O adatoms, one ^{18}O and the other ^{16}O. Therefore, the limiting ratio of $C^{18}O:CO_{total}$ desorbed from a surface in the case of a low coverage of CO and saturated with $^{18}O_2$ should be .5, which compares remarkably well with the value determined from the plot in Fig. 23.

When CO adsorbs on the surface and dissociates into C and O

adatoms, it is necessary to have two adjacent sites vacant. On the

W(110) surface, the C and O adatoms were assumed to occupy every

other row of A sites (Fig. 24). Random dissociative adsorption of CO

according to the above hypothesis results in ~25% of the A sites on the

W(110) surface not having empty adjacent sites (44). The α-CO

(associatively adsorbed CO) will be assumed to be bonded at these

sites. A p(2x1) surface structure was assumed to result from C and O

adatoms from dissociatively adsorbed CO. One-half a molecule would

be adsorbed per unit cell or one molecule in a p(2x2) structure. If

$^{18}O_2$ were dosed on a surface of saturated preadsorbed CO, the

co-adsorbed $^{18}O_2$ could occupy every other site in the rows between

the C and O adatoms (Fig. 24); these oxygen molecules would also

produce a p(2x2) structure or one molecule per unit cell of this

structure. Upon heating the surface in a flash desorption experiment,

the dissociation of adsorbed molecular $^{18}O_2$ occurs according to

$$\underset{*}{\overset{O}{\diagup}} - \underset{*}{\overset{O}{\diagdown}} \rightleftharpoons 2\underset{*}{\overset{O}{\big|}}$$
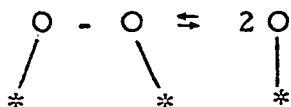
It will be assumed a C adatom can recombine only with an O

adatom for CO desorption. According to the above bonding scheme,

there is a C and ^{18}O adatom per p(2x2) unit mesh and the associatively

co-adsorbed $^{18}O_2$ also formed a p(2x2) unit mesh. Therefore, each

p(2x2) unit mesh has C and ^{16}O adatoms and a molecule of $^{18}O_2$. The probability of an adsorbed $^{18}O_2$ is near the C adatom is .5 and coupled with the assumption only one-half of the $^{18}O_2$ molecules have dissociated at the temperature where CO desorbs results in the C adatom having a choice of oxygen isotopes in the ratio $^{16}O : ^{18}O$ of 1 : .5. The resulting ratio of $C^{16}O : C^{18}O$ desorbed from the β state should be 2 : 1. Therefore, from a surface with a saturated predose of $C^{16}O$ followed by a saturating $^{18}O_2$ dose, 25% of the CO will desorb as associatively adsorbed $C^{16}O$. From 100 sites, the remaining 75 sites should desorb 37.5 molecules of CO as the β state. From the above ratio one-third should be $C^{18}O$ or the limiting ratio of $C^{18}O : CO_{total}$ would be .20. This ratio estimated from Fig. 22 is ~.24.

The above discussion can be summarized very briefly. The isotopic mixing of the oxygen in the desorbing CO molecules can best be interpreted in terms of a model for dissociative adsorption of CO. If the adsorbed CO is in the form of C and O adatoms, it is very understandable why adsorption of oxygen does not displace any preadsorbed CO. The bonding of the C and O adatoms at sites A in Fig. 24 to produce a p(2x1) structure explains the limiting ratio of $C^{18}O : CO_{total}$ desorbed at low CO coverages and is consistent with bonding models for chemisorbed species presented in Chapter II.

Mixed adsorption of CO and $^{18}O_2$ on a W(111) surface

The flash desorption spectra of CO adsorbed on a W(111) surface are plotted in Fig. 25. The CO desorbs in two states, a β state at ~1050°K and an α state at ~450°K. These two states desorb as very sharp symmetric peaks, an indication of the absence of any other states present on the surface. The desorption of CO is unlike the hydrogen desorption from a W(111) surface in which Tamm and Schmidt (2) observed multiple desorption peaks. In the case of CO adsorption, it is not even possible to form any new desorption peaks by the co-adsorption of oxygen on a surface with preadsorbed CO. The results of the mixed adsorption of $C^{16}O$ and $^{18}O_2$ on the W(111) surface are plotted in Figs. 26-29. In Fig. 26, it is observed, for the small predose of $C^{16}O$ followed by increasing coverages of $^{18}O_2$, that the amount of $C^{18}O$ desorbed increases proportionally. At high coverages of $^{18}O_2$, the amount of $C^{18}O$ desorbed is very large compared to $C^{16}O$ desorbed in the high temperature state, but the amount of $C^{18}O$ desorbed in this state decreases as the amount of CO predosed on the surface increases (Figs. 26-29). It is also interesting to note in this series of experiments that the temperature of maximum desorption of this high temperature state decreases as the coverage of oxygen increases. The isotopic mixing of the oxygen in the desorbing CO molecules from a surface with co-adsorbed $C^{16}O$ and $^{18}O_2$ occurs
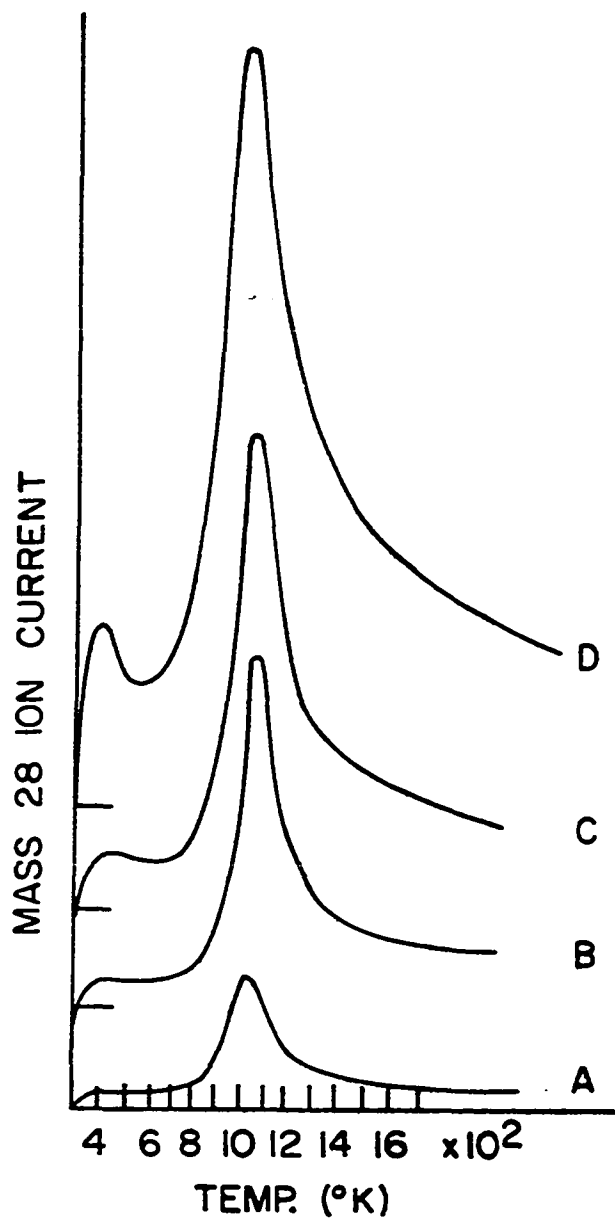
Fig. 25. Flash desorption spectra of CO adsorbed on a W(111) surface
(A - 2.3 L, B - 4.8L, C - 8.0L and D - 19.9L).
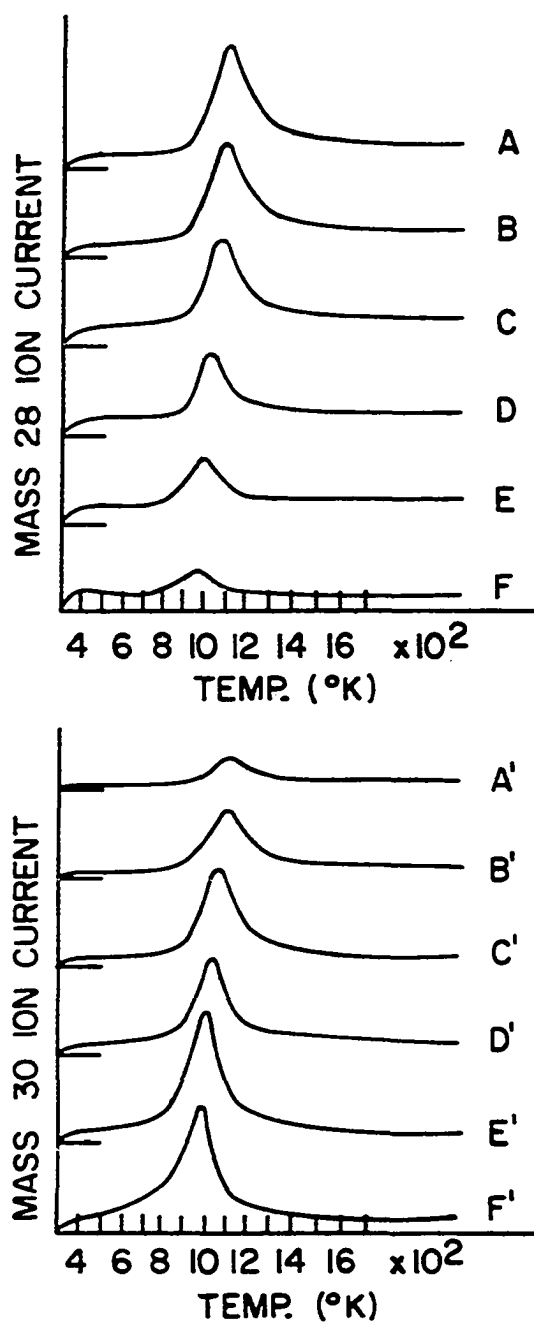
Fig. 26. Flash desorption spectra of CO from a W(111) surface predosed
with 2.3L of $C^{16}O$ followed with increasing dosages of $^{18}O_2$
(A - 0.0L, B - 1.4L, C - 2.5L, D - 5.7L, E - 10.7L and
F - 22.0L).
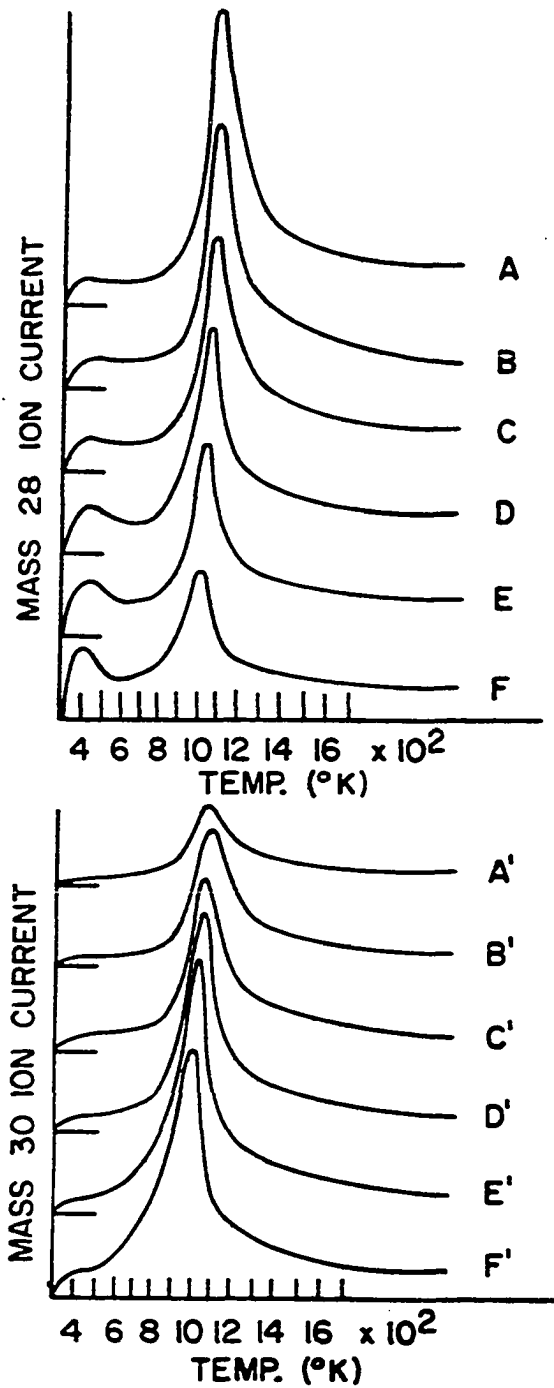
Fig. 27. Flash desorption spectra of CO from a W(111) surface predosed
with 4.8L of $C^{16}O$ followed with increasing dosages of $^{18}O_2$
(A - 0.0L, B - 1.4L, C - 2.5L, D - 5.7L, E - 10.7L and
F - 22.0L).
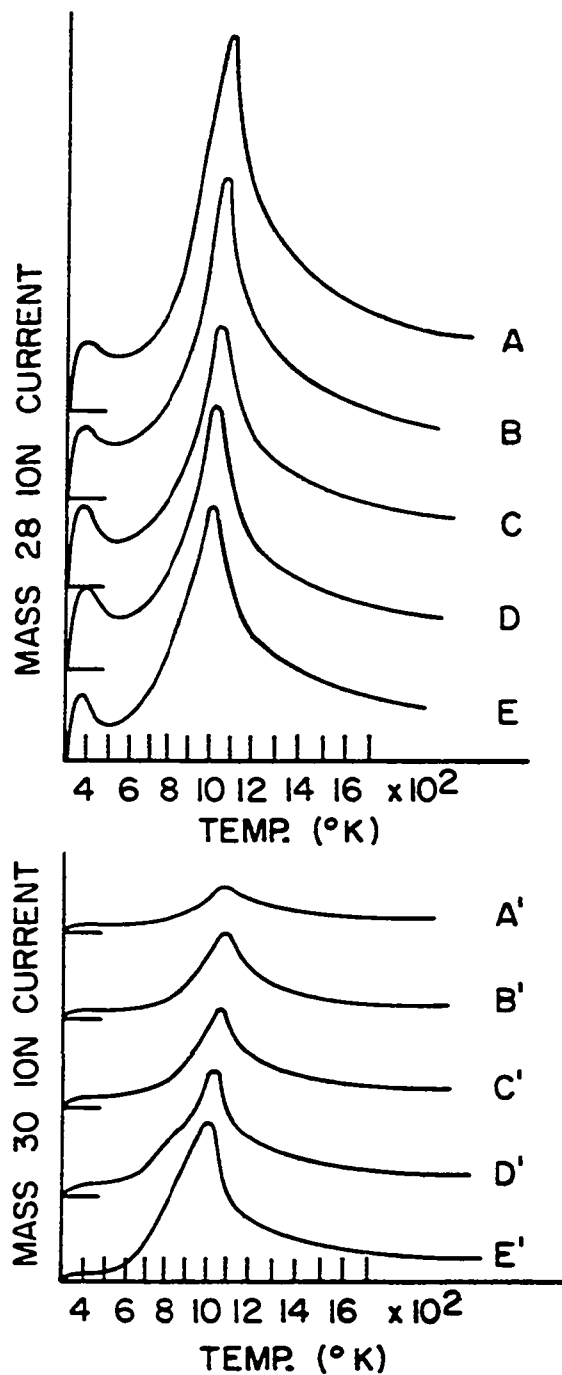
Fig. 28. Flash desorption spectra of CO from a W(111) surface predosed
with 8.0 L of $C^{16}O$ followed with increasing dosages of $^{18}O_2$
(A - 0.0 L, B - 2.5 L, C - 5.7 L, D - 10.7 L and E - 22.0 L).
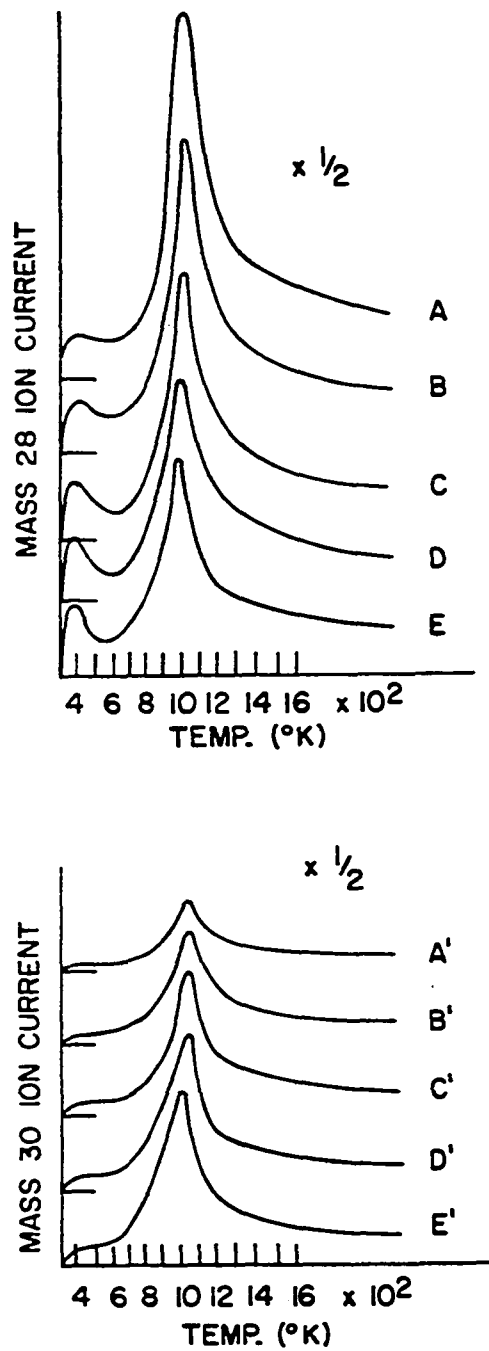
Fig. 29. Flash desorption spectra of CO from a W(111) surface predosed with 19.9L of $C^{16}O$ followed with increasing dosages of $^{18}O_2$ (A - 0.0L, B - 2.5L, C - 5.7L, D - 10.7L and E - 22.0L).

almost exclusively in the CO desorbed in the β state. When oxygen is dosed on a surface with preadsorbed CO, there is no significant increase in the amount of α-CO desorbing. Such an observation suggests no conversion process of α-CO and β-CO is occurring on the surface. If β-CO was formed by conversion of the associatively adsorbed α-CO, the oxygen adsorption should prevent this conversion. Therefore, an increase in the amount of α-CO desorbed would result. No such observations were made (Figs. 26-29) providing no evidence for a conversion process.

In Fig. 30, it is observed that at low coverages of preadsorbed oxygen there is a decrease in the overall amount of CO adsorbed on the surface compared to a clean surface. The preadsorbed oxygen appears to initially block sites for CO adsorption in the β state and create more sites for CO to adsorb as α-CO (Fig. 30). But as the amount of preadsorbed oxygen increases, there is a decrease in the amount of CO desorbed in both states.

As observed on the other tungsten surfaces in this study, oxygen when dosed on a surface with preadsorbed CO is not able to displace any of the CO. Figure 31 shows, that with increasing doses of oxygen on surfaces with constant coverages of preadsorbed CO, the total amount of CO ($C^{16}O + C^{18}O$) desorbed is constant but the ratio of $C^{18}O:CO_{total}$ which is desorbed from the surface (Fig. 32) changes.
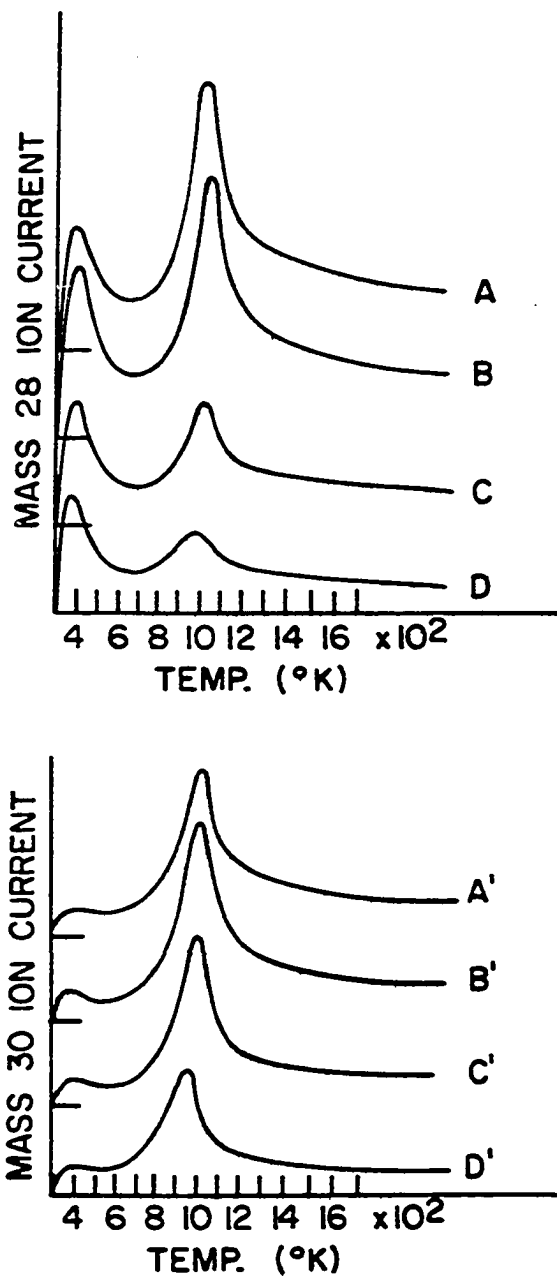
Fig. 30. Flash desorption spectra of CO from a W(111) surface predosed with increasing dosages of $^{18}O_2$ (A - 2.5L, B - 5.7L, C - 10.7L and D - 22.0L) followed by a constant dose of $C^{16}O$ (8.0L).
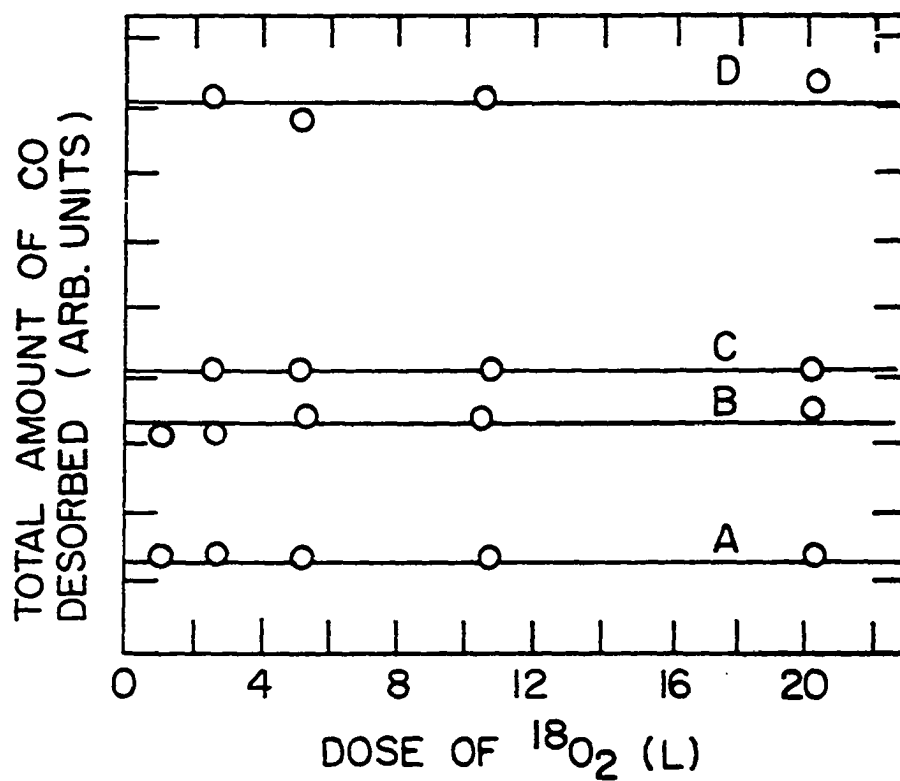
Fig. 31. Total amount of CO ($C^{16}O + C^{18}O$) desorbed from a W(111) surface where the surface was predosed with $C^{16}O$ (A - 2.3 L, B - 4.8 L, C - 8.0 L and D - 19.9 L) with increasing dosages of $^{18}O_2$ (1.4 L, 2.5 L, 5.7 L, 10.7 L and 22.0 L) in each set of $C^{16}O$ doses.
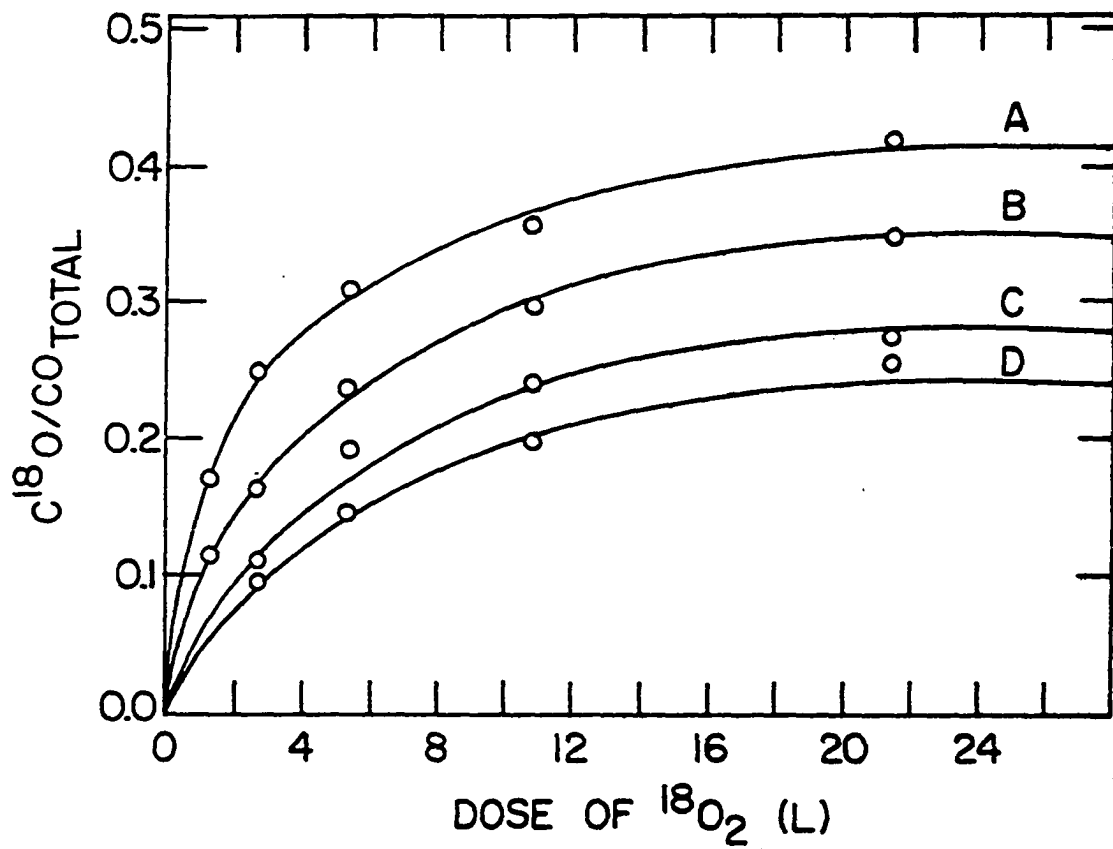
Fig. 32. The ratio of $C^{18}O/CO_{total}$ desorbed from a W(111) surface predosed with $C^{16}O$ (A - 2.3L, B - 4.8L, C - 8.0L and D - 19.9L) with increased dosages of $^{18}O_2$ (1.4L, 2.5L, 5.7L, 10.7L and 22.0L) in each set of $C^{16}O$ doses.

This ratio appears to reach limiting values for a selected predose of

CO followed by a saturating $^{18}O_2$ dose. These limiting ratios of

$C^{18}O:CO_{total}$ which desorb from a surface with preadsorbed CO are

(Fig. 33) 0.65 at low coverages of CO and a surface saturated with

$^{18}O_2$, and 0.24 for a saturated coverage of CO followed by a saturating

$^{18}O_2$ dose.

Following is a summary of the above results which must be

consistent with any proposed model for CO adsorption and interaction

with co-adsorbed $^{18}O_2$.

(1) CO adsorbed on a W(111) surface at room temperature

desorbs as an α state at ~450°K and a β state at ~1050°K.

(2) Co-adsorption of CO and $^{18}O_2$ result in isotopic mixing of

the oxygen in the CO molecules desorbed from the β state.

(3) Preadsorbed CO is not displaced from the surface by dosing

with oxygen nor is the oxygen able to create new desorption states.

The adsorbed oxygen on a surface with preadsorbed CO does not

increase the amount of CO desorbing in the α state providing evidence

to dispute the existence of a conversion process to the β state by

heating the surface.

(4) A surface with preadsorbed $^{18}O_2$ initially blocks sites for

adsorption in the β state and creates more sites for adsorption of

α - CO. A surface with a saturated adlayer of oxygen appears to be
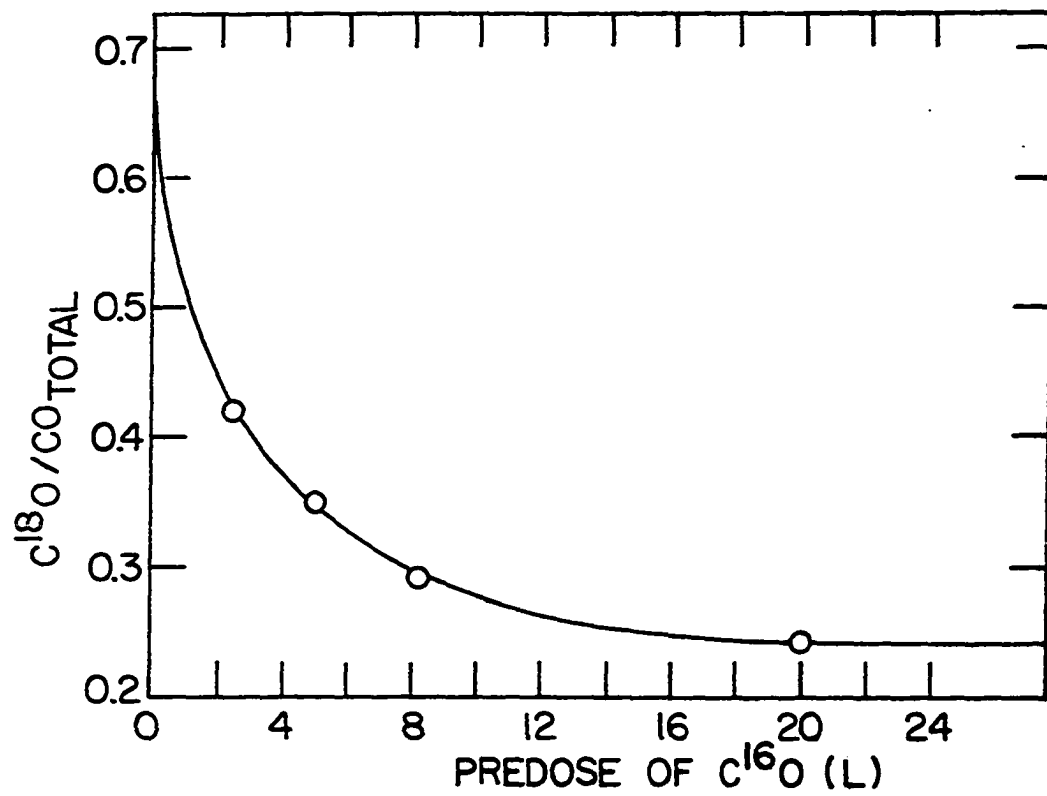
Fig. 33. The limiting ratio of $C^{16}O/CO_{total}$ desorbed from a W(111) surface predosed with $C^{16}O$ (2.3L, 4.8L, 8.0L, 19.9L) followed by a saturated dose of $^{18}O_2$.

able to block subsequent adsorption of CO in any state.

(5) There are limiting ratios of $C^{18}O$:CO_{total} desorbed from a surface with preadsorbed CO followed by a saturating $^{18}O_2$ dose. At low coverage of preadsorbed CO, this ratio appears to be ~.65 and from a surface with a saturated coverage of preadsorbed CO, this ratio appears to be ~.24.

The above results are very similar to those found on the other tungsten surfaces studied and therefore, also imply a model for the dissociative adsorption of CO. The CO in the β state on the W(111) is assumed to be dissociatively adsorbed based on the isotopic mixing of the oxygen in the desorbed CO molecules from a surface of co-adsorbed $C^{16}O$ and $^{18}O_2$. The CO molecules in the α state must be associatively adsorbed because of the lack of any significant isotopic mixing. The decrease in the temperature of maximum desorption of the CO in the β state as the coverage of adsorbed oxygen increases can either result from weakened bonds with the surface due to the co-adsorbed oxygen or from the increased O adatom concentration enabling easier recombination of the C adatom with oxygen.

On the W(111) surface, three symmetric sites seem attractive for bonding chemisorbed species to the surface. In Fig. 34, these sites are illustrated as site A which has three-fold symmetry and is above
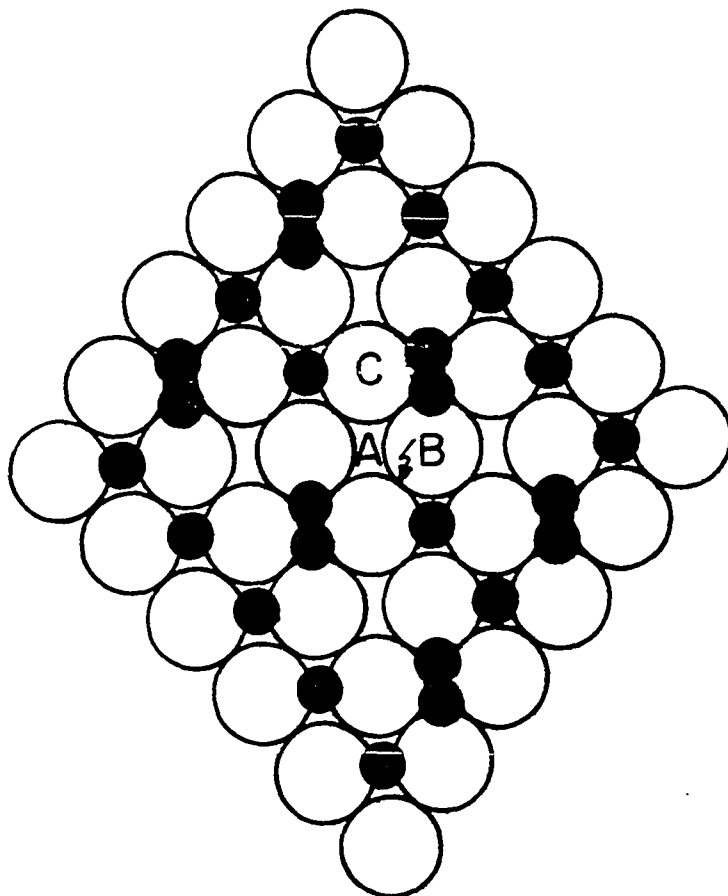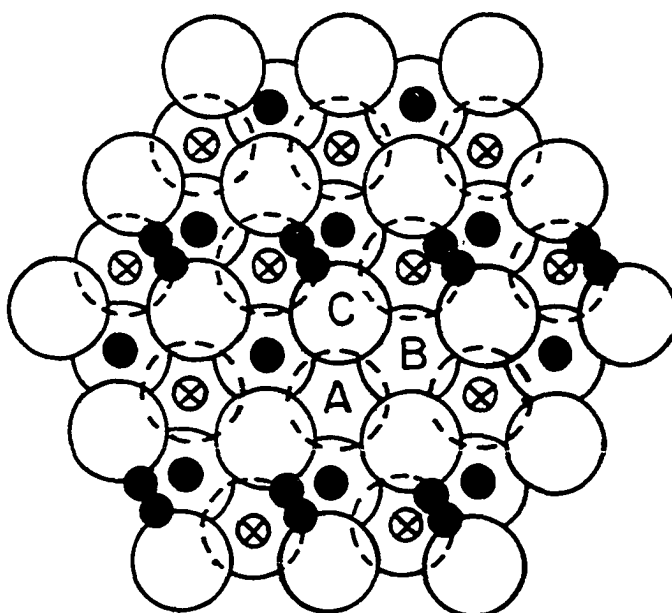
Fig. 34. Possible sites occupied by chemisorbed species from co-
adsorption of CO and $^{18}O_2$ on a W(111) surface (A - 4 CN
site, B - 4 CN' site, C - 1 CN site, ● - Oadatoms, ⊗ -
C adatoms and ●● - associatively adsorbed oxygen).

an atom exposed to the surface and also surrounded by other surface atoms. Site B also has three-fold symmetry and is above a surface atom which is more exposed as a surface atom. The C sites are above the most exposed surface atoms on this surface. Based on the results and prediction in Chapter II, a carbon adatom would probably select site A to satisfy its multi-valent property. The proximity and the easy occupation of site B during dissociative adsorption of CO probably would result in O adatoms selecting these sites. If dissociative adsorption requires an empty site A and an empty adjacent site B, it is very probable, as was found and predicted on the other tungsten surfaces (18, 44), that in random dissociative adsorption $\sim 20\%$ of the A sites would not have available empty adjacent B sites at saturation coverage. These sites could then be occupied by associatively adsorbed CO which would be stable on the surface at room temperature. This is very similar to the model proposed on the other tungsten surfaces.

We therefore assume that adsorption of CO at room temperature results in C and O adatoms bonded at adjacent A and B sites (Fig. 34), which desorb as CO molecules in the β state, and CO adsorbed associatively at A sites where adjacent B sites are unavailable, which desorb as CO molecules in the α state. On a surface with preadsorbed CO, it is easy to understand why the co-adsorption of oxygen was not able to displace any of the preadsorbed CO from these bonding sites.

It was observed that preadsorbed oxygen initially blocked sites for β adsorption while creating more sites for associatively adsorbed CO (Fig. 30). If the preadsorbed oxygen is dissociatively adsorbed at the B sites, this increases the probability of A sites not having an empty adjacent B site for CO to dissociatively adsorb. Therefore, there is an increase in A sites for the associatively adsorbed CO (observed in Fig. 30).

At very low coverages of CO followed by a saturated dose of $^{18}O_2$, the C adatom bonded at A sites would find one ^{16}O adatom in an adjacent B site and two ^{18}O species adsorbed at the other adjacent B sites. Therefore, the limiting ratio of $C^{18}O:CO_{total}$ desorbed should be $\sim.67$ which compares favorably with the value of $\sim.65$ determined from the plot in Fig. 33. On a W(111) surface saturated with preadsorbed $C^{16}O$ and followed with a saturating $^{18}O_2$ dose, the only place for the co-adsorbed $^{18}O_2$ molecules to bond are at the remaining unoccupied C sites. It is very likely that the oxygen molecule would be bridged between two adjacent C sites. In this configuration, there is one-half an adsorbed $^{18}O_2$ molecule per C adatom. Again, it will be assumed that upon heating the surface during flash desorption, the oxygen dissociates according to

$$-\tfrac{1}{2}\, \underset{*}{\overset{O}{\diagup}} - \underset{*}{\overset{\cdot O}{\diagdown}} \rightleftarrows \underset{*}{\overset{O}{|}} \quad .$$
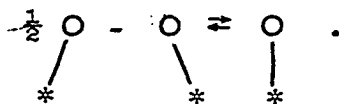
Based upon previous evidence, $\sim 20\%$ of the CO desorbed will be

α-$C^{16}O$ from associatively adsorbed CO at A sites. If the C adatom

will recombine only with oxygen atoms, it has a choice of one ^{16}O adatom

from the dissociated CO molecule and assuming the $^{18}O_2$ dissociation is

only one-half complete, and that only one-half the C adatoms are adjacent

to the adsorbed $^{18}O_2$, then the C adatom has a choice of one-fourth ^{18}O

adatom for every ^{16}O adatom. Therefore, the 80% of the CO desorbed

from the β state will be one-fifth $C^{18}O$. The limiting ratio of

$C^{18}O{:}CO_{total}$ desorbed from the above surface saturated with

preadsorbed CO followed by a saturating dose of $^{18}O_2$ is $\sim .18$ and

compares with the value estimated in Fig. 33 of $\sim .24$.

Summary and Conclusions

A model for dissociative adsorption of CO is consistent with all

the observations in this study where CO chemisorption was examined on

three single crystal surfaces (100, 110, 111) of tungsten. The observa-

tions indicated the CO which desorbed at the high temperatures was

dissociated on the surface at room temperature. On all the surfaces,

a stable associatively adsorbed species was found to desorb at lower

temperatures. All these chemisorbed species were not displaced by

co-adsorbed oxygen. The CO desorbing at the higher temperature was

a mixture of $C^{16}O$ and $C^{18}O$ which resulted from the isotopic mixing

of the oxygen from the dissociative adsorbed CO and the co-adsorbed

$^{18}O_2$ which was at least partially dissociated before the CO desorbed.

On all three tungsten surfaces, it was assumed the associatively

adsorbed CO was bonded at sites where vacant sites needed for the

dissociation of the CO molecule were not present. On the W(100) and

W(111) surfaces, it was proposed that adsorbed oxygen from an oxygen

dose on a clean surface would not occupy the sites preferred for C

adatoms from CO dissociation. Therefore, on the W(100) surface

preadsorbed oxygen at 2 CN sites (Fig. 13) should decrease the

availability of vacant adjacent 5 CN sites needed for CO to adsorb and

dissociate. As observed (Fig. 9), this results in an increase of α-CO

desorbed from the W(100) surface where CO was dosed on a surface

with preadsorbed oxygen. On the W(111) surface, it was assumed the

preadsorbed oxygen occupied sites B in Fig. 34. When the CO adsorbs

at sites A, vacant adjacent sites B are needed for the CO to dissociate.

If these sites are occupied by preadsorbed O adatoms, then they are

not available for CO dissociation. Therefore, as observed in Fig. 30,

there is an increase in the amount of α - CO desorbed from the W(111)

surface where CO was dosed on a surface with preadsorbed oxygen.

On the W(110) surface, the oxygen adatoms from adsorbed oxygen and

the adatoms from dissociated CO were assumed to occupy the same

sites. Therefore, the random adsorption of either CO or O_2 on a W(110)

surface should result in approximately the same number of sites

present on the surface with unavailable vacant adjacent sites. These

sites were assumed to be occupied by associatively adsorbed CO.

Therefore, in contrast to the other surfaces (100, 111), the amount of

α - CO desorbed from a W(110) surface where CO was dosed on a surface

with preadsorbed oxygen (Fig. 20) is about the same as the amount of

α - CO desorbed from a surface where only CO was adsorbed (Fig. 14).

REFERENCES

1. P. W. Tamm and L. D. Schmidt, J. Chem. Phys., 51, 5352 (1969).

2. P. W. Tamm and L. D. Schmidt, J. Chem. Phys., 54, 4775 (1971).

3. P. J. Estrup and J. Anderson, J. Chem. Phys., 45, 2254 (1966).

4. T. E. Madey and J. T. Yates, Jr., Structure et Proprietes des Surface des Solids (Edition de Centre National de la Recherche Scientifique, Paris, 1970) No. 187, p. 155.

5. K. Yonehara and L. D. Schmidt, Surface Sci., 25, 238 (1971).

6. J. A. Delchar and G. Ehrlich, J. Chem. Phys., 42, 2686 (1965).

7. P. J. Estrup and J. Anderson, J. Chem. Phys., 46, 467 (1967).

8. L. R. Clavenna and L. D. Schmidt, Surface Sci., 22, 365 (1970).

9. D. L. Adams and L. H. Germer, Surface Sci., 27, 21 (1971).

10. P. J. Estrup and J. Anderson in: Proc. 27th Annual Physical Electronics Conference, MIT, 1967.

11. N. P. Vas'ko, Yu. G. Ptushinskii and B. A. Chuikov, Surface Sci., 14, 448 (1969).

12. T. E. Madey, Surface Sci., 33, 355 (1972).

13. Yu. G. Ptushinski and B. A. Chuikov, Soviet Phys.-Solid State, 10, 565 (1968).

14. J. T. Yates, Jr., and T. E. Madey, J. Chem. Phys., 45, 1623 (1966).

15. W. H. Weinberg and R. P. Merrill, Surface Sci., 32, 317 (1972).

16. L. R. Clavenna and L. D. Schmidt, Surface Sci., 33, 11 (1972).

17. C. G. Goymour and D. A. King, J. C. S. Faraday I, 69, 736 (1973).

18. C. G. Goymour and D. A. King, J. C. S. Faraday I, 69, 749 (1973).

19. C. G. Goymour and D. A. King, Surface Sci., 35, 246 (1973).

20. R. Hoffmann, J. Chem. Phys., 39, 1397 (1963).

21. J. C. Tracy and J. M. Blakely, Surface Sci., 15, 157 (1969).

22. P. A. Redhead, J. P. Hobson and E. V. Kornelson, The Physical Basis of Ultra-High Vacuum (Chapman and Hall, London, 1968).

23. R. R. Ford, Adv. Catalysis, 21, 51 (1970).

24. D. O. Hayward in: Chemisorption and Reactions on Metallic Films, ed. J. R. Anderson (Academic Press, London and New York, 1971).

25. G. Ehrlich, T. W. Hickmott and F. G. Hudda, J. Chem. Phys., 28, 506 (1958).

26. J. A. Becker, E. J. Becker and R. G. Brandes, J. Appl. Phys., 32, 411 (1961).

27. J. H. Singleton, J. Chem. Phys., 45, 2819 (1966).

28. D. Brennan and M. J. Graham, Disc. Faraday Soc., 41, 95 (1960).

29. P. A. Redhead, Nuovo Cimento. Suppl., 5, 586 (1967).

30. T. E. Madey, J. T. Yates, Jr. and R. C. Stern, J. Chem. Phys., 42, 1372 (1965).

31. T. E. Madey and J. T. Yates, Jr., 6th Int. Symp. on Rarefied Gas Dynamics (Academic Press, Inc., New York, 1969), 2, 1345.

32. F. M. Propst and T. C. Piper, J. Vac. Sci. Technology, 4, 53 (1966).

33. E. J. Wood, Crystal Orientation Manual (Columbia University Press, New York, 1963).

34. J. T. Yates, Jr. and D. A. King, Surface Sci., 32, 479 (1972).

35. J. T. Yates, Jr., National Bureau of Standards, Washington, D. C., private communication.

36. J. Anderson and P. J. Estrup, J. Chem. Phys., 46, 563 (1967).

37. D. Menzel, Ber. Bunsenges. Phys. Chem., 72, 591 (1968).

38. T. E. Madey and J. T. Yates, Jr., Surface Sci., 11, 327 (1968).

39. T. E. Madey and J. T. Yates, Jr., J. Chem. Phys., 51, 1264 (1969).

40. T. E. Madey, Surface Sci., 33, 355 (1972).

41. J. W. May and L. H. Germer, J. Chem. Phys., 44, 2895 (1966).

42. C. Kohrt and R. Gomer, Surface Sci., 24, 77 (1971).

43. J. W. May, L. H. Germer, and C. C. Chang, J. Chem. Phys., 45, 2383 (1966).

44. T. Orent and R. S. Hansen, Iowa State University, unpublished work.

91

ACKNOWLEDGEMENTS

certainly aided by the many hours of discussions provided by the members of the P & I Research Group III (Dr. Jerome McAllister, Dr. Ralph Sheets, Dr. Paul Masterson and Doug Summers) to whom the author is grateful and wishes to express his thanks.

The author wishes to thank his wife, Eileen, for her patience and encouragement during his graduate work and also to our sons, Craig and Todd, for their understanding and the enjoyment they have provided. The author is forever indebted to his father and mother for their continual encouragement and concern during the many years the author spent obtaining his education.

APPENDIX A.

A MOLECULAR ORBITAL INVESTIGATION OF

CHEMISORPTION. I. HYDROGEN ON TUNGSTEN (100) SURFACE

A Molecular Orbital Investigation of

Chemisorption. I. Hydrogen on Tungsten (100) Surface

LEON W. ANDERS AND ROBERT S. HANSEN

Ames Laboratory-USAEC and Department of Chemistry
Iowa State University, Ames, Iowa 50010

AND

L. S. BARTELL

Department of Chemistry, University of Michigan
Ann Arbor, Michigan 48104

Abstract

The relative bonding energies of hydrogen chemisorbed at three

symmetric sites on a W(100) surface were obtained by means of the

Extended Hückel Molecular Orbital Theory (EHMO). The preferred

site for hydrogen chemisorption was found to be the single coordination

number (1 CN) site or the site above a surface tungsten atom. The

W(100) surface was represented by finite arrays of tungsten atoms

which were shown to be adequate for obtaining semi-quantitative

results. The basis set for the calculations contained the valence

orbitals of tungsten and, initially, the 5p orbitals which were non-

bonding but provided the necessary repulsion at small internuclear

separation. The repulsive energy provided by these orbitals was replaced by an analytical exponential repulsive energy term. This allowed the 5p orbitals to be omitted from the basis set to simplify computation. Functionally, the energy change for the reaction $W_n + H \rightarrow W_nH$ was calculated for various assumed configurations of the W_nH "molecule". The bonding between tungsten atoms was found to be changed as a result of W_nH formation, and the change varied with hydrogen position. Energy barriers to surface diffusion were also calculated, and found to agree reasonably with experimental values.

I. INTRODUCTION

In recent years, it has become experimentally possible to study the chemisorption of atoms and molecules on single crystal surfaces. To account for the experimental observations from these well defined surfaces, various bonding models have been proposed, but the detailed description of the adsorbed species remains in the realm of speculation. Unfortunately, no available experimental techniques give conclusive information about the molecular structures or site distributions of the adsorbed species. In view of current experimental limitations and the importance of the implications in the field of catalysis, a theoretical attack seems justified. The prohibitive expense of

ab initio quantum mechanical calculations for such systems make it attractive to explore nonrigorous, semiempirical methods which have been found in the past to account quite well for structural features of molecular systems.

In this paper, we apply the extended Hückel molecular orbital theory, a semiempirical molecular orbital technique, to investigate the preferred structure of the "surface molecule". EHMO has been used previously to study the chemisorption of hydrogen on graphite,[1] and of organic molecules,[2] carbon monoxide[3] and hydrogen[4] on nickel. In the case of carbon monoxide on nickel,[3] the dependence of binding energy on distance at the possible chemisorption sites was not analyzed. The preferred site was selected by comparison of binding energies at a fixed carbon-nickel distance. These investigations used only the valence orbitals in the basis set, and as a result only the hydrogen-graphite interaction produced a minimum in the binding energy curve. The interaction of hydrogen as well as carbon, nitrogen, oxygen and fluorine on graphite[5] was also investigated using CNDO technique in order to alleviate the problem of unreasonable charge transfer which can occur in the EHMO calculations.

Although it is known that this technique has many limitations, it nevertheless has been successful in determining preferred molecular configurations. Therefore, it is a promising tool for

investigating the structure of the elusive surface molecules and for

obtaining a better understanding of the bonding between chemisorbed

atoms and the surface atoms. We have chosen to investigate the

chemisorption of hydrogen on a tungsten (100) surface because of the

experimental data which are available for comparison.[6-11]

II. PROCEDURE

Hoffmann[12] developed a semiempirical molecular orbital theory, including all overlap integrals, referred to as the "extended Hückel" Molecular Orbital theory (EHMO). It was originally utilized to solve

organic conformational problems, but subsequently has been used to

yield insight on other molecular geometric problems, including the

structural chemistry of crystals.[13] Hoffmann stressed that the

method's most reliable characteristic is its ability to predict molecular

geometries and to assess the relative importance of sigma and pi

orbitals. On the other hand, it is quite crude in predicting charge

distributions and excitation energies in electronic transitions.

The molecular orbitals are formed from a linear combination

of atomic orbitals (LCAO),

$$\Psi_j = \sum_q C_{jq} \chi_q \ ,$$

where the atomic orbitals χ_q are the single parameter, Slater-type

atomic orbitals (STO). According to the standard variation principle,

the LCAO function with q atomic orbitals leads to a set of q simul-

taneous linear homogeneous equations, each of which contains q

coefficients C_{jq} ,

$$\sum_q (H_{pq} - \epsilon_j S_{pq}) C_{jq} = 0 \ .$$

For these equations to have nontrivial solutions, the determinant of the

coefficients must vanish,

$$\| H_{pq} - \epsilon_j S_{pq} \| = 0 \ .$$

The eigenvalues ϵ_j given by the solution of this determinant are the

energies of the molecular orbitals. These energies ϵ_j are substituted

back into the set of simultaneous linear homogeneous equations which are

then solved to give the coefficients C_{jq}. These coefficients C_{jq} form

the wave function of the molecular orbital at each energy ϵ_j. In the

Hoffmann formalism, the diagonal elements H_{pp} are set equal to

the valence orbital ionization potential (VOIP) of χ_p; the non-diagonal

elements H_{pq} were approximated by the Mulliken Wolfsberg-Helmholtz

approximation[14]

$$H_{pq} = 0.5K(H_{pp} + H_{qq})S_{pq}$$

with a Helmholtz Factor K equal to 1.80.

The EHMO method does not explicitly account for either electron-

electron or core-core interactions between atoms, but relies on

extensive cancellations which hold approximately for nonpolar molecules.

These cancellations will also hold for other molecules near the equi-

librium internuclear separations where the chemical bond is formed.

Excessive charge transfers, a common problem in the EHMO method,

were partially alleviated by adjusting the VOIP as functions of atomic

charge q and iterating to self-consistency. The atomic charge was

computed by the Mulliken method[15] and the VOIP of the atomic orbitals

were determined as functions of charge q according to the following[16]

$$VOIP(q) = Aq^2 + Bq + C .$$

These adjusted VOIP gave more realistic charge transfers than fixed

VOIP. Bonding energies for different structures in the neighborhood

of their energy minima were similarly shifted by shifts in VOIP so

that conclusions as to preferred sites were unaffected by variations in VOIP.

Table I lists the orbital exponents for the STO and the values for the constants, A, B and C, which are needed to determine the VOIP as a function of atomic charge. The values for the hydrogen 1s orbital were obtained from Basch, Viste and Gray.[16] A value of 1.20 was used for the orbital exponent of the hydrogen 1s orbital. For the tungsten 5p orbital, the value of C was obtained from the tables of Herman and Skillman;[17] the orbital exponent for the STO was obtained by the rules of Burns[18] and assumed to be charge independent. The values of C and the orbital exponents for the STO of the tungsten 5d and 6s orbital were obtained from Lohr and Lipscomb;[19] the values of C for these orbitals agreed with neutral atom ionization measurements of Lotz.[20] A linear charge dependence[21] for the VOIP of the tungsten 5d and 6s orbitals was used with the value of B equal to 3.5 ev/e⁻ .

The EHMO method was first applied to the diatomic molecules, W-W and W-H. These calculations showed that it was necessary to include the inner orbitals of the tungsten atoms as well as the valence orbitals in the basis set to obtain a characteristic potential energy curve; when only valence orbitals were used too few non-bonding orbitals were populated to provide the requisite repulsion at small internuclear separations. It was found that the addition of the inner

orbitals overcame this deficiency, although they made little contribution to the formation of the chemical bond. Therefore, if the repulsive energy could be calculated by an empirical relationship, these orbitals could be omitted, thus reducing the size of the basis set and saving a substantial computation effort. The repulsive energy between atoms in a molecule can be represented approximately by a series of exponential terms of the form

$$E_{Rep} = \sum_{ij} A_{ij} e^{-r_{ij}/\alpha_{ij}}$$

where the parameters, A_{ij} and α_{ij}, are unique for a pair of atoms. These parameters for pairwise interactions were derived from the repulsive energy, E_{Rep}, of the diatomic molecules. The repulsive energy was determined as the difference in bonding energies obtained by a calculation with only valence orbitals and by a calculation which also included the inner orbitals. Comparison of E_{Rep} for WH and W_2H indicated that repulsive energies in the tungsten hydrogen system could be assumed pairwise additive.

In modeling the tungsten (100) surface for the EHMO calculations, it was necessary to truncate the infinite surface to a limited number of metal atoms. These selected surface arrays must represent the possible sites for bonding of a chemisorbed atom. The tungsten (100) appears to offer three distinct symmetric sites which might be considered attractive adsorption sites. These are shown in Figure 1, which also

shows the metal atom arrays used in calculations. The three sites

can be distinguished by the numbers of surface tungsten atoms to

which the hydrogen atom is coordinated (CN). Thus the 1 CN site is on

top of a tungsten atom, the 2 CN site bridges two tungsten atoms, and

the 5 CN site is in the four-fold hole. The size of the surface array

representing the 1 CN and 5 CN sites was increased to 21 tungsten

atoms with an insignificant change in bonding energies. The presence

of edges on these truncated surface arrays caused abnormal charge

distribution, but these effects were reduced by adjusting the VOIP of

the edge atoms. After this initial adjustment, there was no further

adjustment of the tungsten orbitals' VOIP.

III. RESULTS

A. Diatomic Molecules

Energy-distance calculations were made for diatomic molecules

to determine the parameters needed for the exponential repulsive

energy term. These calculations also provided a basis for comparison

with the chemisorbed system, in which the hydrogen was bonded to

larger arrays of tungsten atoms. In Fig. 2, the bonding energy is

plotted as a function of inter-nuclear separation r along the molecular

axis z for the W-W and W-H molecules. The bonding energy was

calculated by subtracting from the total energy the energy of the ions

of the W-H molecule or the energy of the atoms of the W-W molecule

at infinite separation. These arbitrary conventions compensate in part

for the total neglect of coulomb interactions in the EHMO method and

have no influence on any conclusions drawn later.

Figures 2a and 2b display the clear need to include some of

the inner orbitals of tungsten in the basis set in order to obtain a

characteristic potential energy curve. The differences between curves

a and b in Figs. 2a and 2b are the repulsive energies. In Fig. 3,

$\ln \Delta \epsilon$ is plotted as a function of internuclear separation r for W-W

and W-H molecules. From these plots, the values for the parameters

A and α needed to calculate the repulsive energy by the analytical

exponential term were derived. Best values were found to be: $A_{WW} =$

4096.ev, $\alpha_{WW} = 0.289\text{Å}^{-1}$, $A_{WH} = 139.\text{ev}$, $\alpha_{WH} = 0.279\text{Å}^{-1}$.

As previously stated, the VOIP of the valence orbitals were

adjusted as a function of atomic charge and iterated to self-consistency.

For the diatomic molecule W_2 the atomic charge on each tungsten

atom was of course zero, for WH the charge on hydrogen was -0.10

and on tungsten +0.10. Corresponding VOIP are implied by Table I.

The molecular orbitals (LCAO coefficients) for the diatomic molecules

at equilibrium separation are tabulated in Table II. Those for W-H

will prove useful in comparing the bonding of hydrogen to tungsten in

the diatomic molecule with that in "surface molecules" such as W_9H

used to model chemisorption.

Although the diatomic molecules in Table II are not known to exist, their EHMO bond lengths can be compared with the sum of the covalent radii of the atoms in the molecule. The Pauling single bond covalent radii of hydrogen and tungsten are 0.32 and 1.30 angstroms, respectively. The sum of the Pauling covalent radii for the diatomic tungsten molecule gives a bond length of 2.60Å for a single bond. The calculated bond length of 2.14Å implies a multiple bond whose order can be estimated from Pauling's[22] empirical rule

$$D(n) = D(1) - 0.71 \log n \ .$$

Here D(1) is the single bond length (2.60Å), D(n) the observed bond length (2.14Å), and n the bond order. Pauling's rule leads to a value of 4.4 for the bond order in reasonable agreement with the implications of Table II (5 occupied bonding orbitals, 1 occupied anti-bonding orbital). Hence the calculated bond lengths appear to be reasonable and self consistent.

A molecule of a hydrogen atom and two tungsten atoms was used to determine whether the repulsive energies as calculated in the analytical exponential term were pairwise additive. In this molecule, the tungsten atoms were separated by 3.16Å , a characteristic distance on a tungsten (100) surface, and the hydrogen was equidistant

from these two tungsten atoms. The repulsive energies plotted as curve a in Fig. 4 are determined by the differences between the energies calculated by the EHMO technique where the basis set of atomic orbitals included the 5p as well as the valence (6s, 5d) orbitals of the tungsten atoms and those calculated where the 5p orbitals were omitted from the basis set. The repulsive energies, as calculated by the analytical exponential repulsive term for two tungsten-hydrogen interactions, are plotted as curve b in Fig. 4. From the comparison of curves a and b, it is confirmed that the repulsive energy is reasonably well represented by the sum of all pairwise interactions.

B. Hydrogen Chemisorbed on a W(100) Surface

Before calculations were performed with the hydrogen at the proposed chemisorbed sites, it was necessary to make adjustments on the VOIP of the edge tungsten atoms. Because the edge atoms of the surface arrays were missing nearest and next nearest neighbors, their VOIP were adjusted to prevent abnormal charge distribution. The VOIP of the 5d and 6s orbitals of the four corner atoms of the arrays in Figs. 1a and 1b were adjusted to -8.52 ev and -7.52 ev, respectively; these same orbitals on the other four edge atoms were adjusted to -8.76 ev and -7.76 ev, respectively. The orbitals of the eight edge atoms of the array in Fig. 1c were adjusted to -8.68 ev

for the 5d orbitals and -7.68 ev for the 6s orbital. The VOIP of the remaining atoms in these arrays were not adjusted.

Mattheiss'[26] band theory calculation on tungsten provides two check points for our EHMO calculations on the W_9 molecule. First, he finds a d-band width of 10.47 eV. We take as the EHMO analog the difference in energies between highest and lowest molecular orbitals having d character on atom 1 in the surface array of Fig. 1a. The lowest energy of such an orbital is Ψ_2 (shown in Fig. 6a), the highest (not shown because it is unoccupied) is 9.45 eV higher. Second, Mattheiss finds that the bottom of the d band lies 1.36 eV above the bottom of the conduction band. Our analog is the difference between Ψ_1 in Fig. 6a and the first occupied orbital of d character (not totally symmetric and therefore not shown in Fig. 6a); this difference is 1.34 eV, remarkably close to Mattheiss' result.

Calculations were then carried out with hydrogen bonded at the three possible symmetric sites. The minimum charge transfer to the hydrogen occurred with hydrogen bonded at the 5 CN site and the maximum with the hydrogen bonded at the 1 CN site. In the initial calculations, the VOIP of the hydrogen 1s orbital was adjusted as a function of atomic charge q and iterated to self consistency holding the tungsten orbital VOIP constant at values previously given. The final iteration VOIP were -11.34 ev at the 5 CN site, -9.54 ev at the 2 CN site, and -8.84 ev at the 1 CN site. These differences raised

the possibility that energy differences between various absorption

configurations might reflect too strongly the different parametrizations

of the hydrogen 1s VOIP. Since these energy differences were of

principle concern, the calculations were repeated using a VOIP of

-10.30 for all sites. Comparing the two sets of calculations, it was

found that differences in bond energy and equilibrium distances between

configurations were almost unaffected, and most importantly that the

order of bonding energies among the three configurations remained

unchanged. Hence use of a fixed hydrogen VOIP of -10. ev was

adopted for all subsequent calculations for computational simplicity.

The dependence of bonding energy E on internuclear separation

r is plotted in Fig. 5 for hydrogen bonded at each of the three

symmetric sites. The internuclear separation was the distance of

hydrogen to the nearest tungsten atom(s) in the surface atom arrays.

In the case of the 5 CN site, it was the distance to the tungsten atom

in the hole, for the 2 CN site, it was the distance to the two surface

atoms, and for the 1 CN site, it was the distance to the single tungsten

atom. The bond energy E was calculated according to the following

relationship:

$$E = \sum_{W_nH} n_i \, \epsilon_i - \sum_{W_n} n_i \, \epsilon_i - \epsilon_H + \sum_{W_nH} A e^{-r/\alpha}$$

where the first term is the summation over the occupied molecular

orbitals of energy ϵ_i of the surface "molecule" W_nH, the next term

is the summation over the occupied molecular orbitals of energies ϵ_i

of the W_n part of the "molecule" separated from the hydrogen and

the next term is the energy of the singly occupied atomic orbital of a

separated hydrogen atom. The last term, the repulsive energy term,

represents the repulsion of the occupied inner non-bonding orbitals

(omitted from initial calculations), and the summation extends over

all hydrogen-tungsten pairs in the surface array. This term is not

necessary to determine the bond energy if the inner orbitals are

included in the basis set for the MO calculations. Table III presents

bonding energies, equilibrium distances, and charges corresponding

to the energy minima in Fig. 5.

A somewhat simpler description and a better understanding of the

bonding between hydrogen and the surface arrays can be obtained by using

group theory. First, the surface "molecules" must be assigned to a sym-

metry group. The 1 CN and 5 CN sites on the W(100) surface have four-

fold symmetry and the surface arrays in Fig. 1 representing the surface

for each of these symmetric sites belong to the C_{4v} symmetry group. The

2 CN site has twofold symmetry and the surface array representing this

site belongs to the C_{2v} symmetry group. Because the hydrogen 1s orbital

is totally symmetric and belongs to the a_1 irreducible representation

in these symmetry groups, it will interact only with the molecular orbitals

of the tungsten arrays belonging to this same totally symmetric

irreducible representation a_1. For the C_{4v} surface arrays with nine

tungsten atoms (Figs. 1a and 1b), there are twelve totally symmetric

molecular orbitals formed by the valence orbitals of which only five

are occupied. The C_{2v} surface array (Fig. 1c) with twelve tungsten

atoms has twenty totally symmetric molecular orbitals of which eleven

are occupied. An additional totally symmetric molecular orbital

is formed as the hydrogen 1s orbital interacts with molecular orbitals

of the W_n arrays.

Molecular orbital energy diagrams are shown in Fig. 6 for the hydrogen interacting with each of the surface arrays at equilibrium separation. The totally symmetric molecular orbitals of the tungsten arrays are indicated on the left side of the panels in Fig. 6 with the hydrogen 1s orbital on the right side and in the middle are the molecular orbitals formed by the W_nH surface "molecule". The lines joining the molecular orbitals of the separated W_n and H atomic orbital with those of the combined W_nH show the change in energy of the W_n molecular orbitals as they interact with the hydrogen in qualitative form; corresponding quantitative information can be obtained by comparing Tables IV and V (which tabulate the occupied totally symmetric molecular orbitals of the W_9 and W_{12} surface arrays) with Tables VI, VII and VIII (which tabulate the totally symmetric orbitals of the W_nH surface "molecules"). From these tables, it is observed that hydrogen makes only a small contribution to some of the molecular orbitals of the surface "molecule". These are indicated in Fig. 6 as orbitals not joined by a line to the hydrogen 1s orbital.

It is interesting to note that, for the 1 CN and 2 CN sites, interaction of the hydrogen atom with the k occupied molecular orbitals in the totally symmetric a_1 representation leads to k + 1 molecular orbitals all of which are below the highest occupied molecular orbital

(HOMO), and which are correspondingly occupied and contribute to

bonding in the W_nH molecule. In the 5 CN site one of the molecular

orbitals in the W_nH molecule is above the HOMO (Ψ_6 in Fig. 6c)

and so does not contribute to bonding.

IV. DISCUSSION

The observed[6,9] LEED patterns from a C(2x2) surface structure

of hydrogen on the W(100) surface indicate that hydrogen must be chemi-

sorbed at a site with 4-fold symmetry, either the 5 CN or 1 CN site. Evidence

for this comes from the diffraction spots of the C(2x2) surface structure,

where the spots at the half order position [$(\frac{1}{2},\frac{1}{2})$, $(\frac{1}{2},\frac{3}{2})$, etc.] are

diffuse, resulting from C(2x2) domains on the surface which are not

in phase. The facts that the spots at the integral order positions

[(1,0), (1,1), etc.] are sharp and only those at the half order positions

are diffuse indicate that hydrogen must be chemisorbed at sites with 4-

fold symmetry in the C(2x2) surface structure.[23] From the results of

our calculations as shown in Table III, the 1 CN site can be chosen as

the preferred site with 4-fold symmetry for the chemisorbed hydrogen

atom.

Early experimental evidence led to conflicting models for hydrogen

chemisorbed on a W(100) surface including: atoms bonded at a single

site,[6,8] atoms bonded at different sites,[9] and a mixture of atomic and

molecular species bonded to the surface.[7] Recent evidence[10,11]

indicates that atomic species are bonded at one kind of surface site;
the two peaks, β_1 and β_2, in the flash desorption spectrum are a
result of a density dependent interaction on the surface. The high
temperature state, β_2, has been associated with a C(2 x2) surface
structure and as the remaining sites are populated, a (1 x 1) surface
structure results. From the results of our calculating, these sites
must be the 1 CN sites on the W(100) surface.

In the WH molecule, the hydrogen 1s orbital appears only in
the single molecular orbital Ψ_1 (see Table III). In this case the tungsten-
hydrogen bond can be interpreted as a simple single bond involving a
hydrogen 1s orbital and a tungsten sd hybrid orbital. It is tempting
to interpret the 1 CN preference for hydrogen adsorption as reflecting
a preference for simple single bonding to the tungsten atom below it.
The present treatment is not well designed to provide a justification
for such an interpretation. Table VI shows that the molecular
orbitals Ψ_1', Ψ_2', Ψ_4' and Ψ_6 all have substantial hydrogen 1s con-
tributions; while the principal tungsten orbital contributions to Ψ_1' and
Ψ_2' arise from the tungsten atom underlying the hydrogen atom this
atom contributes almost negligibly to Ψ_4' and Ψ_6, whose tungsten
contributions come largely from the d orbitals of the four tungsten
atoms surrounding the adsorption site. Such molecular orbitals are

not well suited for interpretation in terms of localized bonding; for

this purpose optimally localized orbitals are more appropriate as

shown by Ruedenberg and Edmiston.[24] The tungsten atoms which are

involved with the bonding of the hydrogen atom retain their bonds

with the neighboring tungsten atoms, but their strengths change as

a result of the chemisorbed hydrogen.   The reduced overlap population

calculated by the Mulliken[19] method can assess the relative change in

strengths of these tungsten-tungsten bonds.   With hydrogen bonded at

the 1 CN site, the reduced overlap population of the central tungsten

atom with each of its four nearest neighboring tungsten atoms is

reduced 15%.

The small difference in the bonding energy between a 1 CN site

and a 2 CN site can account for the observed mobility of hydrogen on

tungsten surfaces.   Gomer, et. al.[25] observed the diffusion of hydrogen

on a tungsten surface at a temperature of $180°K$ and reported the activa-

tion energy for diffusion E_d was generally 10 to 20% of the bonding

energy E_a, that both E_a and E_d/E_a were lowest on most closely-

packed faces, and that the lowest value of E_d observed was 5.9 kcal

(0.26 ev).   If the diffusion of hydrogen on the W(100) surface occurs

from one 1 CN site to another 1 CN site via a 2 CN site, and the only

energy barrier to diffusion is the difference between bonding energies at

these two sites, then the activation energy for diffusion would be 0.25 ev.

ACKNOWLEDGEMENT

REFERENCES

1. A. J. Bennett, B. McCarroll and R. P. Messmer, Surface Sci. 24, 191 (1971).

2. J. C. Robertson and C. W. Wilmsen, J. Vac. Sci. and Tech. 8, 53 (1971).

3. J. C. Robertson and C. W. Wilmsen, J. Vac. Sci. and Tech. 9, 901 (1972).

4. D. S. M. Fassaert, H. Verbeek and A. Van Der Avoird, Surface Sci. 29, 501 (1972).

5. A. J. Bennett, B. McCarroll and R. P. Messmer, Phys. Rev. B3, 1397 (1971).

6. P. J. Estrup and J. Anderson, J. Chem. Phys. 45, 2254 (1966).

7. P. W. Tamm and L. D. Schmidt, J. Chem. Phys. 51, 5352 (1969).

8. T. E. Madey and J. T. Yates, Jr., _Structure et Proprietes des Surface des Solides_ (Editions du Centre National de la Recherche Scientifique, Paris, 1970) No. 187, p. 155.

9. K. Yonehara and L. D. Schmidt, Surface Sci. 25, 238 (1971).

10. J. T. Yates, Jr. and T. E. Madey, J. Vac. Sci. and Tech. 8, 63 (1971).

11. E. W. Plummer and A. E. Bell, J. Vac. Sci. and Tech. 9, 583 (1972).

12. R. Hoffmann, J. Chem. Phys. 39, 1397 (1963).

13. G. V. Gibbs, M. M. Hamil, S. J. Lavisnathan, L. S. Bartell and H. Yow, Amer. Mineral. 57, 1578 (1972).

14. M. Wolfsberg and C. Helmholtz, J. Chem. Phys. 20, 837 (1952).

15. R. S. Mulliken, J. Chem. Phys. 23, 1833 (1955).

16. H. Basch, A. Viste and H. B. Gray, Theoret. Chim. Acta (Bul.) 3, 458 (1965).

17. F. Herman and S. Skillman, Atomic Structure Calculations (Prentice-Hall, Englewood Cliffs, N. J., 1960).

18. G. Burns, J. Chem. Phys. 41, 1521 (1964).

19. L. L. Lohr, Jr. and W. N. Lipscomb, Inorg. Chem. 3, 22 (1964).

20. W. Lotz, J. Opt. Soc. of Am. 60, 206 (1970).

21. F. A. Cotton and C. B. Harris, Inorg. Chem. 6, 376 (1967).

22. L. Pauling, The Nature of the Chemical Bond, 3rd Ed., (Cornell University Press, 1960).

23. R. L. Park in: The Structure and Chemistry of Solid Surfaces, Ed. G. A. Somorjai (Wiley, New York, 1969) p. 28-1.

24. K. Ruedenberg and C. Edmiston, Rev. Mod. Phys. 35, 457 (1963).

25. R. Gomer, R. Wortman and R. Lundy, J. Chem. Phys. 26, 1147 (1957).

26. L. F. Mattheiss, Phys. Rev. 139, A1893 (1965).

Table I. Atomic orbital parameters for Extended Hückel Molecular
Orbital calculations. Orbital exponents are for Slater type
orbitals. Valence orbital ionization potential (VOIP)
parameters reflect dependence of VOIP on charge q
according to VOIP = Aq^2 + Bq + C.

Atom	Orbital	Orbital Exponent	A (ev/$\|e\|^2$)	B (ev/$\|e\|$)	C (ev)
Hydrogen	1s	1.20	13.60	27.20	13.60
Tungsten	5p	4.91	0.00	0.00	46.07
	5d	2.20	0.00	3.50	9.00
	6s	1.40	0.00	3.50	8.00

Table II. Occupied molecular orbitals for the diatomic molecules, W-W and W-H.

W-W	Ψ_1	Ψ_2	Ψ_3	Ψ_4	Ψ_5	Ψ_6
Energy (ev)	(-10.63)	(-10.57)	(-10.57)	(-9.57)	(-9.57)	(-9.23)
W(1,2)						
$5d_{z^2}$	-.16					-.63
$5d_{xz}$		±.62				
$5d_{x^2-y^2}$				.68		
$5d_{yz}$			±.62			
$5d_{xy}$					.68	
6s	.52					-.16

W-H	Ψ_1	Ψ_2	Ψ_3	Ψ_4	Ψ_5
Energy (ev)	(-12.23)	(-9.42)	(-9.42)	(-9.42)	(-9.42)
H					
1s	-.62				
W					
$5d_{z^2}$	-.47				
$5d_{xz}$		1.00			
$5d_{x^2-y^2}$			1.00		
$5d_{yz}$				1.00	
$5d_{xy}$					1.00
6s	-.26				

Table III. Energies, equilibrium distances, and charges for
hydrogen bonded to different W(100) surface sites.

Site	Bond Energy (ev)	r_e (Å)	Charge $|e|$
1 CN	3.00	1.65	-.36
2 CN	2.74	1.96	-.26
5 CN	1.72	1.61	+.04

Table IV. Totally symmetric molecular orbitals for the surface arrays representing the 1 CN and 5 CN sites.

Molecular Orbital Energy (ev)	Ψ_1 (-12.43)	Ψ_2 (-10.69)	Ψ_3 (-10.38)	Ψ_4 (-9.77)	Ψ_5 (-8.47)
W(1)					
$5d_{z^2}$		-.54		-.10	-.19
6s	-.24				
W(2, 3, 4, 5)					
$5d_{z^2}$		.22	.17	.16	
$5d_{xz}$ (2, 5)		±.15		±.31	±.07
$5d_{x^2-y^2}$		±.12	±.30	±.19	±.05
$5d_{yz}$ (3, 4)		±.15		±.31	±.07
6s	-.18				
W(6, 7, 8, 9)					
$5d_{z^2}$		-.10	-.19		.26
$5d_{xz}$			±.11		±.28
$5d_{yz}$			±.11		±.28
$5d_{xy}$		±.12		±.22	±.10
6s	-.12				

Table V.   Totally symmetric molecular orbitals for the surface array representing the 2 CN site.

	ψ_1 (-12.78)	ψ_2 (-11.31)	ψ_3 (-10.87)	ψ_4 (-10.82)	ψ_5 (-10.25)	ψ_6 (-10.03)	ψ_7 (-9.68)	ψ_8 (-9.62)	ψ_9 (-8.97)	ψ_{10} (-8.72)	ψ_{11} (-8.32)
W(1,2)											
$5d_z2$			-.36	-.09		-.08	.09	-.15			.15
$5d_{x2-y2}$		.33			-.19	-.06	-.05	-.08	-.30	-.14	.08
$5d_{yz}$		±.12	±.08	±.32	±.21		±.17	±.18	±.10	±.12	
$6s$	.18										
W(3,4)											
$5d_z2$			.36	-.09		-.08	-.09	-.15			-.15
$5d_{xz}$		±.12	±.08	±.32	±.21		±.17	±.18	±.10	±.12	
$5d_{x2-y2}$		-.33			-.19	.05	.05	+.08	-.30	.14	.08
$6s$	.18										
W(5, 6, 7, 8)											
$5d_z2$			.12	.05	-.17	.07	.08	.06	.08	-.12	.11
$5d_{xz}$			±.05	±.07	±.14	±.23		±.09			±.26
$5d_{x2-y2}$		-.13	.05	-.11	.10	-.16	.05		-.20	-.05	-.14
$5d_{yz}$						±.07	±.13	±.19	±.14	±.24	±.10
$5d_{xy}$				±.12		±.08	±.24	±.18	±.09	±.18	±.08
$6s$	.10										
W(9, 10, 11, 12)											
$5d_z2$			.12	±.05	.17	.07	.08	.06	.08	-.12	-.11
$5d_{xz}$						±.07	±.13	±.19	±.14	±.24	±.10
$5d_{x2-y2}$		.13	±.05	.11	.10	.16	.05		±.20	.05	-.14
$5d_{yz}$			±.05	±.07	±.14	±.23		±.09			±.26
$5d_{xy}$				±.12		±.08	±.24	±.18	±.09	±.18	±.08
$6s$	.10										

Table VI. Totally symmetric molecular orbitals for the W_9H surface "molecule" where hydrogen is bonded at a 1 CN site.

Molecular Orbital Energy (ev)	Ψ_1'' (-12.74)	Ψ_2' (-11.52)	Ψ_3' (-10.39)	Ψ_4' (-10.01)	Ψ_6 (-9.66)	Ψ_5' (-8.46)
H						
1s	.36	-.49	-.06	.36	.26	-.05
W(1)						
$5d_{z2}$	.16	-.52		-.06		.12
6s	.24	.06		.05		
W(2,3,4,5)						
$5d_{z2}$		.07	-.22	.11	.26	
$5d_{xz}$ (2,5)		±.05		±.30	±.19	±.06
$5d_{x2-y2}$		±.06	±.27	±.10	±.27	±.08
$5d_{yz}$ (3,4)		±.05		±.30	±.19	±.06
6s	.13	.11		-.08	-.05	
W(6,7,8,9)						
$5d_{z2}$			.21		-.07	-.26
$5d_{xz}$			±.11			±.28
$5d_{yz}$			±.11			±.28
$5d_{xy}$		±.04		±.22	±.12	±.11
6s	.10	.07				

Table VII. Totally symmetric molecular orbitals for the $W_{12}H$ surface "molecule" where hydrogen is bonded at a 2 CN site.

Molecular Orbital	Ψ'_1	Ψ'_2	Ψ'_4	Ψ'_3	Ψ'_5	Ψ'_6	Ψ'_7	Ψ'_8	Ψ'_9	Ψ'_{10}	Ψ'_{12}	Ψ'_{11}
Energy (ev)	(-13.15)	(-11.82)	(-11.25)	(-10.85)	(-10.57)	(-10.03)	(-9.84)	(-9.65)	(-9.38)	(-8.73)	(-8.62)	(-8.32)
H												
$1s$	.35	-.44	.13	-.02	-.16	-.02	.18	-.04	-.22	.06	-.21	.02
W(1,2)												
$5d_{z^2}$		.05		-.36	-.09	.08		.16	-.09			.15
$5d_{x^2-y^2}$	-.07	.26	.24		.09			.10	-.10	-.05	-.19	.08
$5d_{yz}$	±.09	±.24	±.27	±.13			±.07		±.14	±.13		
$6s$	.18									-.05		
W(3,4)												
$5d_{z^2}$		-.09	.11	.25	.22	.09	-.16	.06	-.07			-.15
$5d_{xz}$			±.14	±.23	±.31				±.25	±.04	±.07	±.16
$5d_{x^2-y^2}$		-.08	-.32		.15	-.07	.11		.13	.24	-.26	.12
$6s$	.15	.10										
W(5, 6, 7, 8)												
$5d_{z^2}$				.13	.09	-.09	.18			-.12	-.05	.13
$5d_{xz}$		±.05				±.21	±.14		±.20	±.07	±.21	±.23
$5d_{x^2-y^2}$		-.08	-.08		.08	.18	-.11	.06	.26			-.16
$5d_{yz}$			±.06	±.05		±.07	-.14		±.21	±.25		±.10
$5d_{xy}$			±.03	±.09	±.06	±.08	±.05	±.30		±.13	±.15	±.08
$6s$	.06	-.09								.05	-.06	.08
W(9, 10, 11, 12)												
$5d_{z^2}$				-.08	-.17	-.05	-.11	-.09	.07	-.08	-.15	-.08
$5d_{xz}$			±.05			±.06	±.05	±.24	±.05	±.18	±.19	±.11
$5d_{x^2-y^2}$			.14	.09	-.13	-.15		.06	.10	.12	-.20	-.11
$5d_{yz}$				±.07	±.10	±.25	±.09	±.06				±.28
$5d_{xy}$					±.11	±.06	±.26	±.08	±.13	±.21	±.07	±.10
$6s$	.08	.06										

Table VIII. Totally symmetric molecular orbitals for the W_9H surface "molecule" where hydrogen is bonded at a 5 CN site.

| Molecular Orbital | Ψ_1' | Ψ_2' | Ψ_3' | Ψ_4' | Ψ_5' | Ψ_6 |
Energy (ev)	(-13.22)	(-11.75)	(-10.42)	(-9.96)	(8.62)	(7.36)
H						
1s	.44	.29	-.04	-.11	-.13	.17
W						
$5d_{z^2}$	.19	.38	.15	.10	-.11	.54
6s	.16	-.17				
W(2, 3, 4, 5)						
$5d_{z^2}$	-.05	-.11	-.23	.09	-.08	.38
$5d_{xz}$ (2, 5)				±.35		
$5d_{x^2-y^2}$	±.08	±.15	±.25		±.05	±.16
$5d_{yz}$ (3, 4)				±.35		
6s	.12	-.11				
W(6, 7, 8, 9)						
$5d_{z^2}$				.21	.25	.17
$5d_{xz}$				±.10	±.28	
$5d_{yz}$				±.10	±.28	
$5d_{xy}$				-.25	.08	±.12
6s	.06	-.11				-.05

Figure Captions

Figure 1. Surface arrays used to model adsorption on different W(100) surface sites.

Figure 2. Dependence of bond energy on bond distance for W_2 (left figure) and WH (right figure) molecules with and without inclusion of W 5p orbitals.

Figure 3. Dependence of non-bonding (5p orbital) repulsive energy on distance for W_2 and WH molecules.

Figure 4. Additivity of non-bonded orbital repulsive energy.

(a) Difference in E(r) for W_2H between calculations including and omitting W 5p orbitals.

(b) E(r) calculated by pairwise addition of analytic repulsive energy functions.

Figure 5. Bond energies as functions of distances for hydrogen adsorbed on different W(100) surface sites.

Figure 6. Molecular orbital-energy diagrams for the totally symmetric occupied orbitals for hydrogen adsorbed on different W(100) surface sites.

A) 5 CN SITE   B) I CN SITE   C) 2 CN SITF

Figure 1. Surface arrays used to model adsorption on different W(100) surface sites.

Figure 2. Dependence of bond energy on bond distance for W_2 (left figure) and WH (right figure) molecules with and without inclusion of W 5p orbitals.

Figure 3. Dependence of non-bonding (5p orbital) repulsive
energy on distance for W_2 and WH molecules.

Figure 4.   Additivity of non-bonded orbital repulsive energy.

(a) Difference in E(r) for W_2H between calculations including and omitting W 5p orbitals.

(b) E(r) calculated by pairwise addition of analytic repulsive energy functions.

Figure 5. Bond energies as functions of distances for hydrogen adsorbed on different W(100) surface sites.

Figure 6. Molecular orbital-energy diagrams for the totally
symmetric occupied orbitals for hydrogen adsorbed
on different W(100) surface sites.

APPENDİX B.

A MOLECULAR ORBITAL INVESTIGATION OF

CHEMISORPTION. II. NITROGEN ON TUNGSTEN (100) SURFACE

A Molecular Orbital Investigation of

Chemisorption. II. Nitrogen on Tungsten (100) Surface

LEON W. ANDERS AND ROBERT S. HANSEN

Ames Laboratory-USAEC and Department of Chemistry
Iowa State University, Ames, Iowa 50010

AND

L. S. BARTELL

Department of Chemistry, University of Michigan
Ann Arbor, Michigan 48104

Abstract

The relative bonding energies of nitrogen chemisorbed at three
symmetric sites on a W(100) surface, represented by finite arrays of
tungsten atoms,[1] were obtained by means of the Extended Hückel
Molecular Orbital Theory (EHMO). The preferred site for nitrogen
chemisorption was found to be the five coordination number (5 CN) site
or the fourfold site with a tungsten atom below four tungsten atoms
surrounding the nitrogen atom. The 5p orbital repulsive energy, in
the case of hydrogen chemisorption, could be adequately approximated
by the sum over pairs of empirical exponential repulsive terms; in the
case of nitrogen chemisorption this same method was approximately

10% in error at the equilibrium bond distance, and repulsive energies
were therefore obtained from calculations including tungsten 5p
orbitals but with smaller arrays.

I. INTRODUCTION

In a previous paper,[1] the Extended Hückel Molecular Orbital
(EHMO) technique was applied to the bonding of hydrogen to a finite
cluster of tungsten atoms representing a truncated tungsten (100)
surface. The relative stabilities of hydrogen bonded at the three
symmetric sites of a tungsten (100) surface were compared. In addition,
the contributions made by the various orbitals of the surface atoms were
investigated. According to the calculations, hydrogen will preferentially
chemisorb on top of a surface tungsten atom forming a bond closely
resembling that of a WH diatomic molecule.

In this paper this same molecular orbital (EHMO) technique has
been used to investigate the bonding of nitrogen on a tungsten (100) surface.
The nitrogen atom differs from the hydrogen atom particularly in its
ability to form multiple bonds with the surface. The present calculations
should be able to assess the influence of the additional nitrogen orbitals
on a preferred chemisorption site.

II. PROCEDURE

The EHMO theory as formulated by Hoffmann[2] and described in our previous paper[1] has been used to investigate the preferred structure of the W_nN surface "molecule" consisting of nitrogen chemisorbed on a truncated W(100) surface. The surface arrays which represent the three symmetric sites for chemisorption on this surface are shown in Fig. 1. These are the same sites previously described.[1]

Table I lists the orbital exponents for the Slater type orbitals (STO) of the nitrogen 2s and 2p orbitals derived from Slater's rules.[3] It also includes values, taken from the work of Bacch, Viste and Gray,[4] for the parameters A, B, and C which are needed to calculate the valence orbital ionization potential (VOIP) as a function of charge,[1] i. e.,

$$VOIP = Aq^2 + Bq + C \ .$$
$$(1)$$

The EHMO technique was first applied to the WN diatomic molecule. A comparison of curves a and b in Fig. 2 shows that it is necessary to include the 5p orbitals of the tungsten atom as well as the valence orbitals in the basis set to obtain a characteristic potential energy curve. The population of these non-bonding orbitals provides the repulsion needed at small internuclear separations. This repulsive energy can be approximated by

$$E_R = A_e^{-r/\alpha} \ .$$
$$(2)$$

As the nitrogen atom forms a surface molecule, hopefully the repulsive

energy for nitrogen interacting with a larger group of tungsten atoms

can be approximated by the pairwise summation of exponential terms

according to Eq. (2).

III. RESULTS

A. Diatomic Molecule

In Fig. 2, the bonding energy is plotted as a function of inter-

nuclear separation r along the molecular axis z for the WN molecule.

The bonding energy was calculated by subtracting from the total energy

(energy of the occupied molecular orbitals), the energy of the ions of

the W-N molecule at infinite separation.[1] The difference between

curves a and b in Fig. 2 is the repulsive energy resulting from the

presence of the 5p orbitals of tungsten in the basis set. In Fig. 3

$\ln E_{Rep}$ is plotted as a function of internuclear separation r. Values

for the parameters A and α needed to calculate the repulsive energy

according to Eq. (2) were found from this plot to be A_{WN} = 2324.8 ev

and α_{WN} = .234Å^{-1}. For the final iteration, the charge on the

nitrogen atom in the WN molecule at equilibrium separation was -.38

and that on the tungsten atom +.38.

Single bond covalent radii (0.70Å for N and 1.30Å for W)

predict a length of 2.00Å for a W-N single bond. Pauling's empirical

relationship[5] between bond length and bond order (see previous paper[1]),

coupled with the 1.65Å equilibrium bond length indicated by Fig. 2,

gives a value of 3.1 for the bond order of the WN molecule. Table II,

which lists the LCAO for the occupied molecular orbitals of the WN

molecule, shows that there are three molecular orbitals (Ψ_2, Ψ_3 and

Ψ_4) which make major contributions to the bonding; this suggests that

the bond order of 3.1 is a plausible value.

Figure 4 compares the W_2N molecule repulsive energies

determined (curve a) as the difference between the energies calculated

by the EHMO technique with the inclusion and omission of the tungsten

5p orbitals and (curve b) by summing analytical exponential terms

over pairwise interactions. There is about a 10% difference in the

repulsive energies in the neighborhood where the chemical bond is

formed. Because of this difference, larger molecules (W_4N and W_5N)

which still lended themselves to easy computation were investigated;

these molecules are reductions of the surface arrays in Fig. 1. The

tungsten atoms omitted from the surface arrays in Fig. 1 for the above

calculations are at a sufficient distance from the nitrogen atom at each

of the symmetric sites that their 5p orbitals should not contribute to

the repulsive energy when the larger surface arrays are used. In

Fig. 5 the repulsive energies between the nitrogen atom at each of the

bonding sites and the tungsten atoms in the above molecules are plotted.

Curves a in Fig. 5 are based on repulsive energies calculated

from the W_5N or W_4N arrays as explained above, curves b by pair-wise summation of analytical exponential terms. Repulsive energies at bonding distances obtained from curves a are 10% higher for 1 CN site, about the same for the 2 CN site, and about 10% lower for the 5 CN site than those obtained from curves b. Approximation of repulsive energy by pairwise summation of exponential terms (Eq. 2) was therefore judged insufficiently reliable, and it was approximated instead from direct calculations on the abbreviated arrays W_4N and W_5N.

B. Nitrogen Chemisorbed on a W(100) Surface

The adjustments of the VOIP of the edge atoms of the surface arrays in Fig. 1 to reduce charge transfer were the same as those previously adopted.[1] The VOIP of the orbitals of the nitrogen atom were iterated at equilibrium separation to self consistency for charge q at each of the three symmetric sites. On the final iteration, the VOIP for the 2s and 2p orbitals of nitrogen were: -18.93 ev and -10.01 ev at the 5 CN site, -17.17 ev and -8.93 ev at the 2 CN site and -17.31 ev and -9.02 ev at the 1 CN site. To avoid possible oversensitivity of results to VOIP parametrization, the calculations were repeated using -17.77 ev and -9.29 ev for the 2s and 2p orbitals of nitrogen respectively at all the sites. As in the case of hydrogen chemisorption[1] the same ordering in site preference was obtained by both methods

and constant nitrogen 2s and 2p VOIP's were used in further

calculations. The bonding energies as a function of internuclear

separation are plotted in Fig. 6. The internuclear separation was the

distance of nitrogen to the nearest tungsten atom(s) in the surface

atom arrays. In the case of the 5 CN site, it was the distance of the

tungsten atom in the hole, for the 2 CN site, it was the distance to the

two surface atoms, and for the 1 CN site, it was the distance to the

single tungsten atom. The bonding energy E was calculated according

to the following relationship:

$$E = \sum_{W_nN} n_i \epsilon_i - \sum_{W_n} n_i \epsilon_i - \sum_N n_i \epsilon_i + E_{Rep} \qquad (3)$$

where the first term is the summation over occupied molecular orbitals

of energy ϵ_i of the W_nN surface molecule, the next term is the summa-

tion over the occupied molecular orbitals of energies ϵ_i of the W_n part

of the molecule at infinite separation from the nitrogen atom and the

next term is the summation over the occupied atomic orbitals of energy ϵ_i

of the nitrogen atom also at infinite separation. The last term is the

repulsive energy E_{Rep} determined from the W_5N and W_4N molecules and

plotted as curves a in Fig. 5. Table III summarizes the results of

calculations plotted in Fig. 6.

The surface arrays in Fig. 1a and 1b belong to the C_{4v} symmetry

groups and the surface array in Fig. 1c to the C_{2v} symmetry group.[1]

In these groups, the 2s and $2p_z$ orbitals of nitrogen belong to the totally

symmetric a_1 irreducible representation. Therefore, these orbitals

of nitrogen can interact only with the totally symmetric molecular orbitals of the W_n surface arrays. In the C_{4v} symmetry group, the $2p_x$ and $2p_y$ orbitals of nitrogen belong to the e irreducible representation and will interact with molecular orbitals of the W_9 arrays which also belong to this representation. These same orbitals of nitrogen belong to the b_1 ($2p_x$) and b_2 ($2p_y$) irreducible representations in the C_{2v} symmetry group and interact with the molecular orbitals of the W_{12} array belonging to these same irreducible representations.

Molecular orbital energy diagrams for the molecular orbitals belonging to the totally symmetric a_1 irreducible representation are shown in Fig. 7. On the left side of each panel in these figures are the molecular orbitals from the W_n arrays, on the right side are the atomic orbitals of nitrogen and in the middle are the molecular orbitals for the W_nH surface "molecules". The occupied totally symmetric (a_1) molecular orbitals in Fig. 7 are tabulated in Tables IV and V for the W_9 and W_{12} arrays respectively. These can be compared with the totally symmetric molecular orbitals of the W_nN surface "molecules" (Table VI - 1 CN, Table VII - 2 CN and Table VIII - 5 CN). Because of the totally symmetric orbitals ($2s$ and $2p_z$) of nitrogen, there must be two additional totally symmetric molecular orbitals in the W_nN surface "molecule" than in the W_n "molecule". In Fig. 7a and 7c, these molecular orbitals are Ψ_6 and Ψ_7. For nitrogen bonded at the 1 CN

site (Fig. 7a) these molecular orbitals are lower in energy than the highest occupied molecular orbital (HOMO) and therefore are occupied, whereas at the 5 CN site (Fig. 7c) Ψ_7 is above the HOMO. At the 2 CN site (Fig. 7b) the additional molecular orbitals (Ψ_{12} and Ψ_{13}) of the $W_{12}N$ formed by the nitrogen 2s and $2p_z$ orbital interacting with the W_{12} surface array are below the HOMO but one of the totally symmetric orbitals (Ψ_{11}) has become unoccupied in the reordering of all the molecular orbitals in the $W_{12}N$ surface "molecule".

In Fig. 8, molecular orbital energy diagrams are shown which involve the $2p_x$ and $2p_y$ orbitals of nitrogen. In the case of the W_9 arrays for the 1 CN and 5 CN sites (Fig. 8a and c) these molecular orbitals belong to the e irreducible representations and for the 2 CN site (Fig. 8b) they belong to the b_1 and b_2 irreducible representations. The molecular orbitals represented in Fig. 8 for the W_9 and W_{12} are tabulated in Tables IX and X respectively. These can be compared with the molecular orbitals of the W_nN surface "molecule" (Table XI - 1 CN, Table XII - 2 CN, Table XIII - 5 CN).

The additional molecular orbitals formed by the $2p_x$ and $2p_y$ atomic orbitals of nitrogen as they interact with the W_n surface arrays are Ψ_{15} and Ψ_{16} in the case of the W_9N and Ψ_{19} and Ψ_{20} in the $W_{12}N$ surface "molecules". The molecular orbitals Ψ_{19} and Ψ_{20} of the $W_{12}N$ "molecule" are below the highest occupied molecular

(HOMO) and are therefore occupied. But in the case of the W_9N "molecules", Ψ_{15} and Ψ_{16} (having the same energy) are the HOMO; these molecular orbitals of the W_9N "molecule" with nitrogen at the 1 CN site (Fig. 8a) are occupied with a single electron, whereas at the 5 CN site (Fig. 8c), they are occupied with three electrons.

IV. DISCUSSION

Low-energy electron-diffraction (LEED)[6] has indicated that nitrogen adsorbed on a W(100) surface produces a C(2x2) structure and flash desorption spectrometry (FDS)[7] indicates it desorbs as a single β state. It has been proposed that this adsorbed structure has only half the surface sites occupied with atomic species. Estrup and Anderson[6] originally proposed that the preferred chemisorption sites are alternate 5 CN sites. It has also been shown that a molecular bound state can be converted to another β state, presumably also atomically adsorbed nitrogen,[7,8] and proposed that these atoms could be filling 5 CN sites unoccupied in the original C(2x2) structure.

Our calculations indicate that nitrogen prefers the 5 CN site. At this site, the σ bond formed by the 2s and $2p_z$ atomic orbitals of nitrogen with the atoms of the surface array is not as favorable as at the other sites (Fig. 7); hydrogen also formed a weaker σ-bond at this site.[1] But in the case of nitrogen the $2p_z$ and $2p_y$ atomic orbitals

interact more favorably with the tungsten atoms surrounding the 5 CN site (Fig. 8) than at the other sites, and this factor dominates the selection of the 5 CN site for chemisorption. As Table XIII shows, these atomic orbitals are able to form the lowest energy molecular orbitals of e symmetry at the 5 CN site because of their overlap with the appropriate d orbitals of the four surrounding tungsten atoms.

REFERENCES

1. L. W. Anders, R. S. Hansen and L. S. Bartell, J. Chem. Phys. (In press).

2. R. Hoffman, J. Chem. Phys. 39, 1397 (1963).

3. J. C. Slater, Phys. Rev. 36, 57 (1930).

4. H. Basch, A. Viste and H. B. Gray, Theoret. Chim. Acta (Bul.), 3, 458 (1965).

5. L. Pauling, The Nature of the Chemical Bond, 3rd Ed., (Cornell University Press, 1960).

6. P. J. Estrup and J. Anderson, J. Chem. Phys. 46, 567 (1967).

7. L. R. Clavenna and L. D. Schmidt, Surface Sci. 22, 365 (1970).

8. J. T. Yates, Jr. and T. E. Madey, in Proc. Berkeley Intern Mater. Conf. 4th, University of California, Berkeley, June 1968 (1969) p. 19-1.

9. R. S. Mulliken, J. Chem. Phys. 23, 1833 (1955).

Table I. Orbital exponents for STO of the nitrogen atom and parameters needed to calculate VOIP as a function of atomic charge.

Orbital	Orbital Exponent	A $[ev/(e)^2]$	B $[ev/e]$	C $[ev]$
2s	1.950	3.48	20.25	28.02
2p	1.950	3.72	14.14	16.05

Table II. Occupied molecular orbitals for the diatomic molecule WN.

W-N Energy (ev)	Ψ_1 -21.61	Ψ_2 -12.74	Ψ_3 -12.74	Ψ_4 -11.51	Ψ_5 -10.29	Ψ_6 -10.29
N						
2s	.86			.13		
$2p_z$	.08			.72		
$2p_x$		-.69				
$2p_y$			-.69			
W						
$5d_z2$	.21			-.48		
$5d_x2$		-.54				
$5d_{x2-y2}$					1.00	
$5d_{yz}$			-.54			
$5d_{xy}$						1.00
6s	.13			.29		

Table III. Energies, equilibrium distances, and charges for
nitrogen bonded to different W(100) surface sites.

Site	Bond Energy ($\overset{\circ}{A}$)	r_e ($\overset{\circ}{A}$)	Charge
5 CN	-3.25	2.05	-.04
2 CN	-3.15	2.13	-1.36
1 CN	-2.85	1.88	-1.13

Table IV. Totally symmetric molecular orbitals for the surface arrays representing the 1 CN and 5 CN sites.

Molecular Orbital Energy (ev)	Ψ_1 (-12.43)	Ψ_2 (-10.69)	Ψ_3 (-10.38)	Ψ_4 (-9.77)	Ψ_5 (-8.47)
W(1)					
$5d_{z^2}$		-.54		-.10	-.19
6s	-.24				
W(2,3,4,5)					
$5d_{z^2}$		.22	.17	.16	
$5d_{xz}$ (2,5)		±.15		±.31	±.07
$5d_{x^2-y^2}$		±.12	±.30	±.19	±.05
$5d_{yz}$ (3,4)		±.15		±.31	±.07
6s	-.18				
W(6,7,8,9)					
$5d_{z^2}$		-.10	-.19		.26
$5d_{xz}$			±.11		±.28
$5d_{yz}$			±.11		±.28
$5d_{xy}$		±.12		±.22	±.10
6s	-.12				

Table V.   Totally symmetric molecular orbitals for the surface array representing the 2 CN site.

	ψ_1 (-12.78)	ψ_2 (-11.31)	ψ_3 (-10.87)	ψ_4 (-10.82)	ψ_5 (-10.25)	ψ_6 (-10.03)	ψ_7 (-9.68)	ψ_8 (-9.62)	ψ_9 (-8.97)	ψ_{10} (-8.72)	ψ_{11} (-8.32)
W(1,2)											
$5d_{z^2}$			-.36	-.09		-.08	.09	-.15			.15
$5d_{x^2-y^2}$		.33			-.19	-.06	-.05	-.08	-.30	-.14	.08
$5d_{yz}$		±.12	±.08	±.32	±.21		±.17	±.18	±.10	±.12	
$6s$	.18										
W(3,4)											
$5d_{z^2}$			.36	-.09		-.08	-.09	-.15			-.15
$5d_{xz}$		±.12	±.08	±.32	±.21		±.17	±.18	±.10	±.12	
$5d_{x^2-y^2}$		-.33			-.19	.05	.05	+.08	-.30	.14	.08
$6s$	.18										
W(5, 6, 7, 8)											
$5d_{z^2}$			.12	.05	-.17	.07	.08	.06	.08	-.12	.11
$5d_{xz}$			±.05	±.07	±.14	±.23		±.09			±.26
$5d_{x^2-y^2}$		-.13	.05	-.11	.10	-.16	.05		-.20	-.05	-.14
$5d_{yz}$						±.07	±.13	±.19	±.14	±.24	±.10
$5d_{xy}$				±.12		±.08	±.24	±.18	±.09	±.18	±.08
$6s$	.10										
W(9, 10, 11, 12)											
$5d_{z^2}$			.12	±.05	.17	.07	.08	.06	.08	-.12	-.11
$5d_{xz}$						±.07	±.13	±.19	±.14	±.24	±.10
$5d_{x^2-y^2}$		.13	±.05	.11	.10	.16	.05		±.20	.05	-.14
$5d_{yz}$			±.05	±.07	±.14	±.23		±.09			±.26
$5d_{xy}$				±.12		±.08	±.24	±.18	±.09	±.18	±.08
$6s$	.10										

Table VI. Totally symmetric molecular orbital for W_9N surface "molecule" where nitrogen is bonded at a 1 CN site.

Molecular Orbital Energy (ev)	Ψ_6 (-18.33)	Ψ_1' (-12.17)	Ψ_2' (-10.57)	Ψ_3' (-10.38)	Ψ_4' (-9.82)	Ψ_7 (-9.47)	Ψ_5' (-8.43)
N							
2s	.89	-.14	-.21	.04	.04	.03	
$2p_z$		-.03	.46	-.10	-.33	-.65	-.12
W(1)							
$5d_{z^2}$	.17	-.21	.38	-.05	-.07	-.06	.08
6s	.11	.19	-.07				
W(2, 3, 4, 5)							
$5d_{z^2}$			-.21	-.16	.07	-.25	-.08
$5d_{xz}(2, 5)$			±.12	±.06	±.33		±.05
$5d_{x^2-y^2}$			±.08	±.30	±.11	±.22	±.10
$5d_{yz}(3, 4)$			±.12	±.06	±.33		±.05
6s		.18	.08				
W(6, 7, 8, 9)							
$5d_{z^2}$				.10	.19	.10	-.25
$5d_{xz}$					±.11	±.05	±.28
$5d_{yz}$					±.11	±.05	±.28
$5d_{xy}$			±.10		±.23		±.12
6s		.12					

Table VII. Totally symmetric molecular orbitals for the $W_{12}N$ surface "molecule", where nitrogen is bonded at a 2 CN site.

Molecular Orbital	Ψ_{12}	Ψ_1	Ψ_2	Ψ_3	Ψ_4	Ψ_5	Ψ_6	Ψ_7	Ψ_8	Ψ_9	Ψ_{10}	Ψ_{13}	Ψ_{11}
Energy (ev)	(-18.47)	(-12.42)	(-11.35)	(-10.98)	(-10.63)	(-10.22)	(-10.03)	(-9.79)	(-9.62)	(-9.33)	(-8.72)	(-8.55)	(-8.26)
N													
2s	-.86	-.17	.05	.05	-.10	-.16	-.05	.03	-.08		.03	-.03	.03
$2p_z$		.02	.18	.26	-.26	-.47	-.05	.34	-.16	.32	-.01	.28	.17
W(1, 2)													
$5d_{z^2}$			.09	.36			.07	.07	.11	-.07			-.09
$5d_{x^2-y^2}$	.06		.32		.06	-.14			.07	.12	-.08	-.14	-.08
$5d_{yz}$	±.11	±.14	±.14	±.08	±.15	±.17	±.07	±.11	±.13	±.09	±.12		±.06
6s	±.09	.13				-.05							
W(3, 4)													
$5d_{z^2}$				-.31	.14	-.12	.09	.19	-.05	-.05	-.09	-.15	.18
$5d_{xz}$			±.14	±.08	±.37			±.16	±.19	±.07	±.20	±.23	±.08
$5d_{x^2-y^2}$			-.31	.12	.10	-.14	-.11	-.06		.17			-.16
6s		.18				-.05							
W(5, 6, 7, 8)													
$5d_{z^2}$				-.09		-.17	-.14	-.10			-.12		-.14
$5d_{xz}$				±.05		±.16	±.17	±.10		±.19	±.05	±.29	±.13
$5d_{x^2-y^2}$			-.12		.09		.20	.08	.08	.22			.17
$5d_{yz}$			±.05	±.05				±.15	±.08	±.20	±.25		±.10
$5d_{xy}$					±.11		±.08	±.07	±.30	±.11	±.14	±.06	±.05
6s		.12				.05					-.05		
W(9, 10, 11, 12)													
$5d_{z^2}$				.10		.16			-.08	.09	-.10	-.16	
$5d_{xz}$			±.06				±.06	±.17	±.17		±.21	±.14	±.15
$5d_{x^2-y^2}$			.11	-.09		.06	-.13	.07		.11	.10	-.22	.08
$5d_{yz}$							±.26	±.08	±.17				±.31
$5d_{xy}$						±.07		±.22		±.08	±.20	±.07	±.12
6s		.10											

Table VIII - Totally symmetric molecular orbitals for the W_9N surface molecule where nitrogen is bonded at a 5 CN site.

Molecular Orbital Energy (ev)	Ψ_6 (-18.71)	Ψ_1' (-11.97)	Ψ_2' (-10.70)	Ψ_3' (-10.36)	Ψ_4' (-9.39)	Ψ_5' (-8.61)	Ψ_7 (-7.49)
N							
$2s$	-.82	.11	.10		.17	-.09	.06
$2p_z$		-.11	.56	.25	.43	.02	-.21
W(1)							
$5d_z2$	-.12	.28	-.23	.09	-.31		.35
$6s$	-.06	-.21					.08
W(2, 3, 4, 5)							
$5d_z2$			.15	-.17	-.13	-.07	.22
$5d_{xz}(2, 5)$			±.21	±.18	±.16		±.21
$5d_x2_{-y}2$	±.06		±.08	±.24			±.17
$5d_{yz}(3, 4)$			±.21	±.18	±.16		±.21
$6s$	-.05	-.14					
W(6, 7, 8, 9)							
$5d_z2$			-.11	.19	.08	.24	
$5d_{xz}$			±.05	±.07	±.06	±.30	
$5d_{yz}$			±.05	±.07	±.06	±.30	
$5d_{xy}$			±.06	±.10	±.29		±.35
$6s$		-.13			-.09		

Table IX. Molecular orbitals which belong to the e representation in the C_{4v} symmetry group for the W_9 surface arrays representing the 1 CN and 5 CN sites.

Molecular Orbital / Energy (ev)	Ψ_1 (-10.68)	Ψ_2	Ψ_3 (-10.17)	Ψ_4	Ψ_5 (-9.71)	Ψ_6	Ψ_7 (-9.58)	Ψ_8	Ψ_9 (-9.24)	Ψ_{10}	Ψ_{11} (-8.91)	Ψ_{12}	Ψ_{13} (-8.80)	Ψ_{14}
W(1)														
$5d_{xz}$	-.50	.10			.21		.19		.06	.08	-.19		-.07	-.37
$5d_{yz}$	.10	.50			-.21			.19	-.08	.06		-.19	.37	-.07
W(2, 5)														
$5d_{z2}$	±.16		±.13	±.15		±.26	±.11		±.14	±.18	±.10			±.07
$5d_{xz}$	-.23	.05		-.05		.13			-.17	-.22	-.29			.10
$5d_{x2-y2}$	±.12		±.17	±.21		±.14		±.26	±.17	±.22	±.07			
$5d_{yz}$		-.17	.16	-.13	-.16			.35				-.08	.05	
$5d_{xy}$		±.22	±.19	±.15	±.07							±.32	±.07	
6s			±.07	±.08		±.20	±.20		±.12	±.16				±.08
W(3, 4)														
$5d_{z2}$		±.16	±.15	±.13	±.26			±.11	±.18	±.14		±.10	±.07	
$5d_{xz}$	.17		.13	.16		.16	.35				-.08			-.05
$5d_{x2-y2}$		±.12	±.21	±.17	±.14			±.26	±.22	±.17		±.07		
$5d_{yz}$	.05	.23	.05		-.13				.22	-.17		-.29	-.10	
$5d_{xy}$	±.22		±.15	±.18		±.07					±.32			±.07
6s			±.08	±.07	±.20			±.20	±.16	±.12			.08	
W(6, 9)														
$5d_{z2}$			±.21		±.14	±.10					±.26	±.32	±.08	±.11
$5d_{xz}$	.08	-.09	-.08	.19	-.07		.18	.09		.09	.09	-.11	-.21	.11
$5d_{x2-y2}$	±.09	±.06		±.11	±.17	±.24			±.18		±.10	±.08	±.17	±.12
$5d_{yz}$	.06	-.11	-.05	-.20	-.06	.05		.19		.10	-.13	.07		.24
$5d_{xy}$	±.08	±.10	±.07		±.08	±.05				±.26	±.09	±.11	±.25	±.37
6s			±.10		±.19	±.14	±.15	±.18		±.23		±.05	±.05	±.08
W(7, 8)														
$5d_{z2}$				±.21	±.10	±.14			±.05		±.32	±.26	±.11	±.08
$5d_{xz}$	.11	.06	.20	-.05	.05	.06	.19		.10		.07	.13	.24	
$5d_{x2-y2}$	±.06	±.09	±.11		±.24	±.17				±.18	±.08	±.10	±.12	±.17
$5d_{yz}$	-.09	-.08	.19	.08		-.07	.09	.18			.11	.09	-.11	-.21
$5d_{xy}$	±.10	±.07		±.07	±.05	±.08				±.26	±.11	±.09	±.37	±.25
6s				±.10	±.14	±.19	±.18	±.15	±.23		±.05		±.08	±.05

Table X. Molecular orbitals which belong to the b_1 and b_2 representations in the C_{2v} symmetry group for the W_{12} surface array representing the 2 CN site.

Molecular Orbital	ψ_1	ψ_2	ψ_3	ψ_4	ψ_5	ψ_6	ψ_7	ψ_8	ψ_9	ψ_{10}	ψ_{11}	ψ_{12}	ψ_{13}	ψ_{14}	ψ_{15}	ψ_{16}	ψ_{17}	ψ_{18}
Energy (ev)	(-10.92)	(-10.92)	(-10.88)	(-10.88)	(-10.56)	(-10.56)	(-10.01)	(-10.01)	(-9.80)	(-9.80)	(-9.59)	(-9.59)	(-9.38)	(-9.38)	(-9.07)	(-9.07)	(-8.62)	(-8.62)
W(1,2)																		
d_{z^2}	±.18	±.15			±.10				±.18	±.19	±.09	±.07	±.10	±.08			±.14	±.05
d_{xz}	-.17	.21	-.06			-.08	-.10		.17	-.15			.20	-.24	-.13			-.08
$d_{x^2-y^2}$	±.17	±.14	±.05	±.09	±.11			±.05					±.12	±.10			±.27	±.10
d_{yz}						-.21	-.05	.08	-.23			.14	.11	-.19	-.16		.05	
d_{xy}	±.12	±.14	±.14	±.08	±.08	∓.37							±.09	±.11	±.20			±.11
$6s$				±.18	±.08													
W(3,4)																		
d_{z^2}	±.15	±.18			±.10				±.19	±.18	±.07	±.09	±.08	±.10			±.05	±.14
d_{xz}					.05	-.21	.23	.08			.11	-.14	.16	-.19				-.05
$d_{x^2-y^2}$	±.14	±.17	±.09	±.05	±.11	±.05							±.10	±.12			±.10	±.27
d_{yz}	-.21	-.17		-.06	±.08		.10	.15	.17				-.24	-.20		-.13	.08	
d_{xy}	±.14	±.12	±.08	±.14	±.37	±.08							±.11	±.09	±.20			±.11
$6s$			±.18	±.09	±.08													
W(5,8)																		
d_{z^2}	±.09				±.12	±.07			±.27	±.16	±.09	.08			±.09	±.14	±.14	
d_{xz}					-.11		±.23			.09		-.18	.11	.09	-.14	-.27	-.18	-.08
$d_{x^2-y^2}$		±.17			±.11	±.08					±.21	±.18	±.18	±.12	±.14	±.09		±.13
d_{yz}		.15					.09		.08	±.16	.18	.15	-.10			-.13	-.24	-.18
d_{xy}	±.08				±.07			±.30	±.07	±.09	±.08	±.08		±.20·	±.07	±.18		±.15
$6s$			±.23	±.16	±.12													
W(6,7)																		
d_{z^2}		±.09			±.07	±.10	±.09		±.14	±.28	±.06	±.11			±.10	±.13	±.12	±.07
d_{xz}					.10	.06	-.17	.16	±.08		.17	-.07	-.11	-.09	-.17	.26	.09	-.18
$d_{x^2-y^2}$	±.17				±.10		±.08				±.23	±.15	±.15	±.16	±.13	±.11	±.09	±.10
d_{yz}	.15					-.06	-.07	-.17	.06	.19	.13		±.10	.06	-.12	-.07	.29
d_{xy}		±.08			±.09	±.19	±.23	±.09	±.06	±.05	±.09	±.19			±.19	±.08	±.13
$6s$				±.28	±.10													
W(9,12)																		
d_{z^2}	±.09				±.10	±.07		.09	±.28	±.14	±.11	±.06			±.13	±.10	±.07	±.12
d_{xz}		-.15					.07	-.07	.06	.17	.13	-.19	.10	-.15	-.12	-.06	.29	.07
$d_{x^2-y^2}$		±.17			±.10		±.08				±.15	±.23	±.16	±.11	±.11	±.13	±.10	±.09
d_{yz}					-.10	.16	.17		-.08	.07	.17	-.09	-.19	-.26	-.17	.18	.09
d_{xy}	±.08				∓.04	±.21	±.19	±.06	±.09	±.09				±.19		±.13	±.08
$6s$			±.28	±.08	±.10													
W(10,11)																		
d_{z^2}		±.09			±.12		±.07	±.16	±.27	±.08	±.09			±.14	±.09		±.14	
d_{xz}	.15						.09	-.16	-.08	.15	-.18		-.10	-.13		-.18	.24
$d_{x^2-y^2}$	±.17				±.11		±.08			±.18	±.21	±.12	±.18	±.09	±.14	±.13	
d_{yz}					.11	-.23		-.09		.18		.09	-.11	.27	-.14	.08	-.18
d_{xy}		±.08			±.07	±.10		±.09	±.07	±.08	±.08	±.20		±.18	-.07	±.15
$6s$			±.16	±.23	±.12													

Table XI. Molecular orbitals which belong to the e representation for the W_9N surface "molecule" where nitrogen is bonded at a 1 CN site.

Molecular Orbital / Energy (ev)	Ψ_1	Ψ_2	Ψ_3	Ψ_4	Ψ_7	Ψ_8	Ψ_5	Ψ_6	Ψ_{13}	Ψ_{14}	Ψ_9	Ψ_{10}	Ψ_{11}	Ψ_{12}	Ψ_{15}	Ψ_{16}
	(-10.92)		(-10.19)		(-9.87)		(-9.70)		(-9.35)		(-9.24)		(-8.90)		(-8.23)	
N																
$2p_x$	-.37		.08	-.08		-.48			-.30	-.25		.05			-.46	.23
$2p_y$		-.37	-.08	-.08	.48				-.25	.30	.05				-.23	-.46
W(1)																
$5d_{xz}$	.55					.14	.10	.16			.05	-.12	-.05	-.06	-.19	.09
$5d_{yz}$		.55			-.14		-.16	.10			-.12	-.05	-.06	.05	-.09	-.19
W(2,5)																
$5d_{z^2}$	±.12		±.16	±.16			±.14	±.23	±.13	±.11	±.08	±.19	±.08	±.10	±.10	±.05
$5d_{xz}$	.19					-.13	.07	.11	-.05		-.11	.27	-.19	-.25		
$5d_{x^2-y^2}$	±.12	±.12	±.18	±.18			±.06	±.10	±.26	±.21	±.08	±.22			±.14	±.07
$5d_{yz}$		-.17	-.11	-.11	-.37		-.11	.07	-.11	.13			-.05		-.05	-.10
$5d_{xy}$			±.20	±.20	±.07		±.06		±.11	±.13			±.23	±.17		
$6s$			±.08	±.08		±.11	±.12	±.19	±.06	±.05	±.08	±.20		±.05	±.12	±.06
W(3,4)																
$5d_{z^2}$		±.12	±.16	±.16			±.23	±.14	±.11	±.13	±.19	±.08	±.10	±.08	±.05	±.10
$5d_{xz}$	-.12		.11	-.11		.37	.07	.11	-.13	-.11				-.05	-.10	.05
$5d_{x^2-y^2}$		±.12	±.18	±.18			±.10	±.06	±.21	±.26	±.22	±.08			±.07	±.14
$5d_{yz}$		.19			.13		-.11	.07		.05	.27	.11	-.25	.19		
$5d_{xy}$	±.17		±.20	±.20		±.07		±.06	±.13	±.11			±.17	±.23		
$6s$			±.08	±.08	±.11		±.19	±.12	±.05	±.06	±.20	±.08	±.05		±.06	±.12
W(6,9)																
$5d_{z^2}$				±.20	±.05	±.05		±.17				±.05	±.42	±.05		
$5d_{xz}$	-.07	-.06	.18	.09		.16		.06	-.20		-.05	-.06	-.11	.16	.22	
$5d_{x^2-y^2}$	±.05	±.05	±.08		±.13	±.11	±.28	±.08		±.12	±.15	±.07		±.06	±.10	±.29
$5d_{yz}$	-.06	-.07	-.18	.09	-.16			.07	-.20			-.07	-.06	-.18	.19	.11
$5d_{xy}$	±.05	±.05		±.10	±.07	±.08		±.10		±.24	±.13	±.29			±.30	±.10
$6s$				±.12	±.09	±.11	±.06	±.25		±.09	±.10	±.22	±.09			±.11
W(7,8)																
$5d_{z^2}$			±.20		±.05	±.05	±.17				±.05		±.05	±.42		
$5d_{xz}$	-.07	.06	-.09	-.18		.16	.07			-.20	.07		.18	-.06	.11	-.19
$5d_{x^2-y^2}$	±.05	±.05		±.08	±.11	±.13	±.07	±.28	±.12		±.07	±.15	±.06		±.29	±.10
$5d_{yz}$	.06	-.07	.09	-.18	-.16		-.06			.20	-.06	.05	.16	.11	-.10	.22
$5d_{xy}$	±.05	±.05	±.10		±.08	±.07	±.10			±.24	±.29	±.13				±.30
$6s$			±.12		±.11	±.09	±.25	±.06		±.09	±.22	±.10		±.09		±.11

Table XII. Molecular orbitals which belong to the b_1 and b_2 representations for the $W_{12}N$ surface molecule where nitrogen is bonded at a 2 CN site.

Molecular Orbital	Ψ_1	Ψ_2	Ψ_3	Ψ_4	Ψ_5	Ψ_6	Ψ_7	Ψ_8	Ψ_9	Ψ_{10}	Ψ_{11}	Ψ_{12}	Ψ_{13}	Ψ_{14}	Ψ_{15}	Ψ_{16}	Ψ_{19}	Ψ_{20}	Ψ_{1-}	Ψ_{18}
Energy (ev)	(-11.18)	(-11.14)	(-10.90)	(-10.89)	(-10.70)	(-10.63)	(-10.28)	(-10.02)	(-9.86)	(-9.84)	(-9.67)	(-9.61)	(-9.55)	(-9.46)	(-9.23)	(-9.07)	(-8.93)	(-8.72)	(-8.59)	(-8.50)
N																				
$2p_x$	.35		-.03		.10		-.08		-.22		-.1o		-.31	.34			-.53	.34		
$2p_y$		.39		-.02	-.25		.33		.15		-.21		-.15			.02	.44			-.20
W(1,2)																				
$5d_{z^2}$		±.23			±.14		±.13		±.22		±.12		±.13							±.11
$5d_{xz}$	.19		.21			-.09		-.13			-.24			-.23	-.10		.14			
$5d_{x^2-y^2}$		±.17		±.16			±.16		±.05				±.05							±.23
$5d_{yz}$		.21		-.05	.27		-.14		.06		.14		-.05			.22				.06
$5d_{xy}$	±.28					±.31		±.07		±.05		±.07		±.10	±.19				±.06	±.15
$6s$		±.06		±.20			±.07													
W(3,4)																				
$5d_{z^2}$	±.18		±.11					±.07		±.27		±.14		±.06	±.12				±.23	
$5d_{xz}$			.07			-.22		.23		-.06		.11		-.30	-.05				.06	
$5d_{x^2-y^2}$	±.08		±.22				±.13	±.05						±.16	±.05				±.16	±.23
$5d_{yz}$		.19		-.12	-.09		.19		.11		.22		.21			-.11	.27			
$5d_{xy}$		±.07		±.11	±.40		±.16							±.10		±.21	±.15			±.07
$6s$	±.10		±.16				±.11													
W(5,6,7,8)																				
$5d_{z^2}$		±.07	±.07				±.11		±.08	±.20	±.07	±.20	±.14	±.06	±.05	±.12	±.21	±.09	±.09	±.05
$5d_{xz}$	.05				±.10			-.10	±.23	.07	±.15	.14		-.06	.10	±.27	±.08	.16	.08	±.13
$5d_{x^2-y^2}$	±.05	±.10	±.12				±.11	±.07						±.36	±.06	±.09	±.10		±.13	±.08
$5d_{yz}$	±.08	±.06		.06	.07		-.10	±.08	-.08	±.13	.13	±.05	-.15	±.11		-.12	.10	±.28	±.12	-.22
$5d_{xy}$		±.08			±.07		±.19	±.11	±.13	±.08	±.07	±.11		±.12	±.08	±.20	±.20	±.08	±.23	±.12
$6s$	±.05	±.08	±.10	±.25		±.07	±.10													
W(9,10,11,12)																				
$5d_{z^2}$		±.05	±.05	±.05	±.05	±.06	±.12	±.05	±.08	±.27	±.10	±.09	±.08	±.11	±.12	±.09	±.06	±.11	±.10	±.08
$5d_{xz}$	-.06	±.06	.09		±.10				±.19			.17		-.21	.10	±.06	±.07		-.18	±.22
$5d_{x^2-y^2}$	±.05	±.07	±.08	±.09	±.05	±.13	±.10			±.08		±.30		±.12	±.07	±.14	±.05	±.08	±.10	±.12
$5d_{yz}$					.06	±.10		±.19	-.10	±.14	.11	±.09	-.11	±.06	±.27	-.15			±.17	.16
$5d_{xy}$	±.07				±.05			±.29				±.23			±.20	±.05	±.06	±.08		±.19
$6s$	±.13		±.19	±.12		±.15								±.05						

Table XIII. Molecular orbitals which belong to the e representation for the W_9N surface "molecule" where nitrogen is bonded at a 5 CN site.

Molecular Orbital	Ψ_1	Ψ_2	Ψ_9	Ψ_{10}	Ψ_3	Ψ_4	Ψ_5	Ψ_6	Ψ_7	Ψ_8	Ψ_{11}	Ψ_{12}	Ψ_{13}	Ψ_{14}	Ψ_{15}	Ψ_{16}
Energy (ev)	(-11.30)		(-10.31)		(-10.16)		(-9.68)		(-9.51)		(-8.94)		(-8.81)		(-8.35)	
N																
$2p_z$		-.51	.30		-.02	.09	.05		.08			.05	-.02		-.11	.12
$2p_y$	-.51			-.30	-.09	-.02		.05		.08	.05			.02	-.12	-.11
W(1)																
$5d_{xz}$		-.40	-.24				-.13		-.19			-.22	-.37		.11	-.13
$5d_{yz}$	-.40			.24				-.13		-.19	-.22			.37	.13	.11
W(2,5)																
$5d_{z^2}$		±.16			±.05	±.19	±.30		±.05			±.17	±.08			
$5d_{xz}$			-.33				-.19		-.22			±.24	.06		.10	-.12
$5d_{x^2-y^2}$		±.22	±.07		±.08	±.33			±.11				±.07			
$5d_{yz}$				-.31	.11				.05	-.33	-.09					
$5d_{xy}$	±.20				±.23	±.06		±.05				±.28		±.05	±.06	±.05
$6s$		±.05	±.07			±.07	±.23		±.21			±.10	±.10	±.11	±.07	±.09
W(3,4)																
$5d_{z^2}$	±.16				±.19	±.05		±.30		±.05	±.17			±.08		
$5d_{xz}$			.31			-.11			-.33	-.05		-.09	-.05			
$5d_{x^2-y^2}$	±.22			±.07	±.33	±.08				±.11				±.07		
$5d_{yz}$				.33				-.19		-.22	-.24			-.06	.12	.10
$5d_{xy}$		±.20			±.06	±.23	±.05	±.23				±.28	±.11		±.05	±.06
$6s$	-.05			±.07	±.07					±.21	±.10			±.10	±.09	±.07
W(6,9)																
$5d_{z^2}$					±.18	±.11	±.14	±.11			±.30	±.27	±.06	±.06	±.19	
$5d_{xz}$			.15		-.19	-.09			-.14	-.14	-.16		.10	-.22	.14	-.33
$5d_{x^2-y^2}$			±.10	±.11		±.06	±.17	±.22	±.14	±.14			±.17	±.17		±.32
$5d_{yz}$			.06	-.15		.21						-.16	.22	-.10	.18	.30
$5d_{xy}$			±.09	±.08	±.09	±.05	±.09	±.07	±.11	±.11	±.13	±.11	±.30	±.30	±.19	
$6s$			±.07	±.06	±.06		±.21	±.17	±.14	±.14	±.10	±.09	±.07	±.07	±.11	
W(7,8)																
$5d_{z^2}$					±.11	±.18	±.11	±.14			±.27	±.30	±.06	±.06		±.19
$5d_{xz}$			.15	.06	.21				-.15	-.15	.16		.10	.22	.30	-.18
$5d_{x^2-y^2}$	±.11			±.10	±.06		±.22	±.17	±.10	±.10			±.17	±.17	±.32	
$5d_{yz}$				-.15	.09	-.19			.05	.05		.16	-.22	-.10	.33	.14
$5d_{xy}$	±.08	±.09			±.05	±.09	±.07	±.09	±.16	±.16	±.11	±.13	±.30	±.30		±.19
$6s$		±.06	±.07			±.06	±.17	±.21	±.20	±.20	±.09	±.10	±.07	±.07		±.11

Figure Captions

Figure 1. Surface arrays used to model adsorption on different W(100)

surface sites.

Figure 2. Dependence of bond energy on bond distance for WN molecule

with and without inclusion of W 5p orbitals.

Figure 3. Dependence of non-bonding (5p orbital) repulsive energy on

distance for the WN molecules.

Figure 4. Additivity of non-bonded orbital repulsive energy.

a) Difference in $E(r)$ for W_2N between calculations including

and omitting W 5p orbitals.

b) $E(r)$ calculated by pairwise addition of analytic repulsive

energy functions.

Figure 5. Additivity of non-bonded orbital repulsive energy of abbreviated

surface arrays.

a) Difference in $E(r)$ for W_nN (n = 4, 5) between calculations

including and omitting W 5p orbitals.

b) $E(r)$ calculated by pairwise addition of analytic repulsive

energy functions.

Figure 6. Bond energies as functions of distances for nitrogen adsorbed

on different W(100) surface sites.

Figure 7. Molecular orbital - energy diagrams for the totally symmetric

occupied orbitals for nitrogen adsorbed on different W(100)

surface sites.

Figure 8. Molecular orbital - energy diagrams for the occupied

orbitals belonging to the representations $e(W_9)$, and b_1

and b_2 (W_{12}) for nitrogen adsorbed on different W(100)

surface sites.

Figure 1. Surface arrays used to model adsorption on different W(100) surface sites.

Figure 2. Dependence of bond energy on bond distance for WN molecule with and without inclusion of W 5p orbitals.

Figure 3. Dependence of non-bonding (5p orbital) repulsive energy on distance for the WN molecules.

Figure 4.   Additivity of non-bonded orbital repulsive energy.

a)   Difference in E(r) for W_2N between calculations including and omitting
W 5p orbitals.

b)   E(r) calculated by pairwise addition of analytic repulsive energy
functions.

Figure 5. Additivity of non-bonded orbital repulsive energy of abbreviated surface arrays.

a) Difference in E(r) for W_nN (n = 4, 5) between calculations including and omitting W 5p orbitals.

b) E(r) calculated by pairwise addition of analytic repulsive energy functions.

Figure 6. Bond energies as functions of distances for nitrogen adsorbed on different W(100) surface sites.

Figure 7. Molecular orbital - energy diagrams for the totally
symmetric occupied orbitals for nitrogen adsorbed
on different W(100) surface sites.

Figure 8. Molecular orbital - energy diagrams for the occupied orbitals belonging to the representations e(W_9), and b_1 and b_2 (W_{12}) for nitrogen adsorbed on different W(100) surface sites.

APPENDIX C.

A MOLECULAR ORBITAL INVESTIGATION OF

CHEMISORPTION. III. OXYGEN ON TUNGSTEN (100) SURFACE

A Molecular Orbital Investigation of

Chemisorption. III. Oxygen on Tungsten (100) Surface

LEON W. ANDERS AND ROBERT S. HANSEN

Ames Laboratory-USAEC and Department of Chemistry

Iowa State University, Ames, Iowa 50010

AND

L. S. BARTELL

Department of Chemistry, University of Michigan

Ann Arbor, Michigan 48104

Abstract

The relative bonding energies of oxygen chemisorbed at three symmetric sites on a W(100) surface represented by finite arrays of tungsten atoms[1] were obtained by means of Extended Hückel Molecular Orbital Theory (EHMO). The preferred site for chemisorbed oxygen was the 2 CN site. The selection of this site by an O adatom is consistent with the usual divalent property of oxygen. Based upon this site selection, a surface structure for O adatoms on the W(100) can be proposed for observed (2 x 1) LEED patterns (8).

I. INTRODUCTION

In applying the Extended Hückel Molecular Orbital (EHMO) technique

to the chemisorption of hydrogen[1] and nitrogen[2] on a tungsten (100) surface,

we have found that the preferred site, for these atoms are different.

Hydrogen preferred a site where it could most effectively bond to a single

surface atom and nitrogen a site where it could interact with five tungsten

atoms satisfying its multiple valency. An atom with yet different bonding

properties is the next obvious step in the study of trying to develop an

overall understanding of chemisorption and sites selected by adsorbates

on any surface. In this paper, we have selected oxygen because of its

usual divalent properties. This should add an additional test in determin-

ing if a metal surface will accept an adsorbate at a site determined by

the chemical properties of the adsorbate atom.

II. PROCEDURE

The EHMO procedure has been outlined in our two previous papers.[1,2]

In Table I are listed the orbital exponents for the Slater type orbitals

(STO) of the oxygen 2s and 2p orbitals which have been derived from

Slater's rules.[3] The valence orbital ionization potential

$$VOIP(q) = Aq^2 + Bq + C \qquad (1)$$

was calculated as a function of atomic charge from the parameters A,

B and C which are also listed in Table I. These values were taken from

the work of Basch, Viste and Gray.[4] As in the previous studies,[1,2] we

are reporting the results of the diatomic molecule, WO, and the surface "molecules", W_nO, where the oxygen atom is placed at each of the three symmetric sites of the surface arrays in Fig. 1.

III. RESULTS

A. Diatomic Molecule

For the diatomic molecule, WO, the bonding energy E as a function of internuclear separation r is plotted in Fig. 2. The presence of the 5p orbitals of tungsten in the basis set produced a minimum in curve a, because the complete occupation of these non-bonding orbitals provide the repulsion at smaller internuclear separation. $\ln E_{Rep}$ (difference between curves a and b) is plotted as a function of r in Fig. 3. An analytical exponential term of the form previously indicated[1]

$$E = A e^{-r/\alpha} \tag{2}$$

can be used to approximate this repulsive energy. The values for the parameters A and α needed to calculate the repulsive energy by this analytical exponential term can be determined from the plot of Fig. 3 ($A_{WO} = 4308.6$ ev and $\alpha_{WO} = .209 \text{ Å}^{-1}$).

From the sum of the single bond covalent radii (0.66Å for O and 1.30Å for W) and the equilibrium bond length for the WO molecule of 1.68Å (Fig. 2), Pauling's empirical relationship[5] between bond length and bond order gives a value of 2.4 for the bond order. From Table II, it is

observed that Ψ_2, Ψ_3 and Ψ_4 are the most significant bonding

molecular orbitals, as was the case for the WN molecule which had a

bond order of 3.1. The resulting smaller bond order for the WO

molecule can be explained by a comparison of overlap population of the

atomic orbitals forming the σ and π bonds of these diatomic molecules.

The overlap population in the σ bond for the WN molecule was .69

compared to .48 for the WO molecule and in the π bond for WN

molecule, the overlap population was .86 compared to .62 in the WO

molecule. The total overlap population for the WN molecule

is 1.55 compared to 1.10 for the WO molecule. This

reduction in overlap population can account for the reduction in bond

order.

It was originally proposed that the computation could be simpli-

fied if the non-bonding 5p orbitals which provide the repulsive energy

could be omitted from the basis set. In the case of hydrogen[1] this

was possible, but it was shown[2] that nitrogen bonded to larger groups

of atoms would not allow the repulsive energy to be calculated by the

summation of pairwise interactions. A similar comparison is made

for the interaction of oxygen with larger arrays of atoms. The

repulsive energies resulting from the presence of the 5p orbitals

of tungsten in the basis set are plotted as curves a in Fig. 4. The

repulsive energies calculated by the summation of pairwise repulsions

determined by the analytical exponential term are plotted as curves b.

As the case with nitrogen, it is also observed that the repulsive

energies can not be properly approximated by the pairwise summation

of exponential term when the oxygen is bonded to larger arrays of

tungsten atoms. Therefore, it was approximated instead by direct

calculation of the reduced arrays of Fig. 1 (W_5 - 1 CN and 5 CN sites

and W_4 - 2 CN sites).

B. Oxygen Chemisorbed on a W(100) Surface

The previous[1] adjustments of the VOIP for the orbitals of the

edge atoms of the surface atom arrays (Fig. 1) were used to reduce

charge transfer resulting from edge effects. With no further adjust-

ment of the VOIP of the tungsten atoms, the VOIP for the orbitals of

the oxygen atom were iterated to charge self-consistency at equilibrium

separation at each of the symmetric sites. On the final iteration, the

VOIP for the 2s and 2p orbitals of oxygen were: -23.53 ev and

-8.77 ev at the 1 CN site, -23.73 ev and -8.92 ev at the 2 CN site

and -25.91 ev and -10.64 ev at the 5 CN site. To insure the

results were not dependent upon VOIP parametrization,[1,2] the calculations were repeated using -23.73 ev and -8.92 ev for the 2s and 2p orbitals of oxygen respectively at all the sites. From these calculations, the bonding energies for oxygen on each of the surface arrays were determined as a function of internuclear separation r and plotted in Fig. 5. The internuclear separation r was the distance to the nearest tungsten atom(s) for the oxygen at each of the sites. The bonding energy E was calculated according to the following relationship:

$$E = \sum_{W_nO} n_i \epsilon_i - \sum_{W_n} n_i \epsilon_i - \sum_{O} n_i \epsilon_i + E_{Rep} \qquad (3)$$

where the first term is the summation over the energies ϵ_i of the occupied molecular orbitals of the surface "molecule" W_nO, the next term is the summation over the energies ϵ_i of the occupied molecular orbitals of the W_n surface "molecule" representing the surface for each site, and the next term is the summation over the energies ϵ_i of the occupied atomic orbitals of the oxygen atom at infinite separation. The repulsive energy E_{Rep} is that determined in prior calculation using abbreviated surface arrays in which the 5p orbitals could be included in the basis set. A summary of the above results where oxygen is at equilibrium separation at each site is found in Table III.

The only molecular orbitals of interest from the W_n surface arrays are those belonging to the same irreducible representation in the appropriate symmetry groups (W_9 - C_{4v} and W_{12} - C_{2v}) as the atomic orbitals of oxygen. In Fig. 6, the molecular orbital energy diagrams are shown for the molecular orbitals belonging to the totally symmetric irreducible representation for surface "molecules" with oxygen bonded to each of the surface arrays in Fig. 1. On the sides of each panel in Fig. 6 are the occupied totally symmetric molecular orbitals of the W_n arrays and the atomic orbitals of oxygen (2s and $2p_z$). The occupied totally symmetric molecular orbitals of the W_nO surface molecules are represented in the center of the panels. The totally symmetric orbitals for the W_9 and W_{12} arrays are tabulated in Tables IV and V and can be compared with the tabulated totally symmetric orbitals for the W_nO surface "molecules" (Table VI - 1 CN, Table VII - 2 CN and Table VIII - 5 CN). From these tables, it is observed that the lowest molecular orbital in each surface "molecule" is extensively 2s in character. The other additional molecular orbital formed as a result of the $2p_z$ atomic orbital interacting with the totally symmetric orbitals for each of the W_n arrays (Ψ_7 - 1 CN and 5 CN and Ψ_{13} - 2 CN) increase in energy in going from the 1 CN to the 2 CN to the 5 CN site. The Ψ_7 molecular orbital at the 5 CN is even above the highest occupied molecular orbital (HOMO). Similar behavior was also observed for the interaction of the totally symmetric

atomic orbital of hydrogen[1] and nitrogen[2] with the W_n arrays.

The $2p_x$ and $2p_y$ orbitals of oxygen, as in the case of nitrogen,[2] play a very important role in the selection of the site for preferred bonding. In Fig. 7 the molecular orbital energy diagrams are shown for these atomic orbitals interacting with the appropriate molecular orbitals of the W_n arrays forming the molecular orbitals of the W_nO surface "molecules". A comparison can be made between the tabulated molecular orbitals (Table XI - 1 CN, Table XII - 2 CN and Table XIII - 5 CN) for the W_nO surface "molecules" with the tabulated molecular orbitals (Table IX - W_9, Table X - W_{12}) of appropriate symmetry for the W_n arrays. With oxygen at the 5 CN site, the $2p_x$ and $2p_y$ orbitals interact primarily with three sets of degenerate orbitals of the W_9 array. The resulting orbitals of the W_9O "molecule" are not as energetically favorable as those similar molecular orbitals of the W_9N "molecule".[2] The influence of these p orbitals of oxygen in selecting the 2 CN site is consistent with the usual divalent property of oxygen.

IV. DISCUSSION

As reported by Madey,[6] the adsorption oxygen on W(100) surface is a complex process. Oxygen will not desorb from the W(100) surface as molecular oxygen, but as oxides of tungsten and even as atomic

oxygen.[7] Estrup and Anderson[8] reported an oxygen (2 x 1) LEED

pattern formed by heating a streaked (4 x 1) structure formed by room

temperature of oxygen.

Our calculations indicate that oxygen prefers the 2 CN site. The

divalent property of oxygen has predominated in selecting the bonding

site. In Fig. 5, the equilibrium internuclear W-O distance (2. 05Å) is

comparable to the sum of the W metallic radius (1.37Å) and the O

covalent radius (.66Å). The bonding of oxygen at the 2 CN sites can

be effectively described as two single bonds to each tungsten atom at

this site. If the oxygen atoms were bonded on the W(100) surface at

2 CN sites as depicted in Fig. 8, each oxygen atom would be bonded to

two tungsten atoms and these two tungsten atoms would not be bonded

to any other oxygen atom. Such a surface structure of adsorbed

oxygen would account for the observed (2 x 1) LEED pattern.

References

1. L. W. Anders, R. S. Hansen and L. S. Bartell, J. Chem. Phys. (in press).

2. L. W. Anders, R. S. Hansen and L. S. Bartell (to be published).

3. J. C. Slater, Phys. Rev., 36, 57 (1930).

4. H. Basch, A. Viste and H. B. Gray, Theoret. Chim. Acta (Bul.), 3, 458 (1965).

5. L. Pauling, The Nature of the Chemical Bond, 3rd Ed. (Cornell University Press, 1960).

6. T. E. Madey, Surface Sci., 33, 355 (1972).

7. Yu. G. Ptushinski and B. A. Chuikov, Soviet Phys.-Solid State, 10, 565 (1968).

8. P. J. Estrup and J. Anderson, in Proc. 27th Annual Physical Electronics Conference, MIT, 1967.

Table I. Orbital exponents for STO of the oxygen atom and parameters
needed to calculate VOIP as a function of atomic charge.

Orbital	Orbital Exponent	A $[ev/(e)^2]$	B $[ev/e]$	C $[ev]$
2s	2.275	3.46	22.89	32.33
2p	2.275	3.46	18.57	15.80

Table II. Occupied Molecular Orbitals for the diatomic molecule WO.

W-O Energy (ev)	Ψ_1 (-27.21)	Ψ_2 (-12.50)	Ψ_3 (-12.50)	Ψ_4 (-11.95)	Ψ_5 (-9.80)	Ψ_6 (-9.80)
O						
2s	.93			.10		
$2p_z$				.84		
$2p_x$			-.81			
$2p_y$		-.81				
W						
$5d_{z^2}$	.13			-.35		
$5d_{xz}$			-.44			
$5d_{x^2-y^2}$					1.00	
$5d_{xy}$						1.00
6s				.18		

Table III. Energies, equilibrium distances, and charges for oxygen bonded to different W(100) surface sites.

Site	Bond Energy (ev)	r_e (Å)	Charge $|e|$
1 CN	-1.06	1.93	-.45
2 CN	-1.30	2.05	-.40
5 CN	-.80	1.98	±.90

Table IV. Totally symmetric molecular orbitals for the surface arrays representing the 1 CN and 5 CN sites.

Molecular Orbital Energy (ev)	Ψ_1 (-12.43)	Ψ_2 (-10.69)	Ψ_3 (-10.38)	Ψ_4 (-9.77)	Ψ_5 (-8.47)
W(1)					
$5d_{z^2}$		-.54		-.10	-.19
6s	-.24				
W(2, 3, 4, 5)					
$5d_{z^2}$		.22	.17	.16	
$5d_{xz}$ (2, 5)		±.15		±.31	±.07
$5d_{x^2-y^2}$		±.12	±.30	±.19	±.05
$5d_{yz}$ (3, 4)		±.15		±.31	±.07
6s	-.18				
W(6, 7, 8, 9)					
$5d_{z^2}$		-.10	-.19		.26
$5d_{xz}$			±.11		±.28
$5d_{yz}$			±.11		±.28
$5d_{xy}$		±.12		±.22	±.10
6s	-.12				

Table V. Totally symmetric molecular orbitals for the surface array representing the 2 CN site.

	ψ_1 (-12.78)	ψ_2 (-11.31)	ψ_3 (-10.87)	ψ_4 (-10.82)	ψ_5 (-10.25)	ψ_6 (-10.03)	ψ_7 (-9.68)	ψ_8 (-9.62)	ψ_9 (-8.97)	ψ_{10} (-8.72)	ψ_{11} (-8.32)
W(1,2)											
$5d_{z^2}$			-.36	-.09		-.08	.09	-.15			.15
$5d_{x^2-y^2}$		.33			-.19	-.06	-.05	-.08	-.30	-.14	.08
$5d_{yz}$		±.12	±.08	±.32	±.21		±.17	±.18	±.10	±.12	
$6s$	.18										
W(3,4)											
$5d_{z^2}$			.36	-.09		-.08	-.09	-.15			-.15
$5d_{xz}$		±.12	±.08	±.32	±.21		±.17	±.18	±.10	±.12	
$5d_{x^2-y^2}$		-.33			-.19	.05	.05	+.08	-.30	.14	.08
$6s$	.18										
W(5, 6, 7, 8)											
$5d_{z^2}$			.12	.05	-.17	.07	.08	.06	.08	-.12	.11
$5d_{xz}$			±.05	±.07	±.14	±.23		±.09			±.26
$5d_{x^2-y^2}$		-.13	.05	-.11	.10	-.16	.05		-.20	-.05	-.14
$5d_{yz}$						±.07	±.13	±.19	±.14	±.24	±.10
$5d_{xy}$				±.12		±.08	±.24	±.18	±.09	±.18	±.08
$6s$	.10										
W(9, 10, 11, 12)											
$5d_{z^2}$			.12	±.05	.17	.07	.08	.06	.08	-.12	-.11
$5d_{xz}$						±.07	±.13	±.19	±.14	±.24	±.10
$5d_{x^2-y^2}$		.13	±.05	.11	.10	.16	.05		±.20	.05	-.14
$5d_{yz}$			±.05	±.07	±.14	±.23		±.09			±.26
$5d_{xy}$				±.12		±.08	±.24	±.18	±.09	±.18	±.08
$6s$	.10										

183

15

Table VI. Totally symmetric molecular orbital for W_9O surface "molecule" where oxygen is bonded at a 1 CN site.

Molecular Orbital	Ψ_6	Ψ_1'	Ψ_2'	Ψ_3'	Ψ_4'	Ψ_7	Ψ_5'
Energy (ev)	(-23.98)	(-12.23)	(-10.49)	(-10.37)	(-9.78)	(-9.23)	(-8.42)
O							
2s	.95	.09	.14	-.05	.03	-.05	
$2p_z$		.02	-.31	.11	-.18	.78	-.16
W(1)							
$5d_z2$	.10	.17	-.37	.10	-.09	.15	.07
6s	.07	-.20	.06				
W(2, 3, 4, 5)							
$5d_z2$			.25	.12	.14	.20	-.08
$5d_{xz}$ (2, 5)			±.14	±.09	±.32	±.05	
$5d_{x2-y2}$			±.05	±.32	±.17	±.15	±.10
$5d_{y2}$ (3, 4)			±.14	±.09	±.32	±.05	
6s		-.18	-.07				
W(6, 7, 8, 9)							
$5d_z2$			-.13	-.16		-.09	-.25
$5d_{xz}$				±.11		±.06	±.28
$5d_{yz}$				±.11		±.06	±.27
$5d_{xy}$			±.11	±.06	±.22		±.12
6s		-.12					

185

17

Table VIL. Totally symmetric molecular orbitals for the $W_{12}O$ surface "molecule" where oxygen is bonded at a 2 CN site.

Molecular Orbital / Energy (ev)	Ψ_{12} (-24.07)	Ψ_1' (-12.49)	Ψ_2' (-11.32)	Ψ_3' (-10.92)	Ψ_4' (-10.63)	Ψ_5' (-10.08)	Ψ_6' (-10.02)	Ψ_8' (-9.71)	Ψ_7' (-9.59)	Ψ_9' (-9.27)	Ψ_{10}' (-8.72)	Ψ_{13} (-8.53)	Ψ_{11} (-8.26)
O													
2s	-.93	.11	.03	.02	-.07	.10	-.06	-.03	-.09	.03	-.02	.02	.02
$2p_z$	-.01	-.02	.11	-.17	-.03	.31	-.09	-.32	-.29	.45		-.32	.21
W(1, 2)													
$5d_{z2}$			.05	-.37			.07	-.14		-.05		-.06	-.08
$5d_{x2-y2}$		-.08	.31		.06	.14		-.08		.15	.09	.12	-.08
$5d_{yz}$	±.07	±.12	±.16		±.14	±.11	±.09	±.09	±.21		±.13		±.06
6s	±.06	-.14											
W(3, 4)													
$5d_{z2}$				.32	.16		.10	-.14	-.12				.18
$5d_{xz}$			±.14	±.11	±.36			±.24	±.09	±.07	±.09	±.14	±.09
$5d_{x2-y2}$			-.32	-.08	.11	.11	-.14			.20	-.20	.21	-.16
6s		-.18											
W(5, 6, 7, 8)													
$5d_{z2}$				.11		.14	-.18				.12		-.15
$5d_{xz}$						±.24	±.11			±.17		±.30	±.12
$5d_{x2-y2}$			-.12		.10		.21		.11	.20			.17
$5d_{yz}$			±.06	±.05		±.07		±.12	±.17	±.17	±.25		±.10
$5d_{xy}$			±.05	±.10			±.07	±.19	±.23	±.15	±.15		
6s		-.12									.05		
W(9, 10, 11, 12)													
$5d_{z2}$				-.10	-.12	-.17			-.05	.09	.10	.16	
$5d_{xz}$		±.06					±.05	±.23	±.08		±.21	±.13	±.15
$5d_{x2-y2}$			.12	.08	-.14	-.11	-.11	-.07		.12	-.10	.22	.07
$5d_{yz}$				±.06	±.10	±.06	±.26	±.07					±.31
$5d_{xy}$					±.14	±.15		±.10	±.24		±.20	±.07	±.12
6s		-.10											

Table VIII. Totally symmetric molecular orbitals for the $W_9 O$ surface "molecule" where oxygen is bonded at a 5 CN site.

Molecular Orbital	Ψ_6	Ψ_1'	Ψ_3'	Ψ_2'	Ψ_4'	Ψ_5'	Ψ_7
Energy (ev)	(-24.15)	(-12.01)	(-10.49)	(-10.18)	(-9.38)	(-8.62)	(-7.59)
O							
2s	.91	-.09	.04		.15	-.08	-.07
$2p_z$		.07	.25	-.45	.56	.04	.23
W(1)							
$5d_{z^2}$	.07	-.25	-.23	.04	-.33	-.05	-.27
6s	.04	.21			-.04		-.07
W(2, 3, 4, 5)							
$5d_{z^2}$		.06	.24		-.11	-.08	-.22
$5d_{xz}$ (2,5)			±.07	±.31	±.11		±.21
$5d_{x^2-y^2}$	±.04	±.10	±.20	±.15		±.06	±.17
$5d_{yz}$ (3,4)			±.07	±.31	±.11		±.21
6s	.03	.14					
W(6, 7, 8, 9)							
$5d_{z^2}$			-.20	-.07	.07	.24	
$5d_{xz}$			±.09		±.06	±.29	
$5d_{yz}$			±.09		±.06	±.29	
$5d_{xy}$				±.16	±.25		±.36
6s		.13			-.09		.05

Table IX. Molecular orbitals which belong to the *e* representation in the C_{4v} symmetry group for the W_9 surface arrays representing the 1 CN and 5 CN sites.

Molecular Orbital / Energy (ev)	Ψ_1	Ψ_2	Ψ_3	Ψ_4	Ψ_5	Ψ_6	Ψ_7	Ψ_8	Ψ_9	Ψ_{10}	Ψ_{11}	Ψ_{12}	Ψ_{13}	Ψ_{14}
	(-10.68)		(-10.17)		(-9.71)		(-9.58)		(-9.24)		(-8.91)		(-8.80)	
W(1)														
$5d_{xz}$	-.50	.10				.21	.19		.06	.08	-.19		-.07	-.37
$5d_{yz}$	.10	.50			-.21			.19	-.08	.06		-.19	.37	-.07
W(2,5)														
$5d_{z2}$	±.16		±.13	±.15		±.26	±.11		±.14	±.18	±.10			±.07
$5d_{xz}$	-.23	.05		-.05	.13				-.17	-.22	-.29			.10
$5d_{x2-y2}$	±.12		±.17	±.21		±.14	±.26		±.17	±.22	±.07			
$5d_{yz}$		-.17	.16	-.13	-.16			.35				-.08	.05	
$5d_{xy}$		±.22	±.19	±.15	±.07							±.32	±.07	
6s			±.07	±.08		±.20	±.20		±.12	±.16				±.08
W(3,4)														
$5d_{z2}$		±.16	±.15	±.13	±.26			±.11	±.18	±.14		±.10	±.07	
$5d_{xz}$	.17		.13	.16		.16	.35				-.08			-.05
$5d_{x2-y2}$		±.12	±.21	±.17	±.14			±.26	±.22	±.17		±.07		
$5d_{yz}$	.05	.23	.05		-.13				.22	-.17		-.29	-.10	
$5d_{xy}$	±.22		±.15	±.18		±.07					±.32			±.07
6s			±.08	±.07	±.20			±.20	±.16	±.12			.08	
W(6,9)														
$5d_{z2}$			±.21		±.14	±.10					±.26	±.32	±.08	±.11
$5d_{xz}$	.08	-.09	-.08	.19	-.07		.18	.09		.09	.09	-.11	-.21	.11
$5d_{x2-y2}$	±.09	±.06		±.11	±.17	±.24			±.18		±.10	±.08	±.17	±.12
$5d_{yz}$	.06	-.11	-.05	-.20	-.06	.05		.19		.10	-.13	.07		.24
$5d_{xy}$	±.08	±.10	±.07		±.08	±.05				±.26	±.09	±.11	±.25	±.37
6s			±.10		±.19	±.14	±.15	±.18		±.23		±.05	±.05	±.08
W(7,8)														
$5d_{z2}$				±.21	±.10	±.14			±.05		±.32	±.26	±.11	±.08
$5d_{xz}$	.11	.06	.20	-.05	.05	.06	.19		.10		.07	.13	.24	
$5d_{x2-y2}$	.06	±.09	±.11		±.24	±.17				±.18	±.08	±.10	±.12	±.17
$5d_{yz}$	-.09	-.08	.10	.08		-.07	.09	.18			.11	.09	-.11	-.21
$5d_{xy}$	.10	±.07		±.07	±.05	±.08				±.26	±.11	±.09	±.37	±.25
6s				±.10	±.14	±.19	±.18	±.15		±.23		±.05	±.08	±.05

Table X   Molecular orbitals which belong to the b_1 and b_2 representations in the C_{2v} symmetry group for the W_{12} surface array representing the 2 CN site.

Molecular Orbital	ψ_1	ψ_2	ψ_3	ψ_4	ψ_5	ψ_6	ψ_7	ψ_8	ψ_9	ψ_{10}	ψ_{11}	ψ_{12}	ψ_{13}	ψ_{14}	ψ_{15}	ψ_{16}	ψ_{17}	ψ_{18}
Energy (ev)	(-10.42)	(-10.42)	(-10.88)	(-10.88)	(-10.56)	(-10.56)	(-10.01)	(-10.01)	(-9.80)	(-9.80)	(-9.59)	(-9.59)	(-9.38)	(-9.38)	(-9.07)	(-9.07)	(-8.62)	(-8.62)
W(1,2)																		
$5d_{z^2}$	±.18	±.15			±.10				±.18	±.19	±.09	±.07	±.10	±.08			±.14	±.05
$5d_{xz}$	-.17	.21	-.06			-.08	-.10		.17	-.15			.20	-.24	-.13			-.08
$5d_{x^2-y^2}$	±.17	±.14	±.05	±.09	±.11			±.05					±.12	±.10			±.27	±.10
$5d_{yz}$					-.24	-.05	.08	-.23			.14	.11	-.19	-.16			.05	
$5d_{xy}$	±.12	±.14	±.14	±.08	±.08	±.17							±.09	±.11	±.20			±.11
$6s$				±.18	±.08													
W(3,4)																		
$5d_{z^2}$	±.15	±.18				±.10			±.19	±.18	±.07	±.09	±.08	±.10			±.05	±.14
$5d_{xz}$					.05	-.23	.23	.08			.11	-.14	.16	-.19				-.05
$5d_{x^2-y^2}$	±.14	±.17	±.09	±.05	±.11	±.05							±.10	±.12			±.10	±.27
$5d_{yz}$	-.21	.17		-.06	±.08			.10	.15	.17			-.24	-.20	-.13	.08		
$5d_{xy}$	±.14	±.12	±.08	±.14	±.17	±.08							±.11	±.09		±.20	±.11	
$6s$			±.18	±.09	±.08													
W(5,6)																		
$5d_{z^2}$	±.09				±.12	±.07			±.27	±.16	±.09	.08			±.09	±.14	±.14	
$5d_{xz}$					-.11		±.23			.09		-.18	.11	.09	-.14	-.27	-.18	-.08
$5d_{x^2-y^2}$		±.17			±.11		±.08				±.21	±.18	±.18	±.12	±.14	±.09		±.13
$5d_{yz}$		.15					.09		.08	±.16	.18	.15	-.10			-.13	-.24	-.18
$5d_{xy}$	±.08				±.07			±.10	±.07	±.09	±.08	±.08		±.20	±.07	±.18		±.15
$6s$			±.23	±.16	±.12													
W(6,7)																		
$5d_{z^2}$		±.09			±.07	±.10	±.09		±.14	±.28	±.06	±.11			±.10	±.13	±.12	±.07
$5d_{xz}$					.10	.06	-.17	.16	±.08		.17	-.07	-.11	-.09	-.17	.26	.09	-.18
$5d_{x^2-y^2}$	±.17				±.10		±.08				±.21	±.15	±.15	±.16	±.13	±.11	±.09	±.10
$5d_{yz}$	.15						-.06	-.07	-.17	.06	.19	.13		±.10	.06	-.12	-.07	.29
$5d_{xy}$		±.08			±.09	±.19	±.23		±.09	±.06	±.05	±.09	±.19			±.19	±.08	±.13
$6s$			±.28	±.10														
W(9,12)																		
$5d_{z^2}$	±.09				±.10	±.07		.09	±.28	±.14	±.11	±.06			±.13	±.10	±.07	±.12
$5d_{xz}$		.15					.07	-.07	.06	.17	.13	-.19	.10	-.15	-.12	-.06	.29	.07
$5d_{x^2-y^2}$		±.17				±.10		±.08			±.15	±.23	±.16	±.11	±.11	±.13	±.10	±.09
$5d_{yz}$					-.10	.16	.17			-.08	.07	.17	-.09	-.19	-.26	-.17	.18	.09
$5d_{xy}$	±.08				±.09	±.23	±.19	±.06	±.09	±.09			±.19			±.13	±.08	
$6s$			±.28	±.08	±.10													
W(10,11)																		
$5d_{z^2}$		±.09			±.12			±.07	±.16	±.27	±.08	±.09			±.14	±.09		±.14
$5d_{xz}$	.15							.09	-.16	-.08	.15	-.18		-.10	-.13		-.18	.24
$5d_{x^2-y^2}$	±.17				±.11		±.08				±.18	±.21	±.12	±.18	±.09	±.14	±.13	
$5d_{yz}$					.11	-.23			-.09		.18		.09	-.11	.27	-.14	.08	-.18
$5d_{xy}$		±.08			±.07	±.10			±.09	±.07	±.08	±.08	±.20		±.18	-.07	±.15	
$6s$			±.16	±.23	±.12													

Table XL. Molecular orbitals which belong to the e representation for the W_9O surface "molecule" where oxygen is bonded at a 1 CN site.

Molecular Orbital	ψ_1	ψ_2	ψ_3	ψ_4	ψ_5	ψ_6	ψ_7	ψ_8	ψ_9	ψ_{10}	ψ_{11}	ψ_{12}	ψ_{13}	ψ_{14}	ψ_{15}	ψ_{16}
Energy (ev)	(-10.78)		(-10.18)		(-9.72)		(-9.69)		(-9.25)		(-9.22)		(-8.90)		(-8.32)	
O																
$2p_x$	.22			-.06	-.19	-.17	-.25	.07		.19	.50	-.05	.06	-.03	-.54	-.34
$2p$		.22	-.06		.17	-.19	-.07	-.25	.19		-.05	-.50	-.03	-.06	.34	-.54
W(1)																
$5d_{xz}$	-.53				.21	.19				.05	-.19		.06		-.21	-.13
$5d_{yz}$		.53			-.19	.21			.05			.19		-.06	.13	.21
W(2,5)																
$5d_{z^2}$	±.15			±.20	±.13	±.11	±.21	±.06		±.25			±.11	±.06	±.06	
$5d_{xz}$	-.22			.05			-.12			-.23	.18		.28	-.15	-.07	
$5d_{x^2-y^2}$	±.12			±.27	±.15	±.13				±.34	±.12				±.10	±.06
$5d_{yz}$		-.15	-.18		-.24	.27	.05	.17				-.08		-.06	.05	-.08
$5d_{xy}$		±.20	±.25	±.05				±.06	±.11			±.16	±.13	±.24		
$6s$			±.10				±.26	±.07		±.17	±.12		±.05		±.09	±.06
W(3,4)																
$5d_{z^2}$		±.15	±.20		±.11	±.13	±.06	±.21	±.25				±.06	±.11		±.06
$5d_{xz}$	-.15			-.18	.27	.24	.17	-.05			.08		.06		.08	-.05
$5d_{x^2-y^2}$		±.12	±.27	±.05	±.13	±.15				±.34		±.12			±.06	±.10
$5d_{yz}$		.22	.05					-.12	-.23			-.18	-.15	-.28		-.07
$5d_{xy}$	±.20		±.05	±.25			±.06			±.11	±.16		±.24	±.13		
$6s$			±.10				±.07	±.26	±.17			±.12		±.05	±.06	±.08
W(6,9)																
$5d_{z^2}$			±.12	±.17		±.09	±.14	±.08					±.12	±.41		±.05
$5d_{xz}$	.08	-.07	.20	-.05	.07	.15	.10		.11	.11	.08	-.09	-.14	-.14		.18
$5d_{x^2-y^2}$	±.07	±.06	±.08	±.06	±.29		±.06	±.10	±.17	±.13	±.05		±.05		±.22	±.05
$5d_{yz}$	.06	-.09	-.11	.17	-.05	.15		.10	.07	.13	.07	-.09	.19		.07	.17
$5d_{xy}$	±.07	±.08	±.05	±.07			±.08		±.08	±.11	±.26	±.31			±.07	±.33
$6s$			±.06	±.09		±.05	±.28	±.16	±.12	±.15	±.08	±.10		±.09		±.09
W(7,8)																
$5d_{z^2}$			±.17	±.12	±.09		±.08	±.16					±.41	±.12	±.05	
$5d_{xz}$	.09	.06	-.17	-.11	.15	.05	.10		-.13	.07	.09	.07		.19	.17	±.07
$5d_{x^2-y^2}$	±.06	±.07	±.06	±.08		±.29	±.10	±.06	±.13	±.17		±.05		±.05	±.05	±.22
$5d_{yz}$	-.07	-.08	-.05	-.20	-.15	.07		.10	.11	-.11	-.09	-.08	-.14	.14	-.18	
$5d_{xy}$	±.08	±.07	±.07	±.05				±.08	±.11	±.08	±.31	±.25			±.33	±.07
$6s$			±.09	±.06	±.05		±.16	±.28	±.15	±.12	±.10	±.08	±.09		±.09	

Table XII. Molecular orbitals which belong to the b_1 and b_2 representations for the $W_{12}O$ surface "molecule" where oxygen is bonded at a 2 CN site.

Molecular Orbital / Energy (ev)	Ψ_1 (-11.04)	Ψ_2 (-11.02)	Ψ_3 (-10.90)	Ψ_4 (-10.88)	Ψ_5 (-10.67)	Ψ_6 (-10.59)	Ψ_7 (-10.19)	Ψ_8 (-10.01)	Ψ_9 (-9.83)	Ψ_{10} (-9.83)	Ψ_{11} (-9.66)	Ψ_{12} (-9.60)	Ψ_{13} (-9.52)	Ψ_{14} (-9.42)	Ψ_{15} (-9.21)	Ψ_{16} (-9.07)	Ψ_{17} (-8.87)	Ψ_{18} (-8.68)	Ψ_{19} (-8.54)	Ψ_{20} (-8.53)
O																				
$2p_x$		.26	-.03			-.09		.05		.16		.08		-.24	.37			.49	.55	
$2p_y$	-.24			.01	-.23		-.31		.14		-.23		.20			-.02	.50			-.28
W(1,2)																				
$5d_{z^2}$		±.23			±.13		±.11	±.24		±.10		±.14				±.07				±.10
$5d_{xz}$	-.21		.19			.09		.12	.23				-.29				-.12			
$5d_{x^2-y^2}$		±.21		±.12			±.13		±.06				±.07			±.24				±.20
$5d_{yz}$		-.16		.05	.28		.21				.17			-.12		.13				
$5d_{xy}$	±.28		±.05			±.33		±.05				±.07			±.19				±.15	
$6s$				±.20	±.06		±.05													
W(3,4)																				
$5d_{z^2}$	±.21		±.09			±.06		±.05		±.27		±.12		±.10	±.09				±.19	
$5d_{xz}$			.07			.23		-.24				-.16		-.27					.06	
$5d_{x^2-y^2}$	±.11		±.21			±.13		±.06						±.16				±.22	±.18	
$5d_{yz}$		-.24			-.39		-.17		.15		.16		-.24			.12	.25			
$5d_{xy}$		±.10		±.15		±.13									±.21	±.17				±.05
$6s$	±.09		±.17			±.10														
W(5,6,7,8)																				
$5d_{z^2}$		±.08	±.07			±.11		±.09	±.24	±.08	±.15	±.13	±.06		±.07	±.12	±.20	±.05	±.10	
$5d_{xz}$	-.05				±.10		±.07	.10	.19	-.05	±.16	-.15	±.07		.11	±.27	±.08	-.16	.05	±.12
$5d_{x^2-y^2}$	±.06	±.12	±.11		±.05		±.07	±.08			±.07		±.36		±.11	±.10	±.14			
$5d_{yz}$	±.09	.08	±.05		.05		.10	±.08	-.09	±.14	.18		.10	±.08		.12	.07	±.30		-.23
$5d_{xy}$		±.08			±.07		±.23	±.11	±.08	±.10	±.06	±.11		±.14		±.19	±.18		±.23	±.13
$6s$	±.05	±.05	±.11	±.25	±.07	±.07	±.07													
W(9,10,11,12)																				
$5d_{z^2}$	±.05	±.06		±.05	±.07	±.06	±.12		±.08	±.29	±.11	±.05	±.07	±.08	±.13	±.09	±.06	±.12	±.08	±.09
$5d_{xz}$	.07	±.08	-.08		±.09				±.19	-.05		-.21		-.15	.11	±.06	±.11	.07	-.16	±.20
$5d_{x^2-y^2}$	±.07	±.10	±.07	±.07		±.13	±.10			±.05		±.29		±.19		±.14	±.06		±.09	±.11
$5d_{yz}$						-.05	±.10	-.05	±.20	-.09	±.12	.14	±.09	.08	±.08	±.27	.15		±.16	.17
$5d_{xy}$	±.08					±.06	±.06	±.28			±.21		±.08	±.06	±.20	±.05		±.07		±.19
$6s$	±.12		±.20	±.13		±.14														

Table XIII. Molecular orbitals which belong to the e representation for the W₉O surface "molecule" where oxygen is bonded at a 5 CN site.

Molecular Orbital	ψ'_1	ψ'_2	ψ'_5	ψ'_6	ψ'_3	ψ'_4	ψ'_7	ψ'_8	ψ'_9	ψ'_{10}	ψ'_{11}	ψ'_{12}	ψ'_{13}	ψ'_{14}	ψ'_{15}	ψ_{16}
Energy (ev)	(-10.98)		(-10.19)		(-10.15)		(-9.68)		(-9.50)		(-8.93)		(-8.80)		(-8.34)	
O																
$2p_x$	-.39		-.23	.12		-.31	.06			-.11	-.04	.05	-.02	-.02	-.16	.14
$2p_y$		-.39	.12	.23	-.31			.06	.11		.05	.04	.02	-.02	.14	.16
W(1)																
$5d_{xz}$	-.47		.10	-.05			-.14			.18	.13	-.17	-.23	-.28	.14	-.12
$5d_{yz}$		-.47	-.05	-.10				-.14	-.18		-.17	-.13	.28	-.23	-.12	-.14
W(2,5)																
$5d_{z^2}$	±.17		±.12	±.06		±.14	±.30			±.06	±.10	±.13	±.05	±.06		
$5d_{xz}$	-.10		.21	-.11		-.18	-.19			.23	.15	-.19		.05	.12	-.10
$5d_{x^2-y^2}$	±.21		±.06			±.36				±.09				±.05		
$5d_{yz}$		.08	.16	.29	-.07				-.32			-.05				
$5d_{xy}$		±.22	±.07	±.14	±.18			±.05			±.23	±.18	±.09	±.07	±.05	±.06
$6s$			±.10	±.06			±.23			±.23	±.06	±.07	±.06	±.08	±.08	±.07
W(3,4)																
$5d_{z^2}$		±.17	±.06	±.12	±.14			±.30	±.06		±.13	±.10	±.06	±.05		
$5d_{xz}$	.08		-.29	.16		.07				.32	.05	-.07				
$5d_{x^2-y^2}$		±.21		±.06	±.36					±.09			±.05			
$5d_{yz}$		-.10	-.11	-.21	.18			-.19	-.23		-.19	-.15	-.05		-.10	-.12
$5d_{xy}$	±.22		±.14	±.07		±.18	±.05				±.18	±.23	±.07	±.09	±.06	±.05
$6s$			±.06	±.10				±.23	±.23		±.07	±.06	±.08	±.06	±.07	±.08
W(6,9)																
$5d_{z^2}$				±.14	±.12	±.10	±.13	±.11			±.05	±.40		±.09		±.18
$5d_{xz}$	.05	.05	-.17		-.20					.14	-.14	-.07	-.11	.21	.32	-.14
$5d_{x^2-y^2}$	±.05	±.05	±.15				±.18	±.21	±.11	±.13	±.05		±.24		±.32	
$5d_{yz}$	.04	.05	.14	.10	-.07	.19				-.14	.12	-.10	.06	.23	-.30	-.18
$5d_{xy}$	±.05	±.05			±.11	±.09	±.09	±.07	±.15	±.13		±.16	±.05	±.42		±.19
$6s$				±.12			±.21	±.17	±.19	±.16		±.12		±.10		±.10
W(7,8)																
$5d_{z^2}$			±.14		±.10	±.12	±.11	±.13			±.40	±.05	±.09		±.18	
$5d_{xz}$	.05	-.04	-.10	.14	.19	.07				.14	.10	.12	.23	-.06	.18	-.30
$5d_{x^2-y^2}$	±.05	±.05		±.15			±.21	±.18	±.13	±.11		±.05		±.24		±.32
$5d_{yz}$	-.05	.05		.17	.09	-.20				-.14	-.07	.14	-.21	-.11	-.14	-.32
$5d_{xy}$	±.05	±.05				±.11	±.07	±.09	±.13	±.15	±.16		±.42	±.05	±.19	
$6s$			±.12				±.17	±.21	±.16	±.19	±.12		±.10		±.10	

Figure Captions

Figure 1. Surface arrays used to model adsorption on different W(100) surface sites.

Figure 2. Dependence of bond energy on bond distance for WO molecule with and without inclusion of W 5p orbitals.

Figure 3. Dependence of non-bonding (5p orbital) repulsive energy on distance for the WO molecules.

Figure 4. Additivity of non-bonded orbital repulsive energy of abbreviated surface arrays.

   a) Difference in $E(r)$ for W_nO ($n = 4, 5$) between calculations including and omitting W 5p orbitals.

   b) $E(r)$ calculated by pairwise addition of analytic repulsive energy functions.

Figure 5. Bond energies as functions of distances for oxygen adsorbed on different W(100) surface sites.

Figure 6. Molecular orbital-energy diagrams for the totally symmetric occupied orbitals for oxygen adsorbed on different W(100) surface sites.

Figure 7. Molecular orbital-energy diagrams for the occupied orbitals belonging to the representations $e(W_9)$, and b_1 and b_2 (W_{12}) for oxygen adsorbed on different W(100) surface sites.

Figure 8. Suggested structure for oxygen adsorbed on the W(100) based upon an oxygen adatom preferring a 2 CN site.

Figure 1. Surface arrays used to model adsorption on different W(100) surface sites.

Figure 2. Dependence of bond energy on bond distance for WO molecule with and without inclusion of W 5p orbitals.

Figure 3. Dependence of non-bonding (5p orbital) repulsive energy on distance for the WO molecules.

Figure 4. Additivity of non-bonded orbital repulsive energy of abbreviated surface arrays.

a) Difference in E(r) for W_nO (n = 4, 5) between calculations including and omitting W 5p orbitals.

b) E(r) calculated by pairwise addition of analytic repulsive energy functions.

Figure 5. Bond energies as functions of distances for oxygen
adsorbed on different W(100) surface sites.

Figure 6. Molecular orbital-energy diagrams for the totally symmetric occupied orbitals for oxygen adsorbed on different W(100) surface sites.

Figure 7. Molecular orbital-energy diagrams for the occupied orbitals belonging to the representations $e(W_9)$, and b_1 and b_2 (W_{12}) for oxygen adsorbed on different W(100) surface sites.

Figure 8. Suggested structure for oxygen adsorbed on the
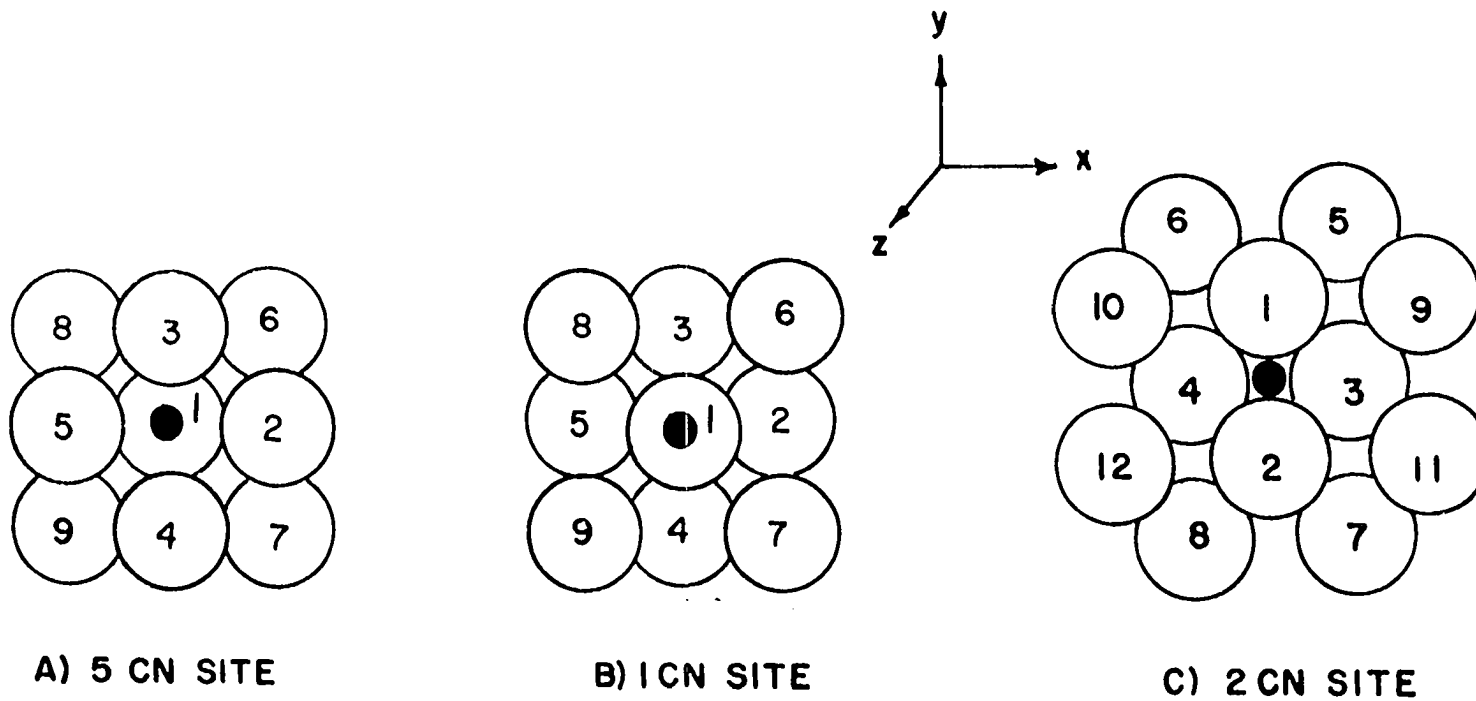W(100) based upon an oxygen adatom preferring
a 2 CN site.

APPENDIX D.

COMPUTER PROGRAM FOR EXTENDED

HÜCKEL MOLECULAR ORBITAL (EHMO) CALCULATIONS

```
C          MAIN PROGRAM TO CALCULATE THE OVERLAP MATRIX
C     ROALD HOFFMANN  CHEMISTRY DEPARTMENT  HARVARD UNIVERSITY CAMBRIDGE
C     THIS PROGRAM CONSTRUCTS AN OVERLAP MATRIX FOR UP TO 140 ORBITALS O
C     UP TO 50 ATOMS.  THE ORBITALS MAY BE OF ANY PRINCIPAL QUANTUM NUMB
C     ANGULAR MOMENTUM S P D OR F  AND THERE IS NO LIMITATION ON THE
C     NUMBER OF ORBITALS OF ANY TYPE EXCEPT THAT THE TOTAL MUST BE LESS
C     THAN 140.
C     THE PROGRAM USES  SEVEN  FILES   5=INPUT  6=OUTPUT  7=PUNCHOUT
C     3,4,8,9 ARE INTERMEDIATE FILES
C     RESTRICTION - NO MORE THAN 5 DIFFERENT TYPE ORBITALS ON ANY ATOM
C     RESTRICTION  DIFFERENT ORBITALS ON SAME CENTER MUST HAVE DIFFERENT
C     INPUT CONSISTS OF THE FOLLOWING
C     FIRST CARD IN FORMAT ( 7I2,F14.6)
C     N, MS, MC, MMM, MORB, MK, CON
C     N IS THE NUMBER OF DIFFERENT ATOMS
C     THE OTHER INTEGERS ARE CONTROL PARAMETERS
C     MK=0 USES  ARITHMETIC MEAN WOLFSBERG HELMHOLTZ FORMULA
C     MK=1 USES DIRECT PROPORTIONALITY OF HAMILTONIAN TO OVERLAP
C     MK=2 USES GEOMETRIC MEAN WOLFSBERG-HELMHOLTZ FORMULA
C     MORB SPECIFIES AN ORBITAL NUMBER FOR WHICH A POPULATION ANALYSIS
C     IN ADDITION TO THE GENERAL ONE WILL BE DONE
C     IF MORB=0 ONLY TOTAL POPULATION ANALYSIS WILL BE PERFORMED
C     MS=1  PUNCHES OUT S
C     MC=1 PUNCHES OUT C
C     MMM=1  BYPASSES POPULATION ANALYSIS
C     MS GREATER THAN 1 PRODUCES TRACE PRINTOUT
C     MR GREATER THAN ZERO, AN EXPONENTIAL REPULSIVE ENERGY WILL BE
C     ADDED TO THE TOTAL ENERGY
C     SECOND CARD IS A TITLE CARD IN FORMAT(72H    )
C     THEN THERE FOLLOW 2N CARDS, TWO FOR EACH ATOM
C     FOR EACH ATOM THE FIRST CARD IS IN FORMAT (I3,F7.3,3F10.6,F12.3,
C     F6.3)
C     THE SECOND CARD IN FORMAT  (5(2I1,F5.3,F6.2))
C     ON THE FIRST CARD ONE READS IN NORB(I)= THE NUMBER OF DIFFERENT TY
C     ORBITALS . ORBITALS  ARE DIFFERENT IF THEY HAVE DIFFERENT N AND L
C     THE NEXT ENTRY ON THIS CARD IS THE CHARGE ON THE ATOM CORE
C     THE NEXT THREE ENTRIES ARE CARTESIAN COORDINATES X,Y,Z OF THE ATOM
C     ON THE SECOND CARD AS MANY 13 CHARACTER SPECIFICATIONS ARE READ IN
C     ARE PROVIDED BY NORB(I) ON THE FIRST CARD    EACH SET SPECIFIES AN
C     FIRST ITS N AND L QUANTUM NUMBERS,THEN THE SLATER EXPONENT,THEN TH
C     COULOMB INTEGRAL
C     THE LAST CARD IN THE DATA IS IN FORMAT(72I1)
C     THIS READS IN THE OCCUPATION NUMBERS OF THE VARIOUS MOLECULAR ORBI
C     STARTING FROM THE MOST BONDING UP TO THE ANTIBONDING ONES
C     THE ORDERING FOR  P    LEVELS IS  Z  X  Y
C     THE ORDERING FOR  D    LEVELS IS  Z**2  XZ  X**2-Y**2  YZ  XY
C     THE ORDERING FOR  P    LEVELS IS  Z  X  Y
C     THE ORDERING FOR  D    LEVELS IS  Z**2  XZ  X**2-Y**2  YZ  XY
C     ONE HAS NO CHOICE AT AL ABOUT THE DIRECTION IN WHICH THE BASIS
C     ORBITALS ARE POINTING   THEY ARE ALWAYS DEFINED WITH RESPECT TO TH
C     ABSOLUTE MOLECULAR COORDINATE SYSTEM
C     ALMOST ALL THE COMMUNICATION TO SUBPROGRAMS IS DONE THROUGH COMMON
C     AS USUAL THE NAMES OF THE SUBROUTINES HAVE LITTLE OR NO
C     RELATION TO THEIR FUNCTION
```
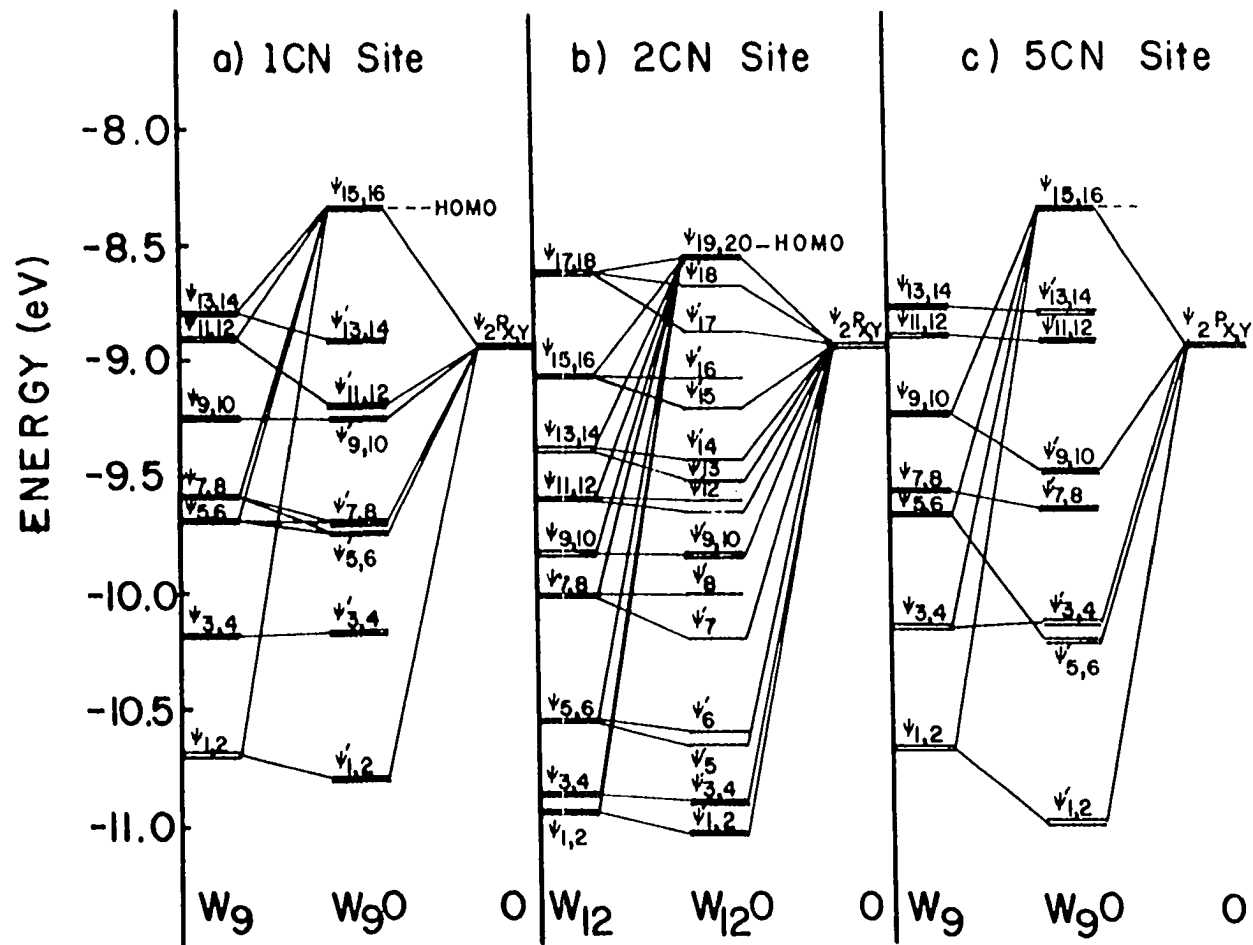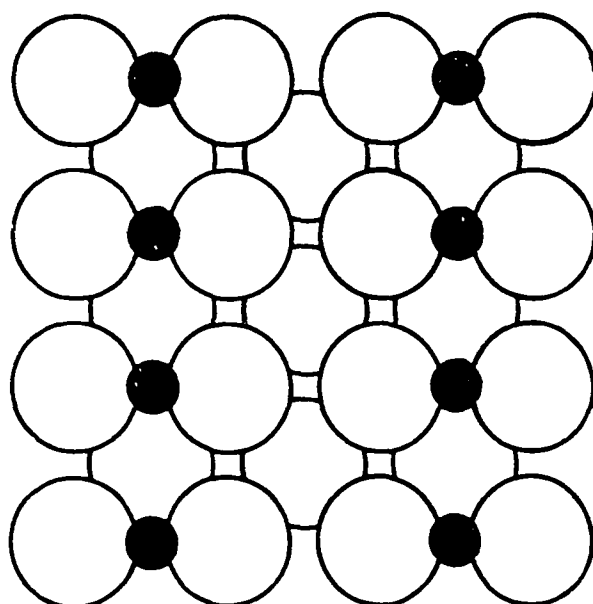
```
C       ONE SET OF DATA MAY BE PLACED IMMEDIATELY FOLLOWING ANOTHER
C       THERE IS A LIMITATION IN THE DIMENSIONING OF AFUNCT AND BFUNCT
C       SO THAT JMAX=N1+N2+L1+L2+1 MUST BE LESS THAN  20 FOR THE HIGHEST
C       POSSIBLE COMBINATION OF THESE ARGUMENTS
C       THIS CAN BE CHANGED BY EXPANDING THE DIMENSION STATEMENT
C       IN AFUNCT AND BFUNCT FOR A AND B  BUT ONE MUST BE CAREFUL
C       IN DOING THIS, SEE NOTE  AT BEGINNING OF B FUNCT
        DIMENSION XX(150),YY(150),ZZ(150),AR(150),AL(150)
        DIMENSION NOR(50,5),SLA(50,5),HII(50,5),NO(50,5),LO(50,5)
         DIMENSION S(140,140)
        DIMENSION ALPHA(150)
        DIMENSION A(100),B(100)
        DIMENSION ICOUNT(50,2)
        DIMENSION CORE(50)
        DIMENSION IOCC(150)
        DIMENSION D1(7),D2(7),M1(7),M2(7),M1SIG(7),M2SIG(7)
        DIMENSION DITTO(84),DITTA(84)
        DIMENSION FACT(25)
        DIMENSION DIM(5)
        DIMENSION NIN(7)
        DIMENSION LQ(150),MQ(150)
        DIMENSION ENER(20),DIS(20),XL(5),YL(5),GL(5),DL(5)
        COMMON   /OAA/ S
        COMMON   /CAB/ ICCC, XX, YY, N, NDIM
        COMMON   /CAC/ ZZ, LQ
        COMMON   /CAD/ A, B
        COMMON   /CAE/ ICOUNT, MC, ALPHA, CORE
        COMMON   /CAF/ MS, MC, MMM, MORB, MK, CON
        COMMON   /CAG/ L1, L2, N1, N2, SK1, SK2
        COMMON   /CAH/ SEPARN, WHEE, MAJ, MAK
        COMMON   /OAI/ NIN
        COMMON   /CAJ/ X1, X2, Y1, Y2, Z1, Z2
        COMMON   /CAK/ DIM
        COMMON   /CAL/ FACT
        COMMON   /CAM/ AR, AL, MR
        COMMON   /CAN/ ER,SUM
      1 FORMAT (7I2,F14.6,2I2)
      6 FORMAT(1H1)
      5 FORMAT(72H
     1                                                         )
      4 FORMAT(5(2I1,F5.3,F6.2))
    715 FORMAT(1H0,50X,20H DISTANCE MATRIX                 ////)
      2 FORMAT(I3,F7.2,3F10.6,F12.3,F6.3)
      8 FORMAT(6I7,3F10.6,F6.3,F6.2,F12.3,F6.3)
      9 FORMAT(110H ORBITAL   ATOM        N       L       M     SIGMA     X
     1 Y         Z       EXP   ALPHA     PRE-EXP    EXPON                )
    814 FORMAT(44HOH(I,J)=0.5*K*S(I,J)*(H(I,I)+H(J,J)) WITH K=   F7.2)
    815 FORMAT(25HOH(I,J)=K*S(I,J) WITH K=        F7.2)
    816 FORMAT(45HOH(I,J)=K*S(I,J)*SQRTF(H(I,I)*H(J,J)) WITH K= F7.2)
    821 FORMAT(40H THE ORBITALS ARE NUMBERED AS FOLLOWS             )
    822 FORMAT(25HOTOO MANY ORBITALS,EXIT               )
    977 FORMAT(72I1)
        NTRN=1
   1111 READ (5,1)N,MS,MC,MMM,MORB,MK,MR,CON,MG,NPP
        IF(N) 3495,3495,3496
```

```
3496 CCNTINLE
     WRITE (6,6)
     REAC (5,5)
     WRITE (6,5)
     CC 10 I=1,N
     READ   ( 5 ,2)NOR(I,1),CCRE(I),XX(I),YY(I),ZZ(I),AR(I),AL(I)
     NCPB=NCR(I,1)
     REAC   ( 5 ,4)(NC(I,J),LC(I,J),SLA(I,J),HII(I,J),J=1,NORB)
  10 CCNTINUE
     WRITE ( 6 ,821)
     hRITE ( 6 ,9)
     K=1
     DC 100 I=1,N
     ICCLNT(I,1)=K
     NCFB=NCR(I,1)
      LC(I)=LC(I,1)
     CC 98 J=1,NORB
     IF(LQ(I)-LO(I,J)) 31,32,32
  31 LQ(I)=LC(I,J)
  32 CCNTINUE
     KF=K+2*LC(I,J)
     KS=KF-K+1
C
C    GECRGE IS A LITTLE SUBRCUTINE WHICH ORDERS M ANC SIGMA FOR A GIVEN
C
     CALL GECRGE(M1,M1SIG,KS)
     CC 20 M=1,KS
     MM=M+K-1
     ALPHA(MM)=HII(I,J)
  20 WRITE ( 6 ,8)MM,I,NO(I,J),LO(I,J),M1(M),M1SIG(M),XX(I),YY(I),
    1ZZ(I),SLA(I,J),ALPHA(MM),AR(I),AL(I)
  98 K=K+KS
 100 ICCUNT(I,2)=K-1
     NCIM=ICCUNT(N,2)
C
C    . ICCLNT IS AN ARRAY WHICH TELLS FOR ATOM I THE NUMBERS OF THE FIRST
C      OREITALS BELONGING TO THAT ATCM
C      THIS IS USEFUL IN THE PCPULATICN ANALYSIS WHEN TOTALS OVER ATOMS A
C
     MKK=MK+1
     GC TO (817,818,819),MKK
 817 WRITE ( 6 ,814)CCN
     GC TO 820
 818 WRITE ( 6 ,815)CON
     GC TO 820
 819 WRITE ( 6 ,816)CCN
 820 CCNTINUE
     IF(NCIM-140) 823,823,824
 824 WRITE ( 6 ,822)
     STCP
 823 CCNTINLE
C
C    NCIM = TCTAL NUMBER OF CRBITALS
C
C    NCW THE CISTANCE MATRIX IS COMPUTED AND PRINTED OUT
```

```
C
      DC 714 I=1,N
      DC 714 J=1,N
  714 S(I,J)=SQRT((XX(I)-XX(J))**2+(YY(I)-YY(J))**2+(ZZ(I)-ZZ(J))**2)
      WRITE ( 6 ,715)
      CALL PEGLEG(S,N)
C
C
      CALL REPU
C
C
C     WE NOW CCMPUTE ALL THE FACTORIALS NECESSARY FOR THE OVERLAP COMPUT
C     HIGHEST IS  FACT(24)    AND FACT(I)=FACTORIAL(I-1)
C     RESTRICTION N1 CR N2 MUST BE LESS THAN 13
C     WHICH IS NOT MUCH OF A RESTRICTION AFTER ALL
C
      FACT(1)=1.0
      DC 2293 I=2,25
      II=I-1
 2293 FACT(I)=FLOAT(II)*FACT(II)
      DC 940 I=1,NDIM
      CC 940 J=1,NDIM
  940 S(I,J)=C.C
```

```
      CITTC(1)=1.0
      CITTA(1)=1.0
      M1(1)=C
      M2(1)=C
      M1SIG(1)=C
      M2SIG(1)=C
      NIN(3)=1
      NIN(5)=1C
      NIN(7)=35
      NM1=N-1
C     THE EVALUATION OF THE OVERLAP IS DONE IN A SET OF EIGHT NESTED
C     DC LCCPS    THE OUTERMOST ONE DEFINES AN ATOM PAUR, J GREATER THAN
C     THE NEXT TWD LOOPS IN DEFINE AN ORBITAL PAIR  II AND JJ IF THERE
C     MCRE THAN ONE CRBITAL ON A GIVEN ATOM    THE NEXT TWC DO LOOPS
C     RUN OVER ALL THE  VALUES OF M AND SIGMA FOR BOTH ORBITALS
C     THE INNERMOST PAIR CF LCCPS RUNS OVER  M AND SIGMA GAIN  THIS TIME
C     THE RESCLVED SET
C     THE ARRAY LQ CONTAINS THE  MAXIMUM L QUANTUM NUMBER FCR A GIVEN AT
C     THE RCTATION SUERCUTINE CERES(WHICH CALLS RTNMXN) THEN    NEED BE
C     CALLEC CNLY CNCE FOR EACH SET CF ATCMS
9999  DC 1000 I=1,NM1
      IP=I+1
      IKIN=    ICCUNT(I,1)
      X1=XX(I)
      Y1=YY(I)
      Z1=ZZ(I)
      NCRBI=NCR(I,1)
      DC 1000 J=IP,N
      JKIN=ICCLNT(J,1)
      N1S=0
      N2S=C
      NI=0
      NJ=C
      X2=XX(J)
      Y2=YY(J)
      Z2=ZZ(J)
      NORBJ=NOR(J,1)
      SEPARN=SCRT((X1-X2)**2+(Y1-Y2)**2+(Z1-Z2)**2)
      LLCI=LC(I)
      LLCJ=LC(J)
      CALL CERES(LLQI,DITTO,SEPARN)
      CALL CERES(LLQJ,DITTA,SEPARN)
      SEPARN=SEPARN/0.529171
      DC 900 II=1,NORBI
      N1=NC(I,II)
      L1=LC(I,II)
      IN=IKIN+NI
      N1S=2*L1+1
      NI=NI+N1S
      NJ=0
      N2S=0
      SK1=SLA(I,II)
      IF(L1) 901,902,901
901   CALL GECRGE(M1,M1SIG,N1S)
```

```
  902 CONTINUE
      DO 910 JJ=1,NORBJ
      N2=NC(J,JJ)
      SK2=SLA(J,JJ)
      L2=LC(J,JJ)
      JIN=JKIN+NJ
      N2S=2*L2+1
      NJ=NJ+N2S
      IF(L2) 903,904,903
  903 CALL GEORGE(M2,M2SIG,N2S)
  904 CONTINUE
C
C     MCLPAB ACQUIRES INFORMATION FROM AFUNCT AND BFUNCT THRU COMMON.
C
      JMAX=N1+N2+L1+L2+1
      CALL AFUNCT(SEPARN*(SK1+SK2)/2.0,JMAX)
      CALL BFUNCT(SEPARN*(SK1-SK2)/2.0,JMAX)
      DO 800 III=1,N1S
      CALL SEAN(III,N1S,DITTO,D1,NIN)
      DO 801 JJJ=1,N2S
      S(IN,JIN)=0.0
      CALL SEAN(JJJ,N2S,DITTA,D2,NIN)
C
C     THE ORBITAL HAS BEEN EXPANDED WRT A LOCAL COORDINATE SYSTEM.
C     JAM AND KAM ARE INDICES RANGING OVER THE LOCAL COORDINATE SYSTEMS
C     CF I AND J RESPECTIVELY.  WHEE REPRESENTS THE OVERLAP INTEGRAL
C     BETWEEN LOCAL ORBITALS JAM AND KAM.
C
      DO 118 JAM=1,N1S
      DO 118 KAM=1,N2S
      IF(M1(JAM)-M2(KAM)) 118,120,118
  120 IF(M1SIG(JAM)-M2SIG(KAM)) 118,121,118
  121 MAJ=M1(JAM)
      MAK=M2(KAM)
      CALL MCLPAB
C     BECAUSE MCLPAB CALCULATES OVERLAPS BETWEEN A RT.-HANDED SYSTEM AND
C     A LEFT-HANDED SYSTEM, WITH Z-AXES POINTING TOWARDS EACH OTHER, WE
C     MUST CHANGE SOME SIGNS.
C
      DO 124 KIX=1,7,2
      IF(L2-(KIX - 1)+MAK) 124,123,124
  124 CONTINUE
      WHEE=-WHEE
  123 S(IN,JIN)=S(IN,JIN)+D1(JAM)*WHEE*D2(KAM)
  118 CONTINUE
  801 JIN=JIN+1
      JIN=JIN-N2S
  800 IN=IN+1
  910 IN=IN-N1S
  900 CONTINUE
 1000 CONTINUE
      DO 1201 I=1,NDIM
      S(I,I)=1.0
      DO 1201 J=I,NDIM
 1201 S(J,I)=S(I,J)
```

```
C
C       THE CCCUPATION NUMBERS ARE READ IN FROM MOST BONDING TO ANTIBONDIN
C       BUT THEN THE DIRECTION HAS TO BE REVERSED BECAUSE THE EIGENVALUES
C       COME OUT IN REVERSE ORDER
C
        READ  ( 5 ,977)(MQ(I),I=1,NDIM)
        DO 856 I=1,NDIM
        J=NDIM-I+1
  856 ICCC(J)=MQ(I)
         CALL IGCR
        IF(MG) 3495, 3495, 3001
 3495 GC TC 1111
 3001 ENER(NTRN)=SUM
        NTRN=NTRN+1
        IF(NTRN.GT.NPP) GO TO 3002
        GC TC 1111
 3002 READ (5,3112) IS,MO,XS,YS,XSF,XM,YSF,YM
 3112 FCRMAT(2I3,6F5.2)
        REAC (5,3113) EINF,(DIS(I),I=1,NPP)
 3113 FCRMAT (F10.4,12F5.3)
        REAC(5,3114) XL,YL,GL,DL
 3114 FCRMAT (20A4)
        WRITE(6,3)
    3 FCRMAT(//12X,'DISTANCE',4X,'ENERGY',/)
        WRITE(6,2013) (DIS(I),ENER(I),I=1,NPP)
        WRITE (6,3)
        DO 3115 I=1,NPP
        ENER(I)=ENER(I)-EINF
        WRITE(6,2013) DIS(I),ENER(I)
 2013 FCRMAT(10X,2F10.3)
 3115 CCNTINUE
        CALL GRAPH(NPP,DIS,ENER,IS,MO,XS,YS,XSF,XM,YSF,YM,XL,YL,GL,DL)
        STCP
        END
```

```
      SUBROUTINE RTNMXN(D)
C     THIS SUBROUTINE CALCULATES THE TRANSFORMATION COEFFICIENTS OF ANGU
C     MOMENTUM FUNCTIONS      THESE ARE CONSTRUCTED BY RECURSION FORMULA
C     RESTRICTION- F ORBITALS ARE THE HIGHEST L THAT CAN BE TRANSFORMED
C     THE ORDERING OF COEFFICIENTS IS SUCH THAT M PRIME VARIES FASTEST
C     FOLLOWED BY SIGMA PRIME FOLLOWED BY M  FOLLOWED BY SIGMA
C     SIGMA =0 IS THE REAL COSINE COMBINATION, SIGMA=1 IS THE SINE
C     THIS SUBROUTINE  ORIGINALLY WRITTEN BY R.M. PITZER AND MODIFIED
C     FOR  THE SPECIAL CASE WHERE  CALPHA=1  SALPHA=0  . ACTUALLY.
C     THE DEFINITION  OF EULER ANGLES OF THE ROTATION WHICH TAKEN THE
C     MOLECULAR COORDINATE SYSTEM INTO THE LOCAL ONE    IS ONE WITH
C     ALPHA AND GAMMA INTERCHANGED FROM THE SYSTEM OF ROSE
      DIMENSION D(84)
      DIMENSION SA(2,4), SG(2,4), IEPS(4), DP(20), DM(10)
      COMMON  /RTN/ LMAX, CBETA, SBETA, CGAMMA, SGAMMA
      SA(1,1)=1.0
      SG(1,1)=1.0
      SA(2,1)=0.0
      SG(2,1)=0.0
      IEPS(1)=1
      DO 10 M=1,LMAX
      SA(1,M+1)=SA(1,M)
      SA(2,M+1)=SA(2,M)
      SG(1,M+1)=SG(1,M)*CGAMMA-SG(2,M)*SGAMMA
      SG(2,M+1)=SG(2,M)*CGAMMA+SG(1,M)*SGAMMA
   10 IEPS(M+1)=2
      IPM1=0
      IPM2=0
      IM=0
      IMM1=0
      IMM2=0
      IP=1
      DP(1)=1.0
      DM(1)=0.0
      DO 200 L=1,LMAX
      LM1=L-1
      LT2M1=L+LM1
      F1=FLOAT(L*LT2M1)
      F2=FLOAT(LM1*LT2M1)
      F3=FLOAT(LM1*L)
      IL=L+1
      DO 190 MPP=1,IL
      MP=MPP-1
      DO 180 MM=1,MPP
      M=MM-1
      IP=IP+1
      IF(MP-LM1) 40,80,120
   40 IPM1=IPM1+1
      IPM2=IPM2+1
      CNST1=F1/SQRT(FLOAT((L-MP)*(L+MP)*(L-M)*(L+M)))
      CNST2=SQRT(FLOAT((LM1-MP)*(LM1+MP)*(LM1-M)*(LM1+M)))/F2
      IF(M) 44,44,60
   44 DP(IP)=CNST1*(CBETA*DP(IPM1)-CNST2*DP(IPM2))
      GO TO 180
```

```
 6C IM=IM+1
    IMM1=IMM1+1
    IMM2=IMM2+1
    CNST3=FLCAT(MP*M)/F3
    DP(IP)=CNST1*(CBETA*DP(IPM1)-CNST2*DP(IPM2)-CNST3*DM(IMM1))
    CM(IM)=CNST1*(CBETA*DM(IMM1)-CNST2*DM(IMM2)-CNST3*DP(IPM1))
    GC TC 18C
 8C IPM1=IPM1+1
    CNST1=F1/SQRT(FLOAT(LT2M1*(L-M)*(L+M)))
    IF(M) 84,84,100
 84 DP(IP)=CNST1*CBETA*DP(IPM1)
    GC TC 18C
1CC IM=IM+1
    IMM1=IMM1+1
    CNST3=FLCAT(MP*M)/F3
    DP(IP)=CNST1*(CBETA*DP(IPM1)-CNST3*DM(IMM1))
    CM(IM)=CNST1*(CBETA*DM(IMM1)-CNST3*DP(IPM1))
    GC TC 18C
12C IF(M-L) 130,160,130
130 CNST4=SQRT(F1/FLOAT((L-M)*(L+M)*IEPS(L)))
    IF(M) 145,140,145
14C IPM1=IPM1-LM1
    IMM1=IMM1-LM1
    GC TC 148
145 IM=IM+1
    IPM1=IPM1+1
    IMM1=IMM1+1
    CM(IM)=-CNST4*SBETA*DM(IMM1)
148 DP(IP)=-CNST4*SBETA*DP(IPM1)
    GC TO 18C
16C IM=IM+1
    IF(M-1) 164,164,168
164 DP(IP)=-CBETA*DP(IPM1)
    CM(IM)=-DP(IPM1)
    GC TC 18C
168 DP(IP)=-.5*(CBETA*DP(IPM1)+DM(IMM1))
    DM(IM)=-.5*(CBETA*DM(IMM1)+DP(IPM1))
18C CCNTINLE
1SC CCNTINLE
200 CCNTINUE
    FSIG=-1.C
    FSIGP=-1.C
    I=1
    C(1)=1.C
    CC 400 L=1,LMAX
    IP=(L*(L+1)*(L+2))/6+1
    IM=((L-1)*L*(L+1))/6
    CC 390 ISIGG=1,2
    ISIG=ISIGG-1
    ICSIG=1-ISIG
    FSIG=-FSIG
    FM=-FSIG
    LL=L+1
    DO 38C MZ=ISIGG,LL
    M=MZ-1
```

```
      MP1=MZ
      FM=-FM
      CC 370 ISIGPP=1,2
      ISIGP=ISIGPP-1
      ICSIGP=1-ISIGP
      FSIGP=-FSIGP
       CC 360 MPZ=ISIGPP,LL
      MP=MPZ-1
      MPP1=MPZ
      I=I+1
      IF(MP-M) 300,330,330
300   I1P=IP+(M*(M+1))/2+MP
      I1M=IM+((M-1)*M)/2+MP
      GC TO 350
330   I1P=IP+(MP*(MP+1))/2+M
      I1M=IM+((MP-1)*MP)/2+M
350   IF(I1M) 351,352,351
351   C(I)=FM*(FSIGP*DP(I1P)*SA(ISIGP+1,MPP1)*SG(ISIG+1,MP1)-FSIG*
     1DM(I1M)*SA(ICSIGP+1,MPP1)*SG(ICSIG+1,MP1))
      GC TO 360
352   C(I)=FM*(FSIGP*DP(I1P)*SA(ISIGP+1,MPP1)*SG(ISIG+1,MP1))
360   CCNTINUE
370   CCNTINUE
380   CONTINUE
390   CCNTINUE
400   CCNTINUE
      RETURN
      END
```

```
      SUBROUTINE BFUNCT (RHO2, IX)
C
C     THIS SUBROUTINE CALCULATES THE B-FUNCTIONS WITH INDICES OF 0 TO IX
C     FOR THE GIVEN VALUE OF RHO2.
C     ORIGINALLY WRITTEN BY R.M. STEVENS
C     IF THE DIMENSION OF B IS CHANGED THAN ONE MUST ALSO MODIFY
C     THE STATEMENT DEFINING IS SO THAT THE SECOND ENTRY IN THE ARGUMENT
C     XMINOF IS THE DIMENSION OF B MINUS 1
C
      DIMENSION A(100),B(100)
      COMMON  /CAD/ A, B
      IA=IFIX(2.0*RHO2)
      IR=IABS(IA)
      IS=MINC(IR+1,99)
      IF (RHO2) 25,35,25
   25 C = EXP(RHO2)
      H = EXP(-RHO2)
      R=C-H
C
C     IF THE VALUE OF RHO2 IS TOO SMALL  THE SINH MUST BE OBTAINED BY
C          SUMMING THE INFINITE SERIES RATHER THAN BY ADDITION OF TWO
C          EXPONENTIALS.
C
      IF (ABS(R)-0.1) 26,28,28
   26 RA=0.0
      T = RHO2
      DO 27 I=2,25
      T = T*RHO2**2/FLOAT((2*I-1)*(2*I-2))
   27 RA = RA+T
      R = (RA+RHO2)*2.
   28 B(1) = R/RHO2
C
C     AS MANY SUCCESSIVE B-FUNCTIONS ARE GENERATED FROM B-0 BY THE RE-
C          CURRENCE FORMULAE AS ACCURACY WILL PERMIT.
C
      DO 51 I=2,IX,IS
      IF (IR) 32,40,32
   32 IL=IS-1
      DO 31 J=1,IL
      K = I+J-1
      IF ((-1)**K) 29,29,30
   29 B(K) = (R+FLOAT(K-1)*B(K-1))/RHO2
      GO TO 31
   30 B(K) = -(C+H-FLOAT(K-1)*B(K-1))/RHO2
   31 CONTINUE
   40 IN=I+IS-1
      IF (IN-IX) 39,39,38
C
C     AFTER THE RECURRENCE FORMULAE HAVE BEEN APPLIED AN APPROPRIATE
C          NUMBER OF TIMES THE NEXT B-FUNCTION IS OBTAINED BY SUM-
C     MATION OF THE INFINITE SERIES.
C
   39 IF((-1)**IN) 44,44,42
   42 TR = RHO2
```

```
105 B(IN) = -2.*TR/FLCAT(IN+1)
    CC 43 J = 1,500
    TR = TR*RHO2**2/FLOAT((2*J)*(2*J+1))
    IF (ABS(TR/B(IN))-.0000001) 51,51,43
 43 B(IN) = B(IN)-2.*TR/FLOAT(IN+1+2*J)
 44 TR = 1.
107 B(IN) = 2.*TR/FLOAT(IN )
    DC 46 J = 1,500
    TR = TR*RHO2**2/FLOAT((2*J)*(2*J-1))
    IF (ABS(TR/B(IN))-.0000001) 51,51,46
 46 B(IN) = B(IN)+2.*TR/FLOAT(IN+2*J)
 51 CCNTINUE
    GC TC 38
C
C       IF THE ARGUMENT IS ZERC A SEPARATE FORMULA MUST BE USED.
C
 35 JY = IX/2+2
    CC 36 I =1,JY
    B(2*I)=0.0
 36 B(2*I-1)=2./FLCAT(2*I-1)
 38 RETURN
    END
```

```
      SUBROUTINE BINCCE(I, J, B)
C
C     THIS SUBROUTINE COMPUTES BINOMIAL COEFFICIENTS
C
      DIMENSION FACT(25)
      COMMON  /CAL/ FACT
      K=J-I
      B=FACT(J+1)/FACT(I+1)/FACT(K+1)
    1 RETURN
      END


      SUBROUTINE SEAN(I, N, DITTO, D, NIN)
C     THIS SUBROUTINE FINDS THE RIGHT ELEMENTS OF DITTO AND PUTS THEM IN
C     SMALLER ARRAY D
      DIMENSION DITTO(84),D(7),NIN(7)
      IF(N-1) 1,2,1
    2 D(1)=1.0
      RETURN
    1 CONTINUE
      LIB=NIN(N)+N*(I-1)
      DO 85 JIB=1,N
      INGRID=JIB+LIB
   85 D(JIB)=DITTO(INGRID)
      RETURN
      END
```

```
      SUBROUTINE SEAN(I, N, DITTO, D, NIN)
C     THIS SUBROUTINE FINDS THE RIGHT ELEMENTS OF DITTO AND PUTS THEM IN
C     SMALLER ARRAY D
      DIMENSION DITTO(84),D(7),NIN(7)
      IF(N-1) 1,2,1
    2 D(1)=1.0
      RETURN
    1 CONTINUE
      LIB=NIN(N)+N*(I-1)
      DO 85 JIB=1,N
      INGRID=JIB+LIB
   85 D(JIB)=DITTO(INGRID)
      RETURN
      END
```

```
      SUBROUTINE AFUNCT (RHO1, J)
C
C     THIS SUBROUTINE CALCULATES THE A-FUNCTIONS WITH INDICES OF 0 TO J
C           FOR THE GIVEN VALUE OF RHO1.
C     ORIGINALLY WRITTEN BY R.M. STEVENS
C
      DIMENSION A(100),B(100)
      COMMON  /CAD/ A, B
      C = EXP(-RHO1)
      A(1) = C/RHO1
      DO 15 I = 2,J
   15 A(I) = (FLOAT(I-1)*A(I-1)+C)/RHO1
      RETURN
      END
```

```
      SUBROUTINE MOLPAB
C
C     THIS SUBROUTINE CALCULATES TWO-CENTER OVERLAP INTEGRALS.
C     THE INTEGRALS ARE CALCULATED BY TRANSFORMATION TO ELLIPSOIDAL
C          COORDINATES AND THEREBY EXPRESSED IN TERMS OF C-FUNCTIONS.
C     (SEE  J.C.P., 24, 201.)
C     ORIGINALLY WRITTEN BY R.M. STEVENS
C
      DIMENSION FACT(25)
      COMMON  /OAG/ L1, L2, N1, N2, SK1, SK2
      COMMON  /OAH/ R, VEST, M1, M2
      COMMON  /OAL/ FACT
      VEST = 0.0
      STRAD = 0.0
      RHOA = R*SK1
      RHOB = R*SK2
      F1=FACT(2*N1+1)
      F2=FACT(2*N2+1)
      IF=L1-M1+1
      F3=FACT(IF)
      IF=L2-M2+1
      F4=FACT(IF)
      IF=L1+M1+1
      F5=FACT(IF)
      IF=L2+M2+1
      F6=FACT(IF)
      TERM = 2.**(N1+N2-L1-L2)*SQRT(FLOAT((2*L1+1)*(2*L2+1))*F3*F4/F1/
     1F2/F5/F6*SK1**(2*N1+1)*SK2**(-2*N1-1))
      JEND = 1+((L1-M1)/2)
      KEND = 1+((L2-M2)/2)
      DO 50 J=1,JEND
      JU=J-1
      IF=2*L1-2*JU+1
      F11=FACT(IF)
      IF=L1-M1-2*JU+1
      F13=FACT(IF)
      F15=FACT(JU+1)
       IF=L1-JU+1
      F17=FACT(IF)
      DO 50 K=1,KEND
      KU=K-1
      IF=2*L2-2*KU+1
      F12=FACT(IF)
      IF=L2-M2-2*KU+1
      F14=FACT(IF)
      F16=FACT(KU+1)
      IF=L2-KU+1
      F18=FACT(IF)
      CALL CFUNCT (N1-L1+2*JU,N2-L2+2*KU,L1-M1-2*JU,L2-M2-2*KU,M1,RHOA,
     1 RHOB,VALUE)
   50 STRAD = STRAD+VALUE*F11*F12/F13/F14/F15/F16/F17/F18*(-1.)**(JU+KU)
      VEST=TERM*STRAD
      RETURN
      END
```

```
      SUBROUTINE GEORGE(M, MSIG, NSBSP)
      DIMENSION M(7),MSIG(7)
      M(1)=0
      MSIG(1)=0
      K=(NSBSP/2)+1
      IF(K-1) 5,5,6
    6 CONTINUE
      DO 10 J=2,K
      M(J)=J-1
      MSIG(J)=0
      L=K+J-1
      M(L)=J-1
   10 MSIG(L)=1
    5 RETURN
      END
```

```
      SLBRCUTINE CFUNCT (IA, IB, IC, IC, IE, RHOA, RHOB, SNAG)
C
C     THIS SUBRCUTINE CALCULATES THE  C-COEFFICIENTS OF ROOTHAAN
C     FCR CVERLAP INTEGRALS CNLY THE C-FUNCTICNS WITH POSITIVE INDICES
C            ARE NECESSARY AND THESE MAY BE CONVENIENTLY CALCULATED BY
C            EXPANSION BY THE BINOMIAL THEOREM.
C     CRIGINALLY WRITTEN BY R.M. STEVENS
C
      DIMENSICN A(100),B(100)
      CCMMCN /CAD/ A, B
   25 CCLNT = C.0
      VEST = TERM*STRAD
      RETURN
      ENC

      IAB = IA+1
      IBB=IB+1
      ICE=IC+1
      ICB=ID+1
      IEB=IE+1
      DC 91 I6=1,IEB
      J6=I6-1
      CALL BINCCE (J6,IE,B6)
      DO 91 I5=1,IEB
      J5=I5-1
      CALL BINCCE (J5,IE,B5)
      DC 90 I4=1,IDB
      J4=I4-1
      CALL BINCCE (J4,IC,B4)
      CC 90 I3=1,ICB
      J3=I3-1
      CALL BINCCE (J3,IC,B3)
      CC 90 I2=1,IBB
      J2=I2-1
      CALL BINCCE (J2,IB,B2)
      CC 90 I1=1,IAB
      J1=I1-1
      CALL BINCCE (J1,IA,B1)
      TERM = B1*B2*B3*B4*B5*B6*(-1.)**(J2+J5+J6+J4+IE+ID)
      IR = J1+J2+2*IE-2*J6+IC-J3+ID-J4+1
      IP = IA-J1+IB-J2+2*IE-2*J5+IC-J3+ID-J4+1
      CCLNT = CCUNT +A(IP)*B(IR)*TERM
   90 CCNTINUE
   91 CCNTINUE
      SNAG = CCUNT*(RHOB /2.)**(IA+IB+IC+ID+2*IE+1)
   92 RETLRN
      ENC
```

```
      SLBROLTINE PEGLEG(A, N)
C     MATRIX OUTPUT SLBROUTINE
      CIMENSION A(140,140)
18 FCRMAT(I4,2X,11F10.6)
19 FCFMAT(1H0/1H0,4X,11(6X,I2,2X)//)
      KITE=0
20 LCW=KITE+1
      KITE=KITE+11
      KITE=MINC(KITE,N)
      WRITE (  6 ,19)(I,I=LOW,KITE)
      CC 32 I=1,N
32 WRITE (  6 ,18)I,(A(I,J),J=LOW,KITE)
      IF(N-KITE) 40,4C,20
4C RETURN
      END
```

```
      SUBROUTINE CERES(LQ, DITTO, SEP)
C     THIS SUBROUTINE   CALCULATES THE EULER ANGLES OF ROTATION AND
C     PROCEEDS TO CALL RTNMXN FOR THE GENERATIONS OF THE TRANSFORMATIONS
C     OF ANGULAR MOMENTUM FUNCTIONS
      DIMENSION DITTO(84)
      COMMON  /CAJ/ X1, X2, Y1, Y2, Z1, Z2
      COMMON  /RTN/ LMAX, CBETA, SBETA, CGAMMA, SGAMMA
  200 FORMAT('ERROR, POSSIBLY ROUNDING OFF ERROR IN CALCULATION OF SEP')
      IF(LQ) 100,100,101
  100 DITTO(1)=1.0
      RETURN
  101 CONTINUE
      LMAX=LQ
      ZZ=Z2-Z1
      IF(X2-X1) 20,5, 20
    5 IF(Y2-Y1) 20, 10, 20
   10 CGAMMA=1.0
      SGAMMA=0.0
      CBETA=SIGN(1.0,ZZ)
      SBETA=0.0
      GO TO 30
   20 ARGU=SEP*SEP-ZZ*ZZ
      IF(ARGU .GE. 0.) GO TO 25
      IF(ARGU .GE. -1.E-6) GO TO 24
      WRITE (6,200)
      STOP
   24 ARGU=0.
   25 SXY=SQRT(ARGU)
          CBETA=ZZ/SEP
      SBETA=SXY/SEP
      CGAMMA=(X2-X1)/SXY
      SGAMMA = (Y2-Y1)/SXY
   30 CALL RTNMXN(DITTO)
      RETURN
      END
```

```
      SUBROUTINE IGOR
C     COMPUTES  H MATRIX FROM S WHICH IS ASSUMED TO BE IN CORE
C     H GOES OUT ON TAPE IH THEN  DIAGONALIZATION AND  POPULATION
C     ANALYSIS ROUTINES ARE CALLED
C     OPTIONS   MS=1 PUNCHES OUT BCD S      MC=1 PUNCHES OUT C
C     MM=1 BYPASSES POPULATION ANALYSIS
C     MK=0 USES ADDITIVE WOLFSBERG-HELMHOLTZ FORMULA
C     MK=1 USES DIRECT PROPORTIONALITY H(I,J)=K*S(I,J)
C     MK=2 USES  GEOMETRIC MEAN WOLFSBERG HELMHOLTZ FORMULA
      DIMENSION A(140,140)
      DIMENSION IX(150)
      DIMENSION ALPHA(150), LATER(150)
      DIMENSION HDIAG(150),B(150)
      DIMENSION IOCC(150)
      DIMENSION CORE(50)
      DIMENSION ICOUNT(50,2)
      COMMON /CAA/ A
      COMMON  /CAB/IX, ALPHA, B, N, NT
      COMMON  /CAE/ ICOUNT,  LATER, HDIAG, CORE
      COMMON  /CAF/ MS, MC, MMM, MORB, MK, CON
      CONP=0.5*CON
      MK=MK+1
      REWIND 4
    1 FORMAT(1H0,50X,23H TOTAL OVERLAP MATRIX          //)
      WRITE (  6 ,1)
      CALL PEGLEG(A,NT)
    4 FORMAT(8F9.6)
      IF(MS-1) 2,3,2
    3 WRITE (  7 ,4)((A(I,J),J=1,NT),I=1,NT)
    2 GO TO (5,6,7),MK
    5 DO 8 I=1,NT
      DO 9 J=1,NT
    9 B(J)=A(I,J)*CONP*(HDIAG(I)+HDIAG(J))
      B(I)=HDIAG(I)
    8 WRITE ( 4)(B(J),J=1,NT)
      GO TO 15
    6 DO 10 I=1,NT
      DO 11 J=1,NT
   11 B(J)=A(I,J)*CON
      B(I)=HDIAG(I)
   10 WRITE ( 4)(B(J),J=1,NT)
      GO TO 15
    7 DO 12 I=1,NT
      DO 13 J=1,NT
   13 B(J)=A(I,J)*CON*SQRT(HDIAG(I)*HDIAG(J))
      B(I)=HDIAG(I)
   12 WRITE ( 4)(B(J),J=1,NT)
   15 CONTINUE
      REWIND 8
      DO 19 I=1,NT
   19 WRITE ( 8)(A(I,J),J=1,NT)
      CALL SCREN
      IF(MC-1) 14,16,14
   16 WRITE (  7 ,4)((A(I,J),J=1,NT),I=1,NT)
```

```
14 IF(MMM-1) 17,18,17
17 CALL MELBA
18 RETURN
   END
```

```
      SUBROUTINE MELBA
C     POPULATION ANALYSIS SUBROUTINE
C     ASSUMES S ON IS   BY RCWS       C IN CORE
      DIMENSION A(140,140),IOCC(150),HDIAG(150),B(150),C(150)
      DIMENSION ICOUNT(50,2), LATER(150)
      DIMENSION CORE(50)
      COMMON   /CAA/ A
      COMMON   /CAB/ IOCC, HDIAG, C, N, NT
      COMMON   /CAE/ ICOUNT,  LATER, B, CORE
      COMMON   /CAF/ MS, MC, MMM, MORB, MK, CON
    3 FORMAT(///40X,35H MULLIKEN OVERLAP POPULATIONS FOR    I3,10H ELECTR
     1ONS//)
      ISUM=0
      DO 5 I=1,NT
    5 ISUM=ISUM+IOCC(I)
      WRITE ( 6 ,3)ISUM
      REWIND 3
      DO 4 J=1,NT
    4 WRITE ( 3)(A(I,J),I=1,NT)
      IF(MORB) 6,6,7
    7 DO 8 I=1,NT
    8 HDIAG(I)=A(I,MORB)
    6 CONTINUE
      CALL CARUSO(IOCC,A,C,NT)
      CALL PEGLEG(A,NT)
      IF(MORB) 9,9,10
   10 REWIND 4
      WRITE ( 4)((A(I,J),J=1,NT),I=1,NT)
      REWIND 8
      DO 11 I=1,NT
   11 READ ( 8)(A(I,J),J=1,NT)
      DO 12 I=1,NT
      DO 12 J=1,NT
   12 A(I,J)=2.0*A(I,J)*HDIAG(I)*HDIAG(J)
      WRITE ( 6 ,13)MORB
   13 FORMAT(1H0,20X,45H OVERLAP POPULATION FOR ELECTRON IN ORBITAL
     1I3//)
      CALL PEGLEG(A,NT)
      CALL JENNY(ICOUNT,A, N, C )
      REWIND 4
      READ ( 4)((A(I,J),J=1,NT),I=1,NT)
    9 CONTINUE
      CALL JENNY(ICOUNT,A, N, C )
      CALL CALLAS(A, NT, C )
      DO 18 I=1,NT
   18 B(I)=0.0
      DO 15 M=1,NT
      RR=FLOAT(IOCC(M))/2.0
      IF(RR) 15,15,17
   17 DO 16 I=1,NT
   16 B(I)=B(I)+RR*A(I,M)
   15 CONTINUE
   78 FORMAT(1H0,50X,20H ORBITAL CHARGES          //)
      WRITE ( 6 ,78)
```

```
19 FORMAT(50X,I4,F10.6)
   WRITE ( 6 ,19)(I,B(I),I=1,NT)
   DO 20 I=1,N
   IN=ICOUNT(I,1)
   IFF=ICOUNT(I,2)
   C(I)=0.0
   DO 21 J=IN,IFF
21 C(I)=C(I)+B(J)
20 C(I)=CORE(I)-C(I)
22 FORMAT(1H0,50X,15H NET CHARGES              //)
23 FORMAT(50X,I4,F10.6)
   WRITE ( 6 ,22)
   WRITE ( 6 ,23)(I,C(I),I=1,N)
   TERT=0
   DO 24 I=1,N
24 TERT=TERT+C(I)
25 FORMAT(1H0,20X,15HTOTAL CHARGE=            F10.6//)
   WRITE ( 6 ,25)TERT
   RETURN
   END
```

```
      SLBROLTINE CALLAS(A, NT, B)
C     CCMPUTES TOTAL GRCSS OVERLAP POPULATION MATRIX
      CIMENSICN A(140,140),B(150)
      REWIND 3
      CC 3 J=1,NT
    3 READ   ( 3)(A(I,J),I=1,NT        )
      CALL CCKI
C      NCW A=SC
      REWINC 3
       CC 1 M=1,NT
       READ   (3) (B(J),J=1,NT)
      CC 1 I=1,NT
    1 A(I,M)=A(I,M)*B(I)*2.0
    2 FCRMAT(1H0,50X,50HCHARGE MATRIX FOR MO'S WITH TWO ELECTRONS IN EAC
     1H                //)
       WRITE (  E ,2)
       CALL PEGLEG(A,NT)
       RETURN
       ENC
```

```
      SLBROUTINE CUPID
C
C     DIAGCNALIZATION OF A REAL SYMMETRIC MATRIX BY THE JACOBI METHOD.
C
C     THERE IS A FACTCR QMULT INSERTED WHICH ESSENTIALLY SETS THE
C     CCNVERGENCE CRITERION FOR THE DIAGCNALIZATION  THIS WAS ORIGINALLY
C     BUT NOW HAS BEEN SET TO 100.0   WHIVH SHOULD GIVE A TCTAL ENERGY
C     TC BETTER THAN CNE PART ON 10 TO THE 8
      CIMENSION H(140,140),IA(150),HDIAG(150),X(150),IQ(150),ARRAY(252)
      CCMMCN   /OAA/ H
      CCMMCN   /CAB/IA, HDIAG, X, NDIM, N
      CCMMON   /CUD/ ARRAY, IPIV, JPIV, CCSINE, SINE
C     THE SUBRCUTINE GPERATES CNLY ON THE ELEMENTS OF H THAT ARE TO THE
C     RIGHT OF THE MAIN DIAGONAL.  THUS, ONLY A TRIANGULAR SECTION NEEC
C     BE STCREC.
C
C     NR IS THE NUMBER CF ROTATIONS
C     LAFITE , MOUTON AND YCUEM ARE SUBROUTINES USED TO PACK WRITE AND R
C     THE VARIOUS QUANTITIES NEEDED TO CCMPUTE THE EIGENVECTORS OUT ON
C     TAPES - THE ROUTINE CAN CNLY HOLC CNE MATRIX IN CORE AT A TIME
C
C     THE EIGENVALUES ARE PUT OUT IN THE VECTOR  HDIAG
C
C     TAPE ITAPEU IS LSED TC STORE IPIV,JPIV,COSINE,SINE FOR EACH
C     RCTATICN, IN ORCER THAT THE EIGENVECTORS MAY BE COMPUTED AFTER
C     CIAGCNALIZATION IS CCMPLETE.
C
      MCM=1
      REWIND 3
  999 FCRMAT(1H0,3HNR=,I5)
      NR=0
      IF (N-1) 1000,1C00,17
C
C     SCAN FCR LARGEST OFF-DIAGONAL ELEMENT IN EACH ROW.  X(I) CONTAINS
C     LARGEST ELEMENT IN THE ITH ROW, AND IQ(I) HOLDS SECOND SUBSCRIPT
C     CEFINING POSITICN OF ELEMENT.
C
   17 NMI1=N-1
      CO 30 I=1,NMI1
      X(I)=0.
      IPL1=I+1
      CC 30 J=IPL1,N
      IF (X(I)-ABS(H(I,J))) 20,20,30
   2C X(I)=ABS(H(I,J))
      IC(I)=J
   3C CCNTINUE
C
C     SET INDICATOR FCR SHUT-CFF.  RAP=2**-27.
C
      RAP=.745058E-08
      CMLLT=10C.0
      RAF=RAP*QMULT
      HCTEST=1.0E38
C
```

```
C        FINC MAXIMUM OF X(I)'S FOR PIVOT ELEMENT, AND TEST FOR END OF
C        PROBLEM.
C
   4C DC 70 I=1,NMI1
         IF (I-1) 60,60,45
   45 IF (XMAX-X(I)) 60,70,70
   6C XMAX=X(I)
         IPIV=I
         JPIV=IC(I)
   7C CONTINUE
C
C        IF XMAX LESS THAN HDTEST, REVISE HDTEST.
C
         IF (XMAX) 1000,1000,80
   8C IF (HDTEST) 9G,90,85
   85 IF (XMAX-HDTEST) 90,90,148
   9C HDIMIN=ABS(H(1,1))
         CD 110 I=2,N
         IF (HDIMIN-ABS(H(I,I))) 110,110,100
  10C HDIMIN=ABS(H(I,I))
  11C CONTINUE
         HDTEST=HDIMIN*RAP
C
C        RETURN IF MAXIMUM H(I,J) LESS THAN (2**-27)*ABSF(H(K,K)-MIN)
C
         IF(HDTEST-XMAX) 148,1000,1000
  148 NR=NR+1
C
C        CCMPUTE TANGENT,SINE, ANC COSINE, H(I,I), H(J,J)
C
  150 TANG=SIGN(2.0,(H(IPIV,IPIV)-H(JPIV,JPIV)))*H(IPIV,JPIV)/(ABS(H(IPI
     1V,IPIV)-H(JPIV,JPIV))+SQRT((H(IPIV,IPIV)-H(JPIV,JPIV))**2+4.0*H(IP
     2IV,JPIV)**2))
         CCSINE=1.0/SQRT(1.0+TANG**2)
         SINE=TANG*COSINE
         HII=H(IPIV,IPIV)
         H(IPIV,IPIV)=COSINE**2*(HII+TANG*(2.*H(IPIV,JPIV)+TANG*
     1H(JPIV,JPIV)))
         H(JPIV,JPIV)=COSINE**2*(H(JPIV,JPIV)-TANG*(2.*H(IPIV,JPIV)-TANG*
     1HII))
         H(IPIV,JPIV)=0.
C
C        PSEUDO-RANK THE EIGENVALUES.  ADJUST SIN AND COS FOR COMPUTATION
C        H(I,K).
C
         IF (H(IPIV,IPIV)-H(JPIV,JPIV)) 152,153,153
  152 HTEMP = H(IPIV,IPIV)
         H(IPIV,IPIV)=H(JPIV,JPIV)
         H(JPIV,JPIV)=HTEMP
C
C
C        RECCMPUTE SINE ANC COS
         HTEMP=SIGN(1.0,-SINE)*COSINE
         CCSINE=ABS(SINE)
         SINE=HTEMP
```

```
  153 CCNTINLE
C
C       INSPECT THE IQ'S BETWEEN I+1 AND N-1 TO DETERMINE WHETHER A NEW
C       MAXIMUM VALUE SHOULD BE COMPUTED, SINCE THE PRESENT MAXIMUM IS IN
C       ROW I CR J.
C
        DO 350 I=1,NMI1
        IF (I-IPIV) 210,350,200
  200 IF (I-JPIV) 210,350,210
  210 IF (IC(I)-IPIV) 230,240,230
  230 IF (IQ(I)-JPIV) 350,240,350
  24C K=IQ(I)
  25C HTEMP=H(I,K)
        H(I,K)=0.
        IPL1=I+1
        X(I)=0.
C
C       SEARCH IN DEPLETED ROW FCR NEW MAXIMUM.
C
        CC 320 J=IPL1,N
        IF (X(I)-ABS(H(I,J))) 300,300,320
  300 X(I)=ABS(H(I,J))
        IC(I)=J
  32C CCNTINUE
        H(I,K)=HTEMP
  35C CCNTINLE
        X(IPIV)=0.
        X(JPIV)=0.
C
C       CHANGE THE OTHER ELEMENTS OF H.
C
        CC 53C I=1,N
        IF (I-IPIV) 370,530,420
  370 HTEMP=H(I,IPIV)
        H(I,IPIV)=COSINE*HTEMP+SINE*H(I,JPIV)
        IF (X(I)-ABS(H(I,IPIV))) 380,390,390
  380 X(I)=ABS(H(I,IPIV))
        IC(I)=IPIV
  39C H(I,JPIV)=-SINE*HTEMP+CCSINE*H(I,JPIV)
        IF (X(I)-ABS(H(I,JPIV))) 400,530,530
  40C X(I)=ABS(H(I,JPIV))
        IQ(I)=JPIV
        GC TO 530
  42C IF (I-JPIV) 430,530,480
  43C HTEMP=H(IPIV,I)
        H(IPIV,I)=COSINE*HTEMP+SINE*H(I,JPIV)
        IF (X(IPIV)-ABS(H(IPIV,I))) 440,450,450
  440 X(IPIV)=ABS(H(IPIV,I))
        IC(IPIV)=I
  450 H(I,JPIV)=-SINE*HTEMP+CCSINE*H(I,JPIV)
        IF (X(I)-ABS(H(I,JPIV))) 400,530,530
  48C HTEMP=H(IPIV,I)
        H(IPIV,I)=COSINE*HTEMP+SINE*H(JPIV,I)
        IF (X(IPIV)-ABS(H(IPIV,I))) 490,500,500
  490 X(IPIV)=ABS(H(IPIV,I))
```

```
      IG(IPIV)=I
 500  H(JPIV,I)=-SINE*HTEMP+CCSINE*H(JPIV,I)
      IF (X(JPIV)-ABS(H(JPIV,I))) 510,530,530
 510  X(JPIV)=ABS(H(JPIV,I))
      IG(JPIV)=I
 530  CCNTINUE
 540  CALL LAFITE(MOM)
      GO TO 40
1000  WRITE ( 6 ,999)NR
      IF(MOM-1) 2014,2014,2015
2015  CALL MCUTON
2014  MCM=1
1002  DO 1004 J=1,N
1004  HDIAG(J)=H(J,J)
      DO 14 I=1,N
      DO 12 J=1,N
      H(I,J)=0.
 12   CCNTINUE
      H(I,I)=1.
 14   CCNTINUE
      IF (NR) 1005,1005,1006
1006  CCNTINUE
      REWIND 3
      NRV=1
1167  IF(NRV-NR) 1168,1168,1100
1168  CCNTINUE
      CALL YCUEM(MOM)
      DO 1101 I=1,N
      HTEMP=H(I,IPIV)
      BCB=CCSINE*HTEMP
      SCB=-SINE*HTEMP
      CCB=SINE*H(I,JPIV)
      H(I,IPIV)=BOB+CCB
      TCB=CCSINE*H(I,JPIV)
      H(I,JPIV)=SOB+TCB
1101  CONTINUE
      NRV=NRV+1
      GO TO 1167
1100  CCNTINUE
1005  NM=N-1
      DO 742 J=1,NM
      JP=J+1
      DO 895 K=1,J
      IF (HDIAG(K)-HDIAG(JP)) 841,895,895
 841  HH=HDIAG(K)
      HDIAG(K)=HDIAG(JP)
      HDIAG(JP)=HH
      DO 1009 I=1,N
      HH=H(I,K)
      H(I,K)=H(I,JP)
      H(I,JP)=HH
1009  CCNTINUE
 895  CCNTINUE
 742  CCNTINUE
      RETURN
```

```
      SLBROUTINE YQUEM(MCM)
C     READS IN THE PACKED  INDICES NEEDED FOR EIGENVECTOR COMPUTATION
C     AND  PUT CN TAPE PREVIOUSLY BY LAFITE AND MOUTON
      DIMENSION ARRAY(252)
      COMMON  /CUC/ ARRAY, IPIV, JPIV, COSINE, SINE
    7 IF(MCM-1) 1,2,1
    2 READ  (3)     (ARRAY(I),I=1,252)
    1 IF(MCM-252) 5,5,6
    6 MCM=1
      GC TC 7
    5 IPIV=ARRAY(MOM)
      JPIV=ARRAY(MOM+1)
      CCSINE=ARRAY(MCM+2)
      SINE=ARRAY(MOM+3)
      MCM=MCM+4
      RETLRN
      END
```

```
      SUBROUTINE LAFITE(M)
C     PACKS QUANTITIES NECESSARY FOR COMPUTATION OF EIGENVECTORS INTO
C     MAXIMUM SIZE RECORDS AND WRITES THEM OUT ON TAPE
      DIMENSION ARRAY(252)
      COMMON  /CUD/ ARRAY, IPIV, JPIV, COSINE, SINE
      ARRAY(M)=IPIV
      ARRAY(M+1)=JPIV
      ARRAY(M+2)=COSINE
      ARRAY(M+3)=SINE
      M=M+4
      IF(M-252) 2,2,3
    3 CONTINUE
      WRITE (   3   )(ARRAY(I),I=1,252)
      M=1
    2 RETURN
      END
```

```
      SUBROUTINE MOUTCN
C     WRITES OUT ON TAPE ANY UNFINISHED RECORD RELATING TO EIGENVECTORS
      DIMENSION ARRAY(252)
      COMMON  /CUD/ ARRAY, IPIV, JPIV, COSINE, SINE
    1 WRITE  (3)     (ARRAY(I),I=1,252)
      RETURN
      END
```

```
      SUBROUTINE CARUSO(IOCC, U, A, NT)
C     COMPUTES  TOTAL OVERLAP POPULATION MATRIX
C     U IS IN CORE    S ON TAPE IS
      DIMENSION U(140,140),A(150),IOCC(150)
      REWIND 8
      REWIND 3
      DO 2 I=1,NT
      DO 2 J=1,NT
    2 U(I,J)=0.0
      DO 3 M=1,NT
      READ  ( 3)(A(J),J=1,NT)
      RMM=2*IOCC(M)
      IF(RMM) 3,3,4
    4 DO 5 I=1,NT
      DO 5 J=1,NT
    5 U(I,J)=U(I,J)+A(I)*A(J)*RMM
    3 CONTINUE
      DO 6 I=1,NT
      READ  ( 8)(A(J),J=1,NT)
      DO 6 J=1,NT
    6 U(I,J)=U(I,J)*A(J)
      RETURN
      END
```

```
      SUBROUTINE SOREN
C     THIS IS THE MATRIX EQUATION SOLVER WHICH REPLACES OLD EIGEN AND
C     FUNCTIONS WITH ONLY ONE MATRIX IN CORE
C     ASSUMES S IS IN CORE AND H  ON TAPE ITAPEH
      DIMENSION A(140,140),IOCC(150),HDIAG(150),B(150),C(150)
      COMMON  /OAA/ A
      COMMON  /OAB/ IOCC, HDIAG, B, NDIM, N
      COMMON  /OAN/ ER,SUM
      REWIND 8
      DO 222 I=1,N
  222 WRITE (8)      (A(I,J),J=1,N)
      REWIND 8
      DO 1988 NN=1,N
      READ (8)       (B(J),J=1,N)
      IF(NN-1)2,3,2
    3 A(NN,NN)=1.
      GO TO 1988
    2 NNN=NN-1
      DO 5988 I=1,NNN
      A(NN,I)=0.
      DO 5988 K=1,I
 5988 A(NN,I)=A(NN,I)+A(K,I)*B(K)
      DO 6988 L=1,NNN
      A(L,NN)=0.
      DO 6988 I=L,NNN
 6988 A(L,NN)=A(L,NN)-A(NN,I)*A(L,I)
      A(NN,NN)=1.
      XNORM=0.
      DO 4988 J=1,NN
 4988 XNORM=XNORM+A(J,NN)*B(J)
      XNORM=1./SQRT(XNORM)
      DO 7988 L=1,NN
 7988 A(L,NN)=A(L,NN)*XNORM
 1988 CONTINUE
      DO 3111 I=2,N
      ING=I-1
      DO 3111 J=1,ING
 3111 A(I,J)=0.
      A(2,1)=0.
 3112 REWIND 9
      DO 3211 I=1,N
 3211 WRITE (9)      (A(J,I),J=1,N)
      REWIND 4
      DO 10 I=1,N
   10 READ (4)       (A(I,J),J=1,N)
      CALL BALDUR
      REWIND 4
      DO 6 J=1,N
    6 WRITE (4)      (A(I,J),I=1,N)
      REWIND 9
      DO 7 J=1,N
    7 READ (9)       (A(J,I),I=1,N)
      REWIND 9
      DO 960 J=1,N
```

```
  960 WRITE (9)     (A(I,J),I=1,N)
      CALL BALL
      CALL CUPID
      WRITE (  6 ,8)(I,HDIAG(I),IOCC(I),I=1,N)
      SUM=0.0
      DO 1965 I=1,N
 1965 SUM=SUM+HDIAG(I)*FLOAT(IOCC(I))
      CRUM=23.07*SUM
      WRITE (  6 ,1972)SUM,CRUM
      ERUM=23.07*ER
      WRITE (6,1973) ER,ERUM
      SUM=SUM+ER
      CRUM=23.07*SUM
      WRITE (  6 ,1974)SUM,CRUM
 1972 FORMAT(//50X,4HSUM,F16.8,3H EV,20X,2H= ,F16.8,5H KCAL//)
 1973 FORMAT(41X,13HREPUL ENERGY,F16.8,3H EV,20X,2H= ,F16.8,5H KCAL//)
 1974 FORMAT(41X,13HTOTAL ENERGY,F16.8,3H EV,20X,2H= ,F16.8,5H KCAL//)
    8 FORMAT(1H0,51X,2HHE(,I3,3H) =,F12.6,6X,I3)
 1234 CALL LCKI
      WRITE (  6 ,9)
    9 FORMAT(1H0,55X,14HEIGENVECTORS  ////)
      CALL PEGLEG(A,N)
      RETURN
      END
```

```
      SLBROUTINE LOKI
C      CALCULATES A=BC WITH C IN CORE ANC B ON TAPE ITAPEB STORED ROWWIS
C      RESULTANT MATRIX IN CORE
       DIMENSICN C(140,140),IX(150),A(150),B(150)
       CCMMCN  /CAA/ C
       CCMMON  /CAB/IX, A, B, NDIM, N
       REWINC 3
       REWINC S
       CC 2 I=1,N
       READ    (S)     (B(J),J=1,N)
       CC 1 K=1,N
       A(K)=0.0
       CC 1 J=1,N
   1 A(K)=A(K)+B(J)*C(J,K)
   2 WRITE   (3)     (A(K),K=1,N)
       REWINC 3
       CC 3 I=1,N
   3 READ    (3)     (C(I,J),J=1,N)
       FETURN
       ENC
```

```
      SUBROUTINE BALDUR
C     CALCULATES A=BC WITH B IN CORE, C ON ITAPEC STORED BY COLUMNS
C     RESULTANT MATRIX IS IN CORE
      DIMENSION B(140,140),IX(150),A(150),C(150)
      COMMON  /CAA/ B
      COMMON  /CAB/IX, A, C, NDIM, N
      REWIND 3
      REWIND 9
      DO 2 I=1,N
      READ   (9)     (C(J),J=1,N)
      DO 1 K=1,N
      A(K)=0.0
      DO 1 J=1,N
    1 A(K)=A(K)+B(K,J)*C(J)
    2 WRITE  (3)     (A(K),K=1,N)
      REWIND 3
      DO 3 I=1,N
    3 READ   (3)     (B(J,I),J=1,N)
      RETURN
      END
```

```
      SUBROUTINE JENNY(ICOUNT, P, N, A)
C     REDUCTION OF OVERLAP POPULATION MATRIX TO ATOM-ATOM
      DIMENSION P(140,140),ICOUNT(50,2),A(150)
      REWIND 9
      DO 1 I=1,N
      IN=ICOUNT(I,1)
      IFF=ICOUNT(I,2)
      DO 2 J=1,N
      A(J)=0.0
       JIN=ICOUNT(J,1)
      JF=ICOUNT(J,2)
      DO 2 K=IN,IFF
      DO 2 L=JIN,JF
    2 A(J)=A(J)+P(K,L)
    1 WRITE ( 9)(A(J),J=1,N)
      REWIND 9
      DO 3 I=1,N
    3 READ  ( 9)(P(I,J),J=1,N)
    4 FORMAT(1H0,40X,50H REDUCED OVERLAP POPULATION MATRIX ATOM BY ATOM
     1             //)
      WRITE (  6 ,4)
      CALL PEGLEG(P,N)
      RETURN
      END
```

```
      SUBROUTINE COKI
C     CALCULATES A=BC WITH C IN CORE AND B ON TAPE ITAPEB STORED ROWWIS
C     RESULTANT MATRIX IN CORE
      DIMENSION C(140,140),IX(150),A(150),B(150)
      COMMON  /CAA/ C
      COMMON  /CAB/IX, A, B, NDIM, N
      REWIND 4
      REWIND 8
      DO 2 I=1,N
      READ   (8)     (B(J),J=1,N)
      DO 1 K=1,N
      A(K)=C.C
      DO 1 J=1,N
 1    A(K)=A(K)+B(J)*C(J,K)
 2    WRITE  (4)     (A(K),K=1,N)
      REWIND 4
      DO 3 I=1,N
 3    READ   (4)     (C(I,J),J=1,N)
      RETURN
      END
```

```
      SLBRCUTINE  BALL
C     CALCULATES A=BC WITH B IN CORE, C CN ITAPEC STORED BY CCLUMNS
C     RESULTANT MATRIX IS IN CCRE
      DIMENSICN B(140,140),IX(150),A(150),C(150)
      CCMMON  /CAA/ B
      CCMMCN  /CAB/IX, A, C, NDIM, N
      REWINC 3
      REWINC 4
      CC 2 I=1,N
      READ    (4)     (C(J),J=1,N)
      CC 1 K=1,N
      A(K)=0.0
      CC 1 J=1,N
    1 A(K)=A(K)+B(K,J)*C(J)
    2 WRITE   (3)     (A(K),K=1,N)
      REWIND 3
      CO 3 1=1,N
    3 READ    (3)     (B(J,I),J=1,N)
      RETURN
      END
```

```
      SUBROUTINE IENNY(ICOUNT, P, N, A)
C     REDUCTION OF OVERLAP POPULATION MATRIX TO ATOM-ATOM
      DIMENSION P(140,140),ICOUNT(50,2),A(150)
      REWIND 4
      DO 1 I=1,N
      IN=ICOUNT(I,1)
      IFF=ICOUNT(I,2)
      DO 2 J=1,N
      A(J)=0.0
      JIN=ICOUNT(J,1)
      JF=ICOUNT(J,2)
      DO 2 K=IN,IFF
      DO 2 L=JIN,JF
2     A(J)=A(J)+P(K,L)
1     WRITE ( 4)(A(J),J=1,N)
      REWIND 4
      DO 3 I=1,N
3     READ  ( 4)(P(I,J),J=1,N)
4     FORMAT(1H0,40X,50H REDUCED OVERLAP POPULATION MATRIX ATOM BY ATOM
     1               //)
      WRITE ( 6 ,4)
      CALL PEGLEG(P,N)
      RETURN
      END
```

```
      SUBROUTINE REPU
C
C     THIS SUBROUTINE CALCULATES AN EXPONENTIAL REPULSION ENERGY.
C     THIS ENERGY DEPENDS ON TWO EMPIRICALLY DETERMINED PARAMETERS.
C
      DIMENSION S(140,140),IOCC(150),XX(150),YY(150),AR(150),AL(150)
      COMMON  /CAA/ S
      COMMON  /CAB/ IOCC, XX, YY, N, NDIM
      COMMON  /CAM/ AR, AL, MR
      COMMON  /CAN/ ER
      ER=0
      IF (MR) 4,4,2
    2 K=N-1
      DO 3 I=1,K
      L=I+1
      DO 3 J=L,N
      ER=ER+SQRT(AR(I)*AR(J))*EXP(-S(I,J)/(AL(I)+AL(J)))
    3 CONTINUE
    4 RETURN
      END
```